Summer 2010

Mathematical models of ion transport through nafion membranes in modified electrodes and fuel cells without electroneutrality

Stephanie Ann Schmidt
University of Iowa

MATHEMATICAL MODELS OF ION TRANSPORT THROUGH NAFION MEMBRANES IN MODIFIED ELECTRODES AND FUEL CELLS WITHOUT ELECTRONEUTRALITY

by

Stephanie Ann Schmidt

An Abstract

Of a thesis submitted in partial fulfillment
of the requirements for the Doctor of
Philosophy degree in Applied Mathematical and Computational Sciences
in the Graduate College of
The University of Iowa

July 2010

Thesis Supervisors: Associate Professor Johna Leddy
Professor Gerhard Strohmer
Assistant Professor Bruce Ayati

ABSTRACT

Electrodes modified with polymer films have distinct permeability. Electroactive redox probes partition from solution into film and are electrolyzed at the electrode. This creates a flux of probe into the polymer film and a flux of electrolyzed probe out of the polymer film. Transport of the probe through the film is governed by diffusion and migration, mathematically described by the Nernst-Planck equation as

$$J_i(x,t) = -D_i \frac{\partial C_i\,(x,t)}{\partial x} - \frac{z_i F}{RT} D_i C_i\,(x,t)\,\frac{\partial \Phi\,(x,t)}{\partial x}$$

where x is the distance from the electrode, t is time, $C_i\,(x,t)$ is the space and time dependent concentration of the probe i, z_i is the charge of the probe i, F is Faraday's constant, R is the gas constant, T is absolute temperature, $J_i(x,t)$ is the flux of the probe i, D_i is the diffusion constant of the probe i, and $\Phi(x,t)$ is the space and time dependent potential.

In most natural systems, charge accumulation is not appreciable and a charged ion is neutralized by a counterion. Electroneutrality is mathematically represented by Laplace's condition on the potential, $\frac{\partial^2 \Phi(x,t)}{\partial x^2} = 0$. In systems where counterions are insufficient to neutralize an ion, local electroneutrality is set by local charge and Poisson's equation replaces Laplace's condition as

$$\frac{\partial^2 \Phi}{\partial x^2} = -\frac{F}{\varepsilon} \sum_i z_i C_i\,(x,t)$$

where ε is the relative permittivity. The Nernst-Planck under Poisson's condition is not solved analytically. The extreme magnitude of F/ε yields a system that resists solution by standard techniques. The first system investigated determines the concentration and potential profiles over the polymer membrane of a fuel cell without the assumption of electroneutrality.

In the second system investigated, the probes physical motion is highly restricted. This gives a more generalized form of the Nernst-Planck equation with spatially varying diffusion coefficient results

$$J = -D\,(x,t)\,\frac{\partial C\,(x,t)}{\partial x} - \frac{zF}{RT} D\,(x,t)\,C\,(x,t)\,\frac{\partial \Phi\,(x,t)}{\partial x}.$$

$D(x,t)$ is the space and time dependent diffusion coefficient, which can include a physical displacement term and an electron hopping term. The second system this thesis investigates is a modified electrode system where electron hopping is responsible for a majority of the probe transport within the film.

Lastly, preliminary methods are presented to determine physical diffusion of a probe at a modified electrode by sweep voltammetry.

Abstract Approved: _____

Thesis Supervisor

_____

Title and Department

_____

Date

Abstract Approved: _____

Thesis Supervisor

_____

Title and Department

_____

Date

Abstract Approved: _____

Thesis Supervisor

_____

Title and Department

_____

Date

MATHEMATICAL MODELS OF ION TRANSPORT THROUGH NAFION MEMBRANES IN MODIFIED ELECTRODES AND FUEL CELLS WITHOUT ELECTRONEUTRALITY

by

Stephanie Ann Schmidt

A thesis submitted in partial fulfillment
of the requirements for the Doctor of Philosophy degree in
Applied Mathematical and Computational Sciences
in the Graduate College of
The University of Iowa

July 2010

Thesis Supervisors: Associate Professor Johna Leddy
Professor Gerhard Strohmer
Assistant Professor Bruce Ayati

Graduate College
The University of Iowa
Iowa City, Iowa

CERTIFICATE OF APPROVAL

PH.D. THESIS

This is to certify that the Ph.D. thesis of

Stephanie Ann Schmidt

has been approved by the Examining Committee for the thesis requirement for the Doctor of Philosophy degree in Applied Mathematical and Computational Sciences at the July 2010 graduation.

Thesis Committee:

Gerhard Strohmer, Thesis Supervisor

Johna Leddy, Thesis Supervisor

Bruce Ayati, Thesis Supervisor

Colleen Mitchell

Tong Li

To My Family

ACKNOWLEDGMENTS

I sincerely thank my advisors, Professor Gerhard Strohmer for his wise direction and patience, Professor Johna Leddy for her caring support and advice and Professor Bruce Ayati for his encouragement and guidance both in research and in life. It was truly a privilege to work with such accomplished scientists. I also wish to thank present and past students of the Leddy lab, especially Luke Haverhals, Chaminda Hettige, Heung Chan Lee, Tim Paschewitz and Perry Motsegood for all their support. I am thankful to my husband Tracy for his loving patience, support and encouragement throughout these long years and my mother, Shirley Ann Bara, for always believing in me. Lastly, I would like to thank my two angelic daughters, Kiranie and Ava Lyn, for always making me smile.

TABLE OF CONTENTS

LIST OF FIGURES

Figure

LIST OF SYMBOLS

Symbol	
α	transfer coefficient, taken to be 0.5
γ	Ratio of diffusion coefficients expressed as $\gamma = \sqrt{\frac{D_s}{D_f}}$
δ	The distance between the centers of two molecules (cm)
ε	relative permittivity, $\varepsilon = \varepsilon_o \varepsilon_r$
κ	Extraction parameter for the concentration of the probe in the film relative to the adjacent solution
λ	eigenvalues
ν	Scan rate for cyclic voltammetry, (V/s)
ρ	Density (g/cm^3)
$\Phi(x,t)$	Potential as a function of distance from the electrode, x, at time t (V)
ω	flux parameter, $\frac{1-\frac{\kappa}{\gamma}}{1+\frac{\kappa}{\gamma}}$
A	Area of the electrode
B	Number of boxes the membrane is divided into
b	The diffusion length relative to the film thickness where $b = B\sqrt{nf2\left(E_2 - E_1\right) / \left(\mathbb{D}_f k_{\max}\right)} = \sqrt{l^2 nf\nu / D_f}$
C^*	Bulk concentration of the probe in solution (mol/cm^3)
$C(x,t)$	Concentration of the probe as a function of distance from the electrode, x, at time t (mol/cm^3)
$\tilde{C}(x,t)$	Dimensionless excess concentration of proton
$\hat{C}(x,t)$	Possible electron hopping equations
$C_{l+/-}$	Concentration of the probe on the film/solution (respectively) side of the film-solution interface

D_j	Diffusion coefficient of probe j
D_f	Diffusion coefficient of the probe in the film
D_{phy}	Physical diffusion rate, typically thought of as the diffusion constant D in the absence of electron hopping
D_s	Diffusion coefficient of the probe in solution
$\mathbb{D}_m$	Dimensionless diffusion coefficient, where $\mathbb{D}_i = D_i \Delta t / (\Delta x)^2$
E	Electric field (V/cm, Ch. 2), Potential (V, Ch. 4)
E^o	Standard potential (V)
$E^{o'}$	Formal potential, an experimentally determined reference potential, specified under given experimental conditions (V)
F	Faraday constant, 96,485.3 C
$f(j,n)$	Fractional concentration at position j and time n, where $f(j,n) = C(x,t)/C^*$
G^o	Gibbs free energy (J)
i	Current at potential E (A)
$J(x,t)$	Flux of proton as a function of distance from the electrode, x, at time t (mol/cm^{2}s)
k	mass action constant
k^o	standard heterogeneous rate constant
k_f, k_b	Forward/backward electron transfer rate
k_{11}	Reaction rate
l	Film thickness (cm)
l^-, l^+	The position just inside and outside the interface at l
N	Concentration of Nafion (mol/cm^3, fixed)
n	Number of electrons transferred, as in $A + ne \rightleftharpoons B$ at E^0

O	A generic oxidizing species
P	A generic redox probe
R	A generic reducing species
R	Molar gas constant, 8.31447 J/mol K
R	Resistance of the outside circuit of a fuel cell
T	Temperature (K)
t	Time since the start of the voltage perturbation (s)
t_k	Total time for the sweep in cyclic voltammetry, $(2\,(E_{final} - E_{init})\,/\nu)$
Δt	Time increment in the simulation; $\Delta t = t_k/k_{\max}$ where t_k is the length of the voltage perturbation
V_o	Potential drop over the membrane (V)
V_L	Potential loss due to the outside circuit of the fuel cell
X_f/X_b	Dimensionless heterogeneous electron transfer rates
x	Distance from the electrode surface where $x = 0$ at the electrode surface
$x_{\max}$	Number of boxes the membrane is divided into
Δx	The size of the spatial increment, defined by $\mathbb{D}_s$
Z	Dimensionless current
z_j	Charge of probe j as, for example, j^{z+}

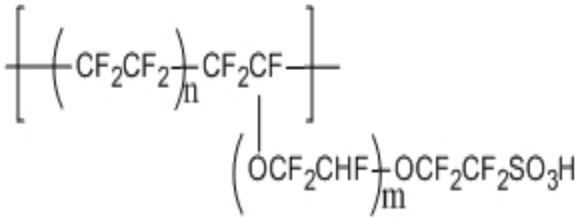

Figure 1. The general chemical structure of Nafion.

CHAPTER 1

INTRODUCTION

In this dissertation, the workings of a hydrogen oxygen fuel cell and a Nafion® modified electrode are specified. The models include a simple mathematical representation of the chemical reactions.

An efficient working fuel cell could replace combustion engines and advance the national goal of becoming less oil dependent. For a fuel cell, an accurate mathematical model is an important tool for optimizing fuel cell efficiency, which makes fuel cell models of current topical interest.

Electron transfer reactions, like those that occur in modified electrodes, are basic chemical reactions that occur in fuel cells, batteries, semiconductors, solar cells, fuel cells, hemoglobin, photography and many industrial electrosynthetic processes. The kinetics of ion transfer reactions are crucial to the efficiency and usefulness of the above technologies and systems, thereby, necessitating a deeper understanding of the systems. [7]

1.1 Nafion Film

The systems studied in this dissertation involve ion transfer reactions within an ion exchange polymer composite matrix supported on an electrode surface. The ion exchange polymer that is used to modify electrodes in these studies is Nafion, the structure of which is shown in Figure 1

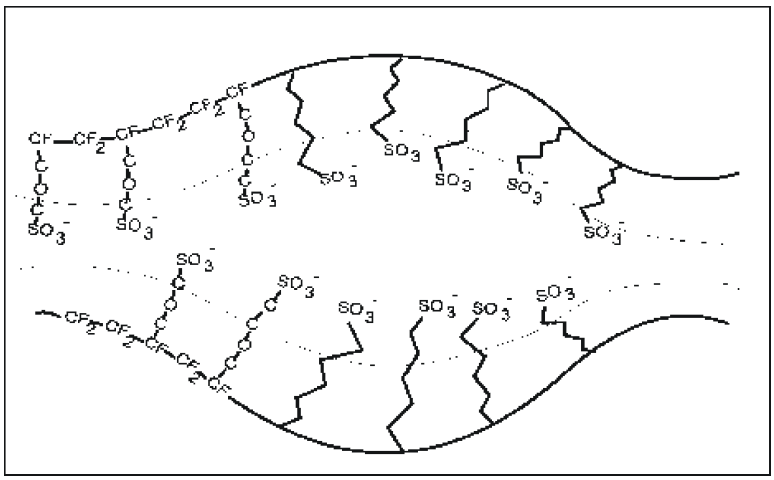

Figure 2. The long standing speculation of the microstructure of Nafion.

where m is typically 1 and n varies from 6 to 14. Structurally, Nafion is a teflon-like, hydrophobic, fluorocarbon backbone with sidechains that terminate in a hydrophilic sulfonic acid. When Nafion is in contact with solution, the proton from the sulfonic acid can easily exchange with cationic species in solution. Nafion provides a cation selective matrix where cationic redox species are preconcentrated within the film. Because Nafion is a polymer, mass transport in the system is slowed. In the acid form, Nafion provides ion conduction through the acidic proton about the superacid sulfonic acid site. The hydrophobic (fluorocarbon) region and hydrophilic (ionic) region are shown in Figure 1 on the left and right sides, respectively. It is long speculated that the microstructure of Nafion is approximated as shown in Figure 2 (image used from reference [1]), where the fluorocarbon phase segregates from the hydrated sulfonic acids to form water filled domains that sustain ionic conduction. In any electrochemical cell where Nafion is used as the separator, ionic flux through the membrane balances the electron flux through the electron conductors (i.e., electrodes and external circuit). This balance of electron and ion (proton) flux is mandatory for all electrochemical cells, that include fuel cells.

1.2 Fuel Cells

A fuel cell is similar to a battery in that it converts chemical energy into electrical energy and is better than a battery in that it does not undergo charge/discharge cycles. A fuel cell provides power as long as it is provided fuel, similar to a combustion engine. A fuel cell is better than a combustion engine because it converts chemical energy directly into electrical energy without traversing through a pressure-volume cycle and is thus, an inherently more efficient process. As an operating device, the hydrogen oxygen fuel cell is environmentally advantageous as compared to the current gasoline combustion engines in automobiles. Further, fuel cells generate minimal heat as compared to combustion engines and do not release carbon dioxide buy rather generate water. Current gasoline combustion engines are subject to the thermodynamic limitations associated with expansion and compression. The Carnot limitations restrict combustion engines to a theoretical maximum efficiency of about 40%. Because a fuel cell converts chemical energy to electrical energy without mechanical cycles, there are no thermodynamic limitations and thus the theoretical efficiency is 100%.

1.2.1 Fuel Cell Workings

A fuel cell consists of two electrodes separated by an ion conducting membrane. As is typical, and for this specific example, the ion conducting membrane will be Nafion and the electrodes will be made of electron conducting materials such as graphite. When catalyst-coated electrodes are pressed against the membrane, interfacial zones are created. At the interfaces, the catalyst, membrane and electrode material intermix to form a gas permeable, ion and electron conducting matrix. The electrochemical reactions occur only at these interfacial zones where three requirements are met: 1) a catalytic site is provided for the reaction to occur; 2) the matrix is sufficiently porous to allow hydrogen and oxygen to reach the catalyst on the anode and cathode, respectively, and 3) a path must exist for the protons to move through the membrane and electrons to move into the

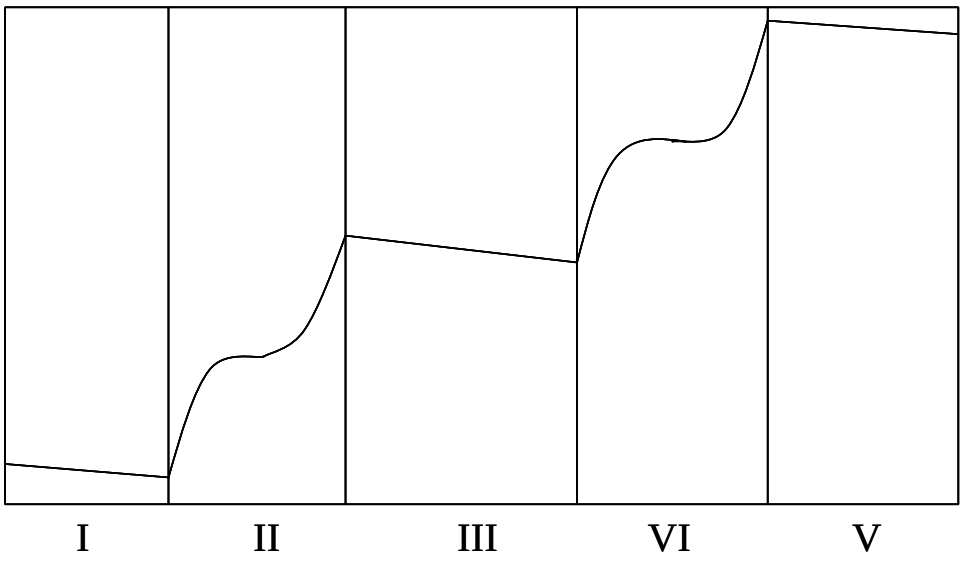

Figure 3. The approximated potential profile through a fuel cell. (Not to scale.)

external circuit.[4]

A local difference in the concentration of protons and electrons is produced because of the reaction. This separation of charge creates a potential difference across the cell. The potential differences are created by the reactions and motion of charge (i.e., ion and electron movement), and differences tend to form at interfaces where resistance are low. The slightly resistive nature of the electrodes and Nafion causes there to be some potential loss in these regions. Figure 3 is a schematic of the approximated potential profile across the cell where I is the anodic electrode, II is the anodic interfacial zone, III is the Nafion membrane, IV is the cathodic interface and V is the cathodic electrode.

Figure **??** is a schematic of a fuel cell. On the left side, hydrogen (H_2) enters the fuel cell. One hydrogen molecule breaks down into two protons and two electrons in the anodic interfacial zone. The protons move through the proton conducting membrane, Nafion, and arrive at the cathode interfacial region. The electrons move through the external circuit, thereby providing electrical power. The electrons then proceed to the cathodic interfacial zone with the protons. This provides

net electrical neutrality. Oxygen (O_2) enters the interfacial zone; oxygen is often provided as air. The free protons and electrons react with the oxygen to produce water. Lastly, water exits the fuel cell. The reaction proceeds provided that the supply of hydrogen and oxygen continues. The interfacial zones are approximately 10 micrometers whereas commercially available Nafion thicknesses can vary from 50 to 175 micrometers.

Thermodynamically, hydrogen and oxygen react spontaneously. However, the kinetics are slow. Hydrogen and oxygen alone are a stable mixture. When they interact in the presence of an appropriate catalyst, water is spontaneously formed. Thermodynamically, the reaction is energetically favorable. The following are the standard potentials, E^o, for the reactions of interest.

$$\begin{aligned} O_2 + 4H^+ + 4e^- &\rightleftharpoons 2H_2O \quad E^o = 1.23V \\ 4H^+ + 4e^- &\rightleftharpoons 2H_2 \qquad E^o = 0.00V \\ \hline O_2 + 2H_2 &\rightleftharpoons 2H_20 \qquad E^o_{cell} = 1.23V \end{aligned} \tag{1}$$

Each of the chemical reactions are written as a reduction, which is addition of electrons to the reactant. Oxidation occurs when electrons are lost from a species. When all species are at standard conditions of 1 M concentration and 1 atm pressure, the reactions occur at E^o, the standard potential determined against a standard hydrogen electrode. The Gibbs free energy for the overall reaction is $\Delta G^o = -nFE^o_{cell}$, where n is the number of electrons, F is the Faraday constant ($96485.3\,\mathrm{C\,mol^{-1}}$), and E^o_{cell} is the calculated cell potential for the overall reaction. Thus, $\Delta G^o = -4 \times 96485.3 \times 1.23 \approx -0.5$ MJ/mole O_2. Because $\Delta G_o < 0$, the reaction is favored and spontaneous as written. The energy per mole of oxygen (-0.5 MJ) is large. This large free energy drives the thermal decomposition of hydrogen and oxygen. It also drives the electrochemical decomposition on which the fuel cell is based. Thus, hydrogen decomposes to electrons and protons at the anode and recombines electrochemically with oxygen at the cathode to yield an electrochemical power source with water as a byproduct. Therefore, even though hydrogen and oxygen are separated by a membrane, it is still energetically favorable for the hydrogen

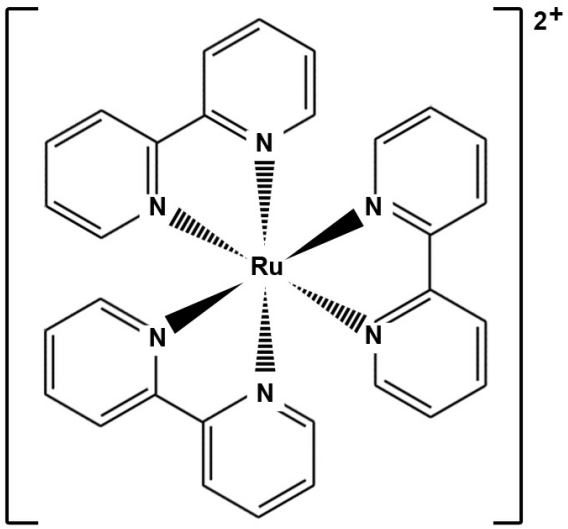

Figure 4. $Ru(bpy)_3^{2+}$ cationic, molecular probe

to decompose and for the fuel cell to operate. The thermal and electrochemical reactions are thermodynamically equivalent.

1.3 Modified Electrodes

In the modified electrode system, we will consider ruthenium tris(2,2′-bipyridine) $\left(Ru(bpy)_3^{2+} \text{and } Ru(bpy)_3^{3+}\right)$ cation moving through Nafion. From cyclic voltametric data, the transport of $Ru(bpy)_3^{2/3+}$ through the film is by diffusion. Because the concentration is high, the redox species are separated by 0.1 nm. Electrons readily exchange between adjacent $Ru(bpy)_3^{2+}$ and $Ru(bpy)_3^{3+}$. This electron exchange (formally, self exchange) is effective for $Ru(bpy)_3^{2/3+}$, the measured diffusion coefficient is well in excess of that by simple physical diffusion, where $Ru(bpy)_3^{2+}$ and $Ru(bpy)_3^{3+}$ must physically exchange positions in space.

Nafion has a strong affinity for $Ru(bpy)_3^{2+}$ and $Ru(bpy)_3^{3+}$ and will preferably bond with either over protons. Thus, when Nafion is placed in a solution that contains $Ru(bpy)_3^{2+}$, all the protons

are replaced with $Ru(bpy)_3^{2+}$ cations. Typically, the solution is an aqueous mixture of an acid such as HNO_3 (0.1 M) and $Ru(bpy)_3Cl_2$ (1 mM). HNO_3 serves as the electrolyte in solution. The cation bound initially to the Nafion is $Ru(bpy)_3^{2+}$, where two sulfonates of Nafion molecules are bound to each $Ru(bpy)_3^{2+}$.

The system is an electrode coated with a Nafion membrane where the large counterelectrode is some large distance away. The counterelectrode is sufficiently distance that the chemical reaction at the counterelectrode will not affect the concentrations of the chemicals at the modified electrode over the short period of the measurement. Thus, for modeling purposes, a single electrode is considered.

When the Nafion coated electrode is placed into the weak acid/$Ru(bpy)_3Cl_2$ solution, all the acidic hydrogen bonds in the Nafion film will be replaced with Nafion-$Ru(bpy)_3^{2+}$ bonds. When $Ru(bpy)_3^{2+}$ is oxidized at the electrode surface to $Ru(bpy)_3^{3+}$, a current is generated. Typically, the $Ru(bpy)_3^{3+}$ is taken to diffuse back through the bulk of the Nafion to the film solution interface. The $Ru(bpy)_3^{3+}$ then extracts from the membrane into the bulk electrolyte solution and $Ru(bpy)_3^{2+}$ is extracted into the membrane. Oxidation proceeds immediately at the electrode surface with $Ru(bpy)_3^{2+}$ fed from the solution and product $Ru(bpy)_3^{3+}$ is jettisoned into the solution. It is important to note that no significant amount of charge builds up in the Nafion as shown by experimental voltammograms. Voltammograms from this system exhibit behavior typical of simple diffusion transport. This is consistent with no observed migration (i.e., potential) effects in these films. Because the Nafion sulfonate anions can not move significantly, this charge balance must be achieved through the movement of positively charge particles. $Ru(bpy)_3^{3+}$ must be the main contributor to the movement of positively charged molecules out of the system. The large affinity of $Ru(bpy)_3^{3+}$ for Nafion precludes repetitive bond breaks between sulfonates and $Ru(bpy)_3^{2/3+}$, which mitigates against large scale physical diffusion of $Ru(bpy)_3^{2/3+}$ into and out of the film. It is more likely that an electron hopping process between the $Ru(bpy)_3^{3+}$ and $Ru(bpy)_3^{2+}$ balances most of the charge.

1.4 Reactions

Two types of reactions will be discussed in this thesis. The following is an overview of each type.

1.4.1 Electrochemical Reactions

Consider the following electrochemical reduction reaction

$$O + e^- \rightarrow R. \tag{2}$$

This is a reduction reaction because molecule O is gaining an electron, $e-$. O is the oxidizer because it is taking the electron. Molecule O is said to be being reduced. This type of reaction can occur when an electrode gives electrons from a molecule O. Consider the reverse electrochemical oxidation reaction

$$R - e^- \rightarrow O. \tag{3}$$

This is an oxidation reaction because molecule R is loosing an electron, $e-$. R is the reducer because it is giving the electron. Molecule R is said to be being oxidized. This type of reaction can occur when an electrode takes electrons from a molecule R.

1.4.2 Self-Exchange Reactions

Homogeneous electron transfer reactions between a redox molecule in two different oxidation states is called a self-exchange reaction [9]; that is,

$$M^n + M^{n\pm1} \rightleftharpoons M^{n\pm1} + M^n \tag{4}$$

where M is the redox species and the notation indicates a change in spatial location for M^n and M^{n+1} can commute with the electron transfer . Under appropriate conditions of high concentration and slow physical diffusion, self exchange reactions enhance apparent diffusion coefficients when

the exchange in space of M^n and $M^{n\pm1}$ is accomplished slowly by physical diffusion but efficiently by electron exchange (electron hopping) between M^n and $M^{n\pm1}$[9]. Self-exchange enhanced diffusion coefficients have been observed for transition metal complexes concentrated in thin films of ion-exchange polymers, such as Nafion in [9]. In this study, self-exchange rates of $Ru(bpy)_3^{2+}$ and $Ru(bpy)_3^{3+}$ are investigated.

1.5 Cyclic Voltammograms

The electrochemical behavior of a system can be studied through a series of steps to different potentials while recording of the current-time curves. In the laboratory, this is done efficiently by an experiment where the potential (E) is swept from some starting potential V_1 to an ending potential V_2 and recording the current (i), thereby creating an i-E curve. The potential is varied linearly with time at sweep rates ν ranging typically from 10 mV/s to 250 V/s with conventional large electrodes. This is known as linear sweep voltammetry. [3]

For an electrochemical reduction reaction, $O + e^- \rightleftharpoons R$, a potential scan begun at V_1 well positive of $E^{o'}$, has only nonfaradaic currents flow initially. As the electrode potential approaches $E^{o'}$, reduction begins and faradaic current starts to flow. As the potential continues to increase negatively, the system reaches a maximum current (i_{pc}) at a particular potential (E_{pc}), after which the surface concentration of the reactant begins to drop and with declining reactant supply, the flux to the electrode surface decreases. The current decays with declining reactant supply until the sweep ends at V_2. The i-E curve observed looks like that of the upper curve depicted in Figure 5. Note that in common plotting convention for cyclic voltammetry, potentials greater than $E^{o'}$ are on the left side of the x-axis while potentials lesser than $E^{o'}$ are on the right. [3]

As the potential scan is reversed and swept in the positive direction (right to left), a large concentration of product R exists near the electrode. As the potential approaches and passes $E^{o'}$, R is converted back to O at the electrode surface. The reactant O is regenerated. As R is oxidized, a current flows. This reversal current has a shape much like that of the forward peak

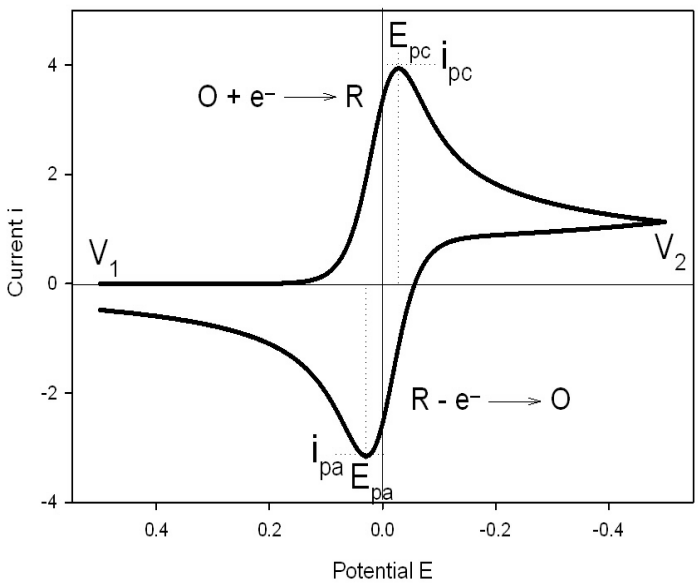

Figure 5. A typical cyclic voltammogram.

for essentially the same reasons, giving a maximum current (i_{pa}) at a particular potential (E_{pa}). Performing the forward and backward sweep experiment together is called cyclic voltammetry and a cyclic voltammogram is a plot of current versus potential.

A typical cyclic voltammogram is shown in Figure 5. Different system characteristics affect the shape of the voltammogram. The morphology of the voltammogram captures the processes occurring in the system. In the system of interest in this dissertation, the voltammograms are shaped as shown in Figure 5. This will effect the boundary conditions and model parameters as this shows that the potential difference must be zero through most of the film with a steep increase and decrease at the electrode sides of the membranes.

1.6 Discretization

Many equations which describe physical systems rely on rates. A rate is simulated mathematically by a derivative. The formula for the derivative of a function of a function $f(x)$

with respect to the variable x $\left(\text{denoted as } f_x(x),\ f'(x) \text{ or } \frac{df}{dx}\right)$ is

$$f_x(x) = f'(x) = \frac{df(x)}{dx} = \lim_{\Delta x \to 0} \frac{f(x+\Delta x) - f(x)}{\Delta x}. \tag{5}$$

Note that $\frac{f(x+\Delta x)-f(x)}{\Delta x}$ is the slope between two points of $f(x)$ separated by a distance of length Δx. For small enough Δx (or close enough values of $f(x)$), $\frac{df(x)}{dx}$ can be approximated by

$$\frac{df(x,t)}{dx} \approx \frac{f(x+\Delta x) - f(x)}{\Delta x}. \tag{6}$$

When a function f is dependant on two variables, say x and t, then any derivative of f is called a partial derivative. A partial derivative is the derivative of f with respect to one variable while the other variable is held constant. This is denoted by

$$\frac{\partial f(x,t)}{\partial x} = \lim_{\Delta x \to 0} \frac{f(x+\Delta x,t) - f(x,t)}{\Delta x} \text{ or } \frac{\partial f(x,t)}{\partial t} = \lim_{\Delta t \to 0} \frac{f(x,t+\Delta t) - f(x,t)}{\Delta t}. \tag{7}$$

Similarly for small enough Δx and Δt, the partial derivatives of f can be approximated by

$$\frac{\partial f(x,t)}{\partial x} \approx \frac{f(x+\Delta x,t) - f(x,t)}{\Delta x} \text{ or } \frac{\partial f(x,t)}{\partial t} \approx \frac{f(x,t+\Delta t) - f(x,t)}{\Delta t}. \tag{8}$$

Second derivatives can also be approximated by taking the partial derivative of the partial derivative with respect to a variable. For example, the second partial derivative with respect to x twice of $f(x,t)$ for fixed Δx is

$$\begin{aligned} \frac{\partial}{\partial x}\left[\frac{\partial f}{\partial x}\right] \frac{\partial^2 f(x,t)}{\partial x^2} &= \lim_{\Delta x \to 0} \frac{\frac{f(x+\Delta x,t)-f(x,t)}{\Delta x} - \frac{f(x,t)-f(x-\Delta x,t)}{\Delta x}}{\Delta x} \\ &\approx \frac{\frac{f(x+\Delta x,t)-f(x,t)}{\Delta x} - \frac{f(x,t)-f(x-\Delta x,t)}{\Delta x}}{\Delta x} \\ &\approx \frac{f(x+\Delta x,t) - 2f(x,t) + f(x-\Delta x,t)}{\Delta x^2}. \end{aligned} \tag{9}$$

When a system is discretized, the length and time of the system perturbation is divided into many Δx and Δt. When looking at a length divided into many Δx, the first box starts a length

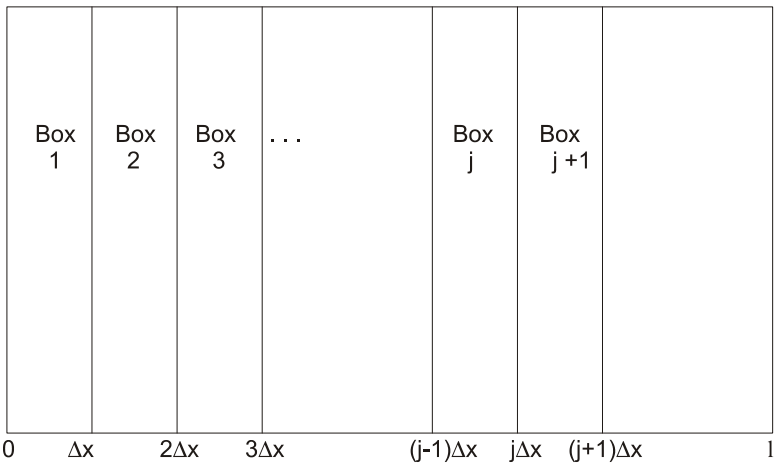

Figure 6. A pictorial representation of discretizing a space into Δx peices.

$x = 0$ and runs to $x = \Delta x$, the second box starts at $x = \Delta x$ and runs to $x = 2\Delta x$, and so on. Box j used to refer to a particular section of length Δx within the system that runs from $x = (j-1)\Delta x$ to $x = j\Delta x$. The section to the left of box j is the $j-1$ box and the section to the right of box j is $j+1$. Similarly, a time of length Δt is identified as time period n, with the Δt time period before as $n-1$ and the time period after as $n+1$. For Δx and Δt sufficiently small, this allows the approximation of the first and second derivatives at a particular location x_o and time t_o more easily for coding a simulation as

$$\frac{\partial f\left(x_o, t_o\right)}{\partial x} \approx \frac{f(j+1,n) - f(j,n)}{\Delta x} \text{ or } \frac{\partial f\left(x_o, t_o\right)}{\partial t} \approx \frac{f(j,n+1) - f(j,n)}{\Delta t} \tag{10}$$

where the x_o is taken to be at the midpoint between $(j-1)\Delta x$ and $j\Delta x$ and t_o is taken to be at the midpoint between $(n-1)\,\Delta t$ and $n\Delta t$. Similarly, second derivatives for fixed Δx can be written as

$$\frac{\partial^2 f\left(x_o, t_o\right)}{\partial x^2} \approx \frac{f(j+1,n) - 2f(j,n) + f(j-1,n)}{\Delta x^2}. \tag{11}$$

For boxes of fixed size Δx, Figure 6 is a pictorial representation of discretizing a space into Δx.

CHAPTER 2

THE MODEL AND SIMULATION OF PROTON TRANSFER WITHIN THE NAFION MEMBRANE OF A FUEL CELL WITHOUT ELECTRONEUTRALITY

Several models have been presented to simulate the proton transport within various regions within a fuel cell ([26], [27], [28], [4]). All previous models have assumed electroneutrality over the membrane within a fuel cell. That is, opposite charges will pair up at every location within the membrane for an overall charge of 0 every where. In reference [4], an earlier attempt to model the interfacial zone of a fuel cell is reported. The equations were solved numerically using Gear's method. This approach does not suffice here because of an integration condition placed on the system of equations. The governing equations are the same as those used here, which served as the model used in this thesis.

2.1 The Physical System

In this chapter, a model is specified for proton movement through the fuel cell system described in section 1.2. Protons can move through the fuel cell by diffusion and migration, collectively called mass transport. Convection occurs by a physical process like stirring and is induced by net solvent motion that cannot occur in a proton exchange membrane fuel cell and is not included here in mass transport consideration.

2.2 Electroneutrality

Electroneutrality occurs when there is no net charge over a region of space; for every negative charge there is a positive charge such that the overall local charge zero and thus neutral. For an electroactive ion, local charge neutrality eliminates migration and mass transport is restricted to diffusion.

Electroneutrality occurs on two scales, local and global throughout the system. Each occurs under specific conditions. Local electroneutrality occurs under two conditions: 1) when the ions of the electroactive probe move sufficiently rapidly to allow counterions to pair rapidly to establish overall charge of zero and 2) when the electrolyte (a non-electroactive species) concentration is large relative to the concentration of electroactive probe. Under condition 2, the electrolyte will carry a majority of the current in the solution to minimize migration as a mode of mass transport for the electroactive species [3]. It has been shown that the electroneutrality assumption is reasonable under these conditions [11].

Global electroneutrality occurs when the total positive ion charge within a system equals the total negative ion charge but the ion and counterion may be too distance to neutralize the charge. Therefore, it is possible to have a charge build up over a portion(s) of the ionic domain (i.e., the membrane) locally, but when the ion charges are integrated over the whole system, there is no excess charge. Locally net charge can exist, but globally, the system is neutral. Local charge build up typically occurs when there is little to no electrolyte and/or a fixed counterion. This novel characteristic will be used in modeling the membrane region of the system in section 1.2.

2.3 The General Equations

From the potential profile in figure 3, protons are moving against the concentration gradient and the electrons are moving against the electric field. The mathematical model must include a coupled migration-diffusion transport process for the charged species. Global charge neutrality dictates that the membrane be electrically neutral overall and thus there is one proton for each ion-exchange site. The membrane need not establish local electroneutrality. Conceptually, as one proton enters the membrane, another leaves, and this maintains global electroneutrality. Proton transport is by a combination of diffusion and migration. Migration can not be the only transport mechanism. As shown later, a migration-only model yields an unrealistic solution, so diffusion must also be considered. However, diffusion is not the primary mode of proton transportation through the

membrane. These constraints determine the boundary conditions and transport equations. Lastly, it is assumed that the forward and backward electron transfer steps at the electrode surface are sufficiently rapid that electrolysis will occur at the mass transport limited rate.

Consider a one dimensional problem. Define $C_j(x,t)$ as the concentration $\left(\text{mol/cm}^3\right)$and $J_j\left(x,t\right)$ as the flux $\left(\text{mol cm}^{-2}\ \text{s}^{-1}\right)$ of species j at time t and location x, where x is normal to the electrode. The time rate of change of species j is

$$\frac{\partial C_j(x,t)}{\partial t} = -\frac{\partial J_j(x,t)}{\partial x} + G_j - L_j, \tag{12}$$

where G_j is the generation and L_j is the loss of species j. Because species are generated and consumed in the interfacial zone and not in the membrane, G_j and L_j are both zero for this simulation. The steady state description is of interest, mathematically represented as $\frac{\partial C}{\partial t} \to 0$. The position in the membrane is measured from $x = 0$ (the left side of the membrane in Figure **??**) at the anode and $x = l$ (the right side of the membrane in Figure **??**) at the cathode.

The Nernst-Planck equation (for a one-dimensional model) gives the equation for the flux in terms of concentration $C_j(x,t)$ and potential $\Phi(x,t)$ of charged species j as:

$$J_j(x,t) = \underbrace{-D_j\frac{\partial C_j(x,t)}{\partial x}}_{\text{diffusion}} - \underbrace{\frac{z_j F D_j}{RT} C_j(x,t)\frac{\partial \Phi(x,t)}{\partial x}}_{\text{migration}} + \underbrace{C_j(x,t)\nu(x,t)}_{\text{convection}} \tag{13}$$

where D_j is the diffusion rate of species j $\left(cm^2 s^{-1}\right)$, z_j is the charge of species j, F is Faraday's constant $\left(C\ mol^{-1}\right)$, R is the gas law constant $\left(J\ K^{-1} mol^{-1}\right)$, T is absolute temperature (K) and $\nu(x,t)$ is the velocity of the solution, which is zero for this system. The terms in equation (13) are the contributions to the flux from diffusion, migration and convection, respectively. Because the only moving species in the fuel cell system are protons, the above species-specific equations will only be considered for protons, which discontinues the need for the j index.

Define $C(x,t)$ as the concentration of proton measured in excess of the protons needed to neutralize sulfonates concentration. Let N be the concentration of sulfonates in the Nafion. It

should be noted that $C(x,t)$ is positive if there is an excess of protons or negative if there is a proton deficit. This gives a time dependent flux equation of

$$J(x,t) = -D\frac{\partial C(x,t)}{\partial x} - \frac{zFD}{RT}\left(C(x,t)+N\right)\frac{\partial \Phi(x,t)}{\partial x} \tag{14}$$

or from equation (12)

$$\frac{\partial C(x,t)}{\partial t} = D\frac{\partial^2 C(x,t)}{\partial x^2} + \frac{zFD}{RT}\left(\left(C(x,t)+N\right)\frac{\partial \Phi(x,t)}{\partial x}\right)_x \tag{15}$$

where $J(x,t)$ is the flux of protons $\left(mol\ cm^{-2}s^{-1}\right)$.

The total current, i, at steady state is set by the flux J_j, or current i_j from each species j at steady state:

$$i = \sum_j i_j = -\sum_j nFAJ_j \tag{16}$$

where n is the number of electrons involved in the reaction and A is the geometric area of the electrode. Because protons are the only moveable species in the system the current equation becomes

$$i = -nFAJ \tag{17}$$

where J is the steady state flux at the electrode.

Modifying Gauss' Law for electricity gives Poisson's equation (see Appendix D), equation (18), which is the relationship between the potential and the concentration of the charged species j in the membrane,

$$\frac{\partial^2 \Phi(x,t)}{\partial x^2} = \frac{-F}{\varepsilon}\sum_j z_j C_j(x,t) \tag{18}$$

where $\varepsilon = \varepsilon_o \varepsilon_r$ and is the relative permittivity. ε_o is the vacuum permittivity and ε_r is the dielectric constant, which is 20 for Nafion [23]. For the system of interest, equation (18) becomes

$$\frac{\partial^2 \Phi(x,t)}{\partial x^2} = \frac{-F}{\varepsilon}C(x,t). \tag{19}$$

Thus, equations (15) and (19) are used to define the proton movement over the Nafion membrane.

Because the magnitudes of the coefficients D and $\frac{F}{\varepsilon}$ differ substantially (the necessity of both terms is discussed in section 2.4), the nonlinear partial differential equations are stiff. For the steady state model used in the simulation program, equation (14) with constant J replaces the time dependant equation 15.

2.4 The Need for Diffusion and Migration in the System Model

Consider equations (19) and (15), that include both diffusion and migration terms. The term is $D \approx 10^{-7}$ whereas the term is $\frac{F}{\varepsilon} \approx 10^{16}$. The twenty-three orders of magnitude difference between terms might suggest that the diffusion term does not contribute appreciably to the overall transport of proton through the Nafion membrane. However, both diffusion and migration play important roles in proton transport and both must be included in an accurate simulation.

2.4.1 Diffusion Only

If only diffusion occurs within the membrane, $\Phi(x,t) = 0$ from equation (15). Strictly diffusion is established experimentally by significantly larger concentration of electrolyte then electroactive species. The electrolyte is electrochemically inert, such as a salt. The electrolyte dissociates into stable positive and negative ions that counters any charge build up in the system due to the electroactive species. Equation (15) then becomes

$$\frac{\partial C}{\partial t} = D\frac{\partial^2 C}{\partial x^2}. \tag{20}$$

At steady state, equation (20) becomes

$$0 = D\frac{\partial^2 C}{\partial x^2}. \tag{21}$$

This has a known steady state solution of $C(x) = ax + b$, where a and b are constants dependent on

boundary conditions and x independent. If the boundary conditions are a fixed concentration C^* at the anode and no overall charge accumulation $\left(\int_0^l C(x) = 0\right)$, the solution for the diffusion-only case is $C(x) = -2C^*x/l + C^*$. Because Nafion is the electrolyte for the system and its anions are immobile, there would be a charge build up over the fuel cell almost everywhere, unless $C^* = 0$. If $C^* = 0$, then the concentration gradient over the membrane would be identically zero. Because there would be no concentration gradient within the system, no diffusion could occur and the system could not run. Therefore, a diffusion-only process does not give a realistic solution for this system. Thus, migration plays a key role in the movement of protons as expected.

2.4.2 Migration Only

From equation (19)

$$\frac{\partial^2 \Phi(x,t)}{\partial x^2} = \frac{-F}{\varepsilon} C(x,t). \tag{22}$$

Integration gives

$$\frac{\partial \Phi(x,t)}{\partial x} = \frac{-F}{\varepsilon} \int_0^x C(s,t)ds + A \tag{23}$$

where A is a constant. Substitute equation (23) into equation (15) gives

$$\frac{\partial C(x,t)}{\partial t} = D\frac{\partial^2 C(x,t)}{\partial x^2} - \frac{zF^2D}{RT\varepsilon}\left((C(x,t)+N)\left[\int_0^x C(s,t)ds + A\right]\right)_x \tag{24}$$

The coefficients of equation (24), $zF^2D(\epsilon RT)^{-1}$ is about 16 orders of magnitude larger than D. The standard way to treat an equation of this type is to assume that the diffusion term, $D\frac{\partial^2 C}{\partial x^2}$, does not contribute significantly to the movement of protons and the migration term dominates mass transport. Thus the only significant portion of equation (24) is

$$\frac{\partial C(x,t)}{\partial t} = -\frac{zF^2D}{RT\varepsilon}\left((C(x,t)+N)\left[\int_0^x C(s,t)ds + A\right]\right)_x, \tag{25}$$

which at steady state becomes

$$\frac{\partial C\left(x,t\right)}{\partial t}=0=\left(\left(C(x,t)+N\right)\left[\int_{0}^{x}C(s,t)ds+A\right]\right)_{x}=\left(\left(C(x)+N\right)\left[\int_{0}^{x}C(s)ds+A\right]\right)_{x} \quad (26)$$

as the equation is no longer time dependant. Let $y(x)=\int_0^x C(s)ds+A$ and $\frac{dy(x)}{dx}=C(x)$ gives $0=\left(\left(\frac{dy(x)}{dx}+N\right)y\left(x\right)\right)_x$ or $\alpha=\left(\frac{dy(x)}{dx}+N\right)y\left(x\right)$. Solving this ODE gives

$$x+\beta=\frac{-1}{N^2}\left(\alpha-Ny-\alpha\ln\left|\alpha-Ny\right|\right) \quad (27)$$

As the system must satisfy the global electroneutrality condition, $y\left(l\right)=A$. In addition, $y\left(0\right)=A$. When these conditions are applied to equation 27, the result is $0=l$. A membrane in a fuel cell must have a length greater than zero. Therefore, diffusion and migration both must contribute to the mass transport of the system.

2.5 The General Solution with Electroneutrality

Local electroneutrality is a common assumption in electrochemical systems and allows the migration term in mass transport to be more easily handled. The local electroneutrality assumption is that there is no charge build up anywhere in the membrane, not even locally. This assumption forces equation (19) to become $\frac{\partial^2\Phi(x,t)}{\partial x^2}=0$, know as Laplace's condition. Thus, equation (24) at steady state becomes

$$0=\frac{\partial^2 C(x,t)}{\partial x^2}-\frac{zFV_o}{RTl}\frac{\partial C(x,t)}{\partial x}, \quad (28)$$

where V_o is the potential difference over the Nafion membrane of length l. Solve for $C(x,t)$ gives

$$C\left(x,t\right)=\frac{a}{r}e^{rx}+b, \quad (29)$$

where $r=\frac{zFV_o}{RTl}$, a is the concentration gradient at the anodic side of the membrane, and b dependent on the steady state assumptions. Assume no excess charge build up over the membrane

or $\int_0^l C(x,t)dx = 0$ to solve $b = a/lr^2\left(1 - e^{rl}\right)$. Thus, equation (29) becomes

$$C(x,t) = a\left(\frac{e^{rx}}{r} + \frac{1 - e^{rl}}{lr^2}\right) \tag{30}$$

where the value of a depends on, as yet, unspecified system condition. Consider concentration profiles for $V_o < 0$ and $V_o > 0$, where monotonically decreasing functions result, either of which profile seems reasonable. The problem with the electroneutrality assumption is not in the mathematics but in the chemistry because local electroneutrality is not necessarily established. Thus, Laplace's condition is replaced with Poisson's condition.

2.6 Existence of a Solution

Define $C(x)$ as the steady state, time-independent concentration of proton and $E(x)$ as the steady state, time-independent electric field $\left(E\left(x\right) = -\frac{\partial\Phi(x)}{\partial x}\right)$. Then equation (13) and equation (18) become

$$\begin{aligned} J &= -D\frac{dC(x)}{dx} + \frac{FD}{RT}C(x)E(x) \\ \frac{dE(x)}{dx} &= \frac{F}{\varepsilon}\left(C - N\right), \end{aligned} \tag{31}$$

where J is the steady state flux at the anode, N is the fixed concentration of sulfonates in the Nafion membrane, F is Faraday's constant, D is the diffusion rate of protons, T is the absolute temperature, R is the gas constant and ε is the relative permittivity constant. Solve for $\frac{dC(x)}{dx}$ and let $a = JD^{-1}$, $b = F\left(RT\right)^{-1}$ and $c = F\varepsilon^{-1}$, gives

$$\begin{aligned} \frac{dC(x)}{dx} &= -a + bC(x)E(x) \\ \frac{dE(x)}{dx} &= c\left(C - N\right). \end{aligned} \tag{32}$$

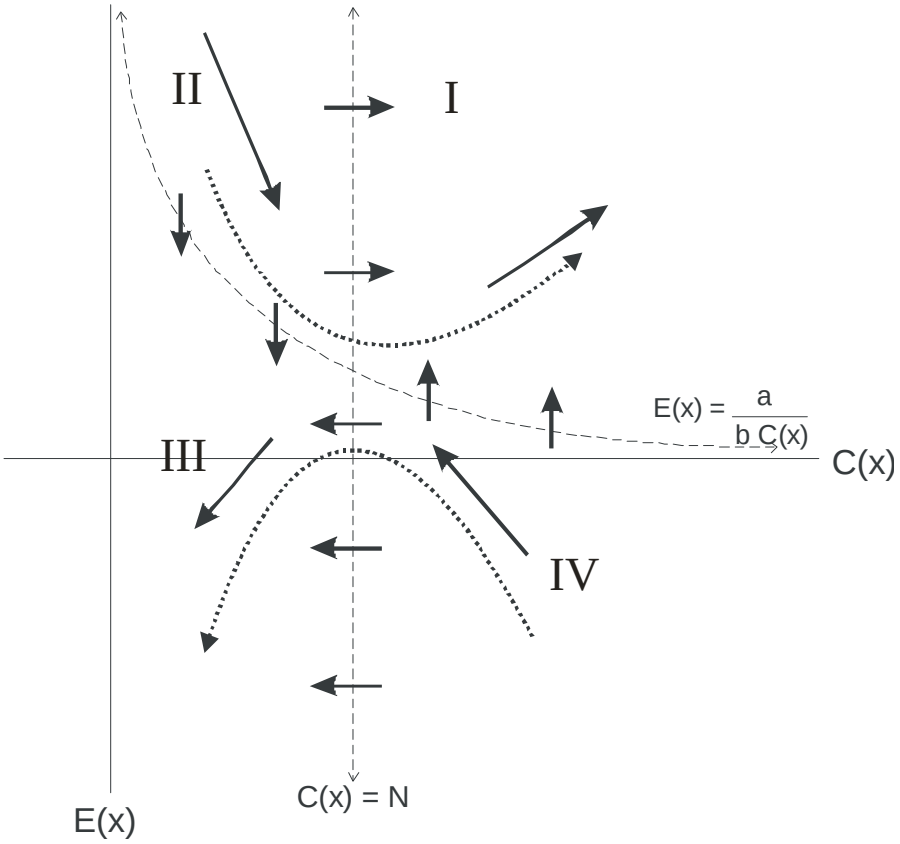

Figure 7. The phase plane diagram for the governing equations of the fuel cell system. The solid arrows are the gradients, the dashed arrows are the equilibrium lines and the dotted arrows are the trend lines. This figure is not drawn to scale.

2.6.1 The Phase Plane Diagram

A phase plane diagram is a plot of the forces applied to points on the plane as determined by the derivatives of the functions describing the system. A two dimensional phase plane would require two differential equations, $\frac{dy_1}{dx} = f_1(y_1, y_2)$ and $\frac{dy_2}{dx} = f_2(y_1, y_2)$. Arrows are drawn on the phase plane, the direction and magnitude determined by the sign and magnitude of $\frac{dy_1}{dx}$ and $\frac{dy_2}{dx}$ as determined by the value of the point on the plane the arrow is being drawn. The phase plane diagram can give insight into how the solution is behaving, for example, if there are any stable equilibrium points or regions that don't make physical sense for a solution to exist.

Figure (7) shows the phase plane diagram of equation set (32) with concentration on the

horizontal axis and electric field strength on the vertical axis. Only $C(x) \geq 0$ were considered, as a negative concentration of proton is not possible. The two dashed lines are equilibrium curves dividing the diagram into four regions. The first equilibrium occurs when $\frac{dE(x)}{dx} = 0$ or $C(x) = N$ whereas the second occurs when $\frac{dC(x)}{dx} = 0$ or $E(x) = a(bC(x))^{-1}$. The intersection of the equilibrium curves gives a single equilibrium point at $\left(N, \frac{a}{bN}\right)$. The solid arrows in the diagram indicate the gradient direction. The length of the arrows does not indicate the gradient magnitude in figure 7. Dotted trend lines where drawn within figure 7 to show flow within each region. In regions I and II, the trend line shows $C(x)$ moves from low concentration to high concentration and goes to an infinite concentration. This behavior for $C(x)$ is not physically real, so an electric field strength greater than $a(bC(x))^{-1}$ is unrealistic. In regions III and IV, the trend line shows $C(x)$ moves from high concentration to low concentration. This behavior is physically realistic and which gives the result of $E(x) \leq a(bC(x))^{-1}$. As shown in the next section, $E(x) \leq a(bC(x))^{-1}$ forces $C(x)$ to be a decreasing or constant function that allows proof of the existence of a solutions for equations (32).

2.6.2 $C(x)$ is a Decreasing Function

From the figure 7, $E(x) \leq a(bC(x))^{-1}$. Applied to $\frac{dC(x)}{dx}$ in equations (32) gives $\frac{dC(x)}{dx} \leq -a + bC(x)\, a(bC(x))^{-1} = 0$. Thus, $\frac{dC(x)}{dx} \leq 0$, and the concentration of protons will never increase over the Nafion membrane.

2.6.3 Existence

It is assumed that $C(x)$ is a continuous function. This is reasonable because the Nafion membrane within the system is uniform.

2.6.3.1 The Trivial Case

If $C(x) = N$ for $x \in [0, l]$ then $\frac{dC(x)}{dx} = 0$ and equations (32) reduce to

$$\begin{aligned} 0 &= -a + bNE(x) \\ \frac{dE(x)}{dx} &= 0. \end{aligned} \tag{33}$$

Thus, $E(x) = \frac{a}{bN}$, which is an unstable equilibrium point.

2.6.3.2 The Non-Trivial Case

$C(x)$ is a decreasing function or $C(x) = N$. Assume that $C(x)$ is not flat everywhere ($C(x) :\neq N$), then $C(x)$ must satisfy a charge neutrality restriction of $\int_0^l (C(x) - N)\, dx = 0$. Thus, there exists region over $[0, l]$ where $C(x) > N$ and a region with $C(x) < N$. Therefore, there exists one interval, $[x_i, x_f] \subset (0, l)$, where $C(x_o) = N$ for $x_o \in [x_i, x_f]$ with $C(x) \geq N$ for $x \in [0, x_i)$ and $C(x) \leq N$ for $x \in (x_f, l]$. It is possible for $x_i = x_f$ making $[x_i, x_f]$ a point. Therefore, there is at least one fixed point within the membrane. In addition to the charge restriction, there is a potential drop over the Nafion membrane of V_o. This means there is a constant V_o such that $V_o = \Phi(l) - \Phi(0) = \int_0^l \frac{d\Phi(x)}{dx} dx$ or $-V_o = \int_0^l E(x)\, dx$. It is easy to see that there is a continuous function which "over-shoots" this potential drop restriction and satisfies the charge neutrality condition, for example $C(x) = -k\left(x - \frac{l}{2}\right) + N$ where k is sufficiently large. Thus, there is a continuous function, $C(x)$, bounded above and below by two other continuous, bounded functions, the trivial solution and the "over-shooting" function. Therefore, there exists a continuous, bounded, decreasing, non-constant function, $C(x)$, on $[0, l]$ solving equations (32).

2.7 The General Equations for the Fuel Cell System without Electroneutrality

Equation (15) provides the transport equation with a condition on $\Phi_{xx}(C(x))$ seen in equation

(19). Instead of considering derivatives of the potential $\Phi(C(x))$, $\Phi(C(x))$ is replaced with a relationship to the electric field $E(C(x))$, where $E(C(x)) = -\frac{\partial \Phi(C(x))}{\partial x}$. This transforms equation (13) to

$$J = -D\frac{\partial C(x)}{\partial x} + \frac{FD}{RT}C(x)E(C(x)) \tag{34}$$

where J is the steady-state, time independent flux and equation (19) to

$$\frac{\partial E(C(x))}{\partial x} = \frac{F}{\varepsilon}(C(x) - N) \tag{35}$$

where $C(x)$ is the actual concentration of proton at steady state.

Equations (34) and (35) appear to have no simulation concerns at first. After investigation of the equations behavior, one will quickly determine that this system is harder to solve than it appears. Standard methods used in ([4, 12–19])

Let $C(x) = N(1 + \tilde{C}(x))$. Then, the above become

$$\begin{aligned} J &= -DN\frac{\partial \tilde{C}(x)}{\partial x} + \frac{FDN}{RT}\left(\tilde{C}(x) + 1\right)E(\tilde{C}(x)), \\ \frac{\partial E(\tilde{C}(x))}{\partial x} &= \frac{FN}{\varepsilon}\tilde{C}(x). \end{aligned} \tag{36}$$

Let $x = l\tilde{x}$ results in

$$\begin{aligned} J &= -\frac{DN}{l}\frac{\tilde{C}(\tilde{x})}{\partial \tilde{x}} + \frac{FDN}{RT}(\tilde{C}(\tilde{x}) + 1)E(\tilde{C}(\tilde{x})), \\ \frac{\partial E\left(\tilde{C}(\tilde{x})\right)}{\partial \tilde{x}} &= \frac{FNl}{\varepsilon}\tilde{C}(\tilde{x}). \end{aligned} \tag{37}$$

Set $\tilde{E}(\tilde{C}(\tilde{x})) = 10^{-3}E\left(\tilde{C}(\tilde{x})\right)$ allows for rearrangement to

$$\begin{aligned} 10^{-3}\frac{\partial \tilde{C}(\tilde{x})}{\partial \tilde{x}} &= -10^{-3}\frac{lJ}{DN} + \frac{Fl}{RT}(\tilde{C}(\tilde{x}) + 1)\tilde{E}\left(\tilde{C}(\tilde{x})\right), \\ \frac{\partial \tilde{E}\left(\tilde{C}(\tilde{x})\right)}{\partial \tilde{x}} &= 10^{-3}\frac{FNl}{\varepsilon}\tilde{C}(\tilde{x}). \end{aligned} \tag{38}$$

This substitution was done because it was thought that the electric field values, $E\left(\tilde{C}(\tilde{x})\right)$, might

be too large and case problems within the simulation, so $E\left(\tilde{C}\left(\tilde{x}\right)\right)$ was multiplied by 10^{-3} to make the simulation values more easily handled. The equations (38) can then be simplified to

$$\begin{aligned} \delta\frac{\partial\tilde{C}\left(\tilde{x}\right)}{\partial\tilde{x}} &= \alpha+\beta\left(\tilde{C}\left(\tilde{x}\right)+1\right)\tilde{E}\left(\tilde{C}\left(\tilde{x}\right)\right), \\ \frac{\partial\tilde{E}\left(\tilde{C}\left(\tilde{x}\right)\right)}{\partial\tilde{x}} &= \gamma\tilde{C}\left(\tilde{x}\right) \end{aligned} \tag{39}$$

where $\alpha=-10^{-3}\frac{lJ}{DN}$, $\beta=\frac{Fl}{RT}$, $\gamma=10^{-3}\frac{FNl}{\varepsilon}$ and $\delta=10^{-3}$. One (trivial) equilibrium state is $\tilde{C}\left(\tilde{x}\right):=0$ and $\frac{\partial\tilde{C}(\tilde{x})}{\partial\tilde{x}}=0$, which gives $\alpha+\beta\tilde{E}\left(\tilde{C}\left(\tilde{x}\right)\right)=0$ or $\tilde{E}\left(\tilde{C}\left(\tilde{x}\right)\right):=-\frac{\alpha}{\beta}$. Define $\hat{E}\left(\tilde{C}\left(\tilde{x}\right)\right)=\tilde{E}\left(\tilde{C}\left(\tilde{x}\right)\right)-E_e$ where $E_e=\frac{\alpha}{\beta}$. Then

$$\begin{aligned} \delta\frac{\partial\tilde{C}\left(\tilde{x}\right)}{\partial\tilde{x}} &= \alpha+\beta(\tilde{C}\left(\tilde{x}\right)+1)(\hat{E}\left(\tilde{C}\left(\tilde{x}\right)\right)+E_e) \\ &= \alpha+\beta E_e+\beta E_e\tilde{C}\left(\tilde{x}\right)+\beta\left(\tilde{C}\left(\tilde{x}\right)+1\right)\tilde{E}\left(\tilde{C}\left(\tilde{x}\right)\right) \\ &= \alpha+\beta\left(\frac{-\alpha}{\beta}\right)+\beta\left(\frac{-\alpha}{\beta}\right)\tilde{C}\left(\tilde{x}\right)+\beta\left(\tilde{C}\left(\tilde{x}\right)+1\right)\tilde{E}\left(\tilde{C}\left(\tilde{x}\right)\right) \\ &= -\alpha\tilde{C}\left(\tilde{x}\right)+\beta(\tilde{C}\left(\tilde{x}\right)+1)\tilde{E}\left(\tilde{C}\left(\tilde{x}\right)\right), \\ \frac{\partial\hat{E}\left(\tilde{C}\left(\tilde{x}\right)\right)}{\partial\tilde{x}} &= \gamma\tilde{C}\left(\tilde{x}\right), \\ \hat{E}\left(\tilde{C}\left(\tilde{x}\right)\right) &= \tilde{E}\left(\tilde{C}\left(\tilde{x}\right)\right)-E_e. \end{aligned} \tag{40}$$

Finally, let $a=\frac{\alpha}{\delta}$, $b=\frac{\beta}{\delta}$, $c=\gamma$ and write each equation as a function of $\tilde{C}$ and $\hat{E}$ gives

$$\begin{aligned} \frac{\partial\tilde{C}\left(\tilde{x}\right)}{\partial\tilde{x}} &= -a\tilde{C}\left(\tilde{x}\right)+b\hat{E}\left(\tilde{C}\left(\tilde{x}\right)\right)+b\tilde{C}\hat{E}\left(\tilde{C}\left(\tilde{x}\right)\right), \\ \frac{\partial\hat{E}\left(\tilde{C}\left(\tilde{x}\right)\right)}{\partial\tilde{x}} &= c\tilde{C}\left(\tilde{x}\right), \\ \tilde{E}\left(\tilde{C}\left(\tilde{x}\right)\right) &= \hat{E}\left(\tilde{C}\left(\tilde{x}\right)\right)+E_e. \end{aligned} \tag{41}$$

Equations (41) are the form the equations in the simulation program in Appendix B.

One equilibrium state occurs when $\tilde{C}\left(\tilde{x}\right)=0$. Deviating too far from $\tilde{C}\left(\tilde{x}\right)=0$ results in an explosion in the migration term. This indicates an instability in the middle of the film. Therefore, any sizable deviation from $\tilde{C}\left(\tilde{x}\right)=0$ would have to take place within a short distance

from the boundaries of the membrane for the system to remain stable. To find out how the system deviates from $\tilde{C}(\tilde{x}) = 0$, it is assumed that $b\tilde{C}(\tilde{x})\hat{E}\left(\tilde{C}(\tilde{x})\right)$ is small compared to the other two terms. To assume that $b\tilde{C}(\tilde{x})\hat{E}\left(\tilde{C}(\tilde{x})\right)$ is negligible, the ratio of $b\tilde{C}(\tilde{x})\hat{E}\left(\tilde{C}(\tilde{x})\right)$ versus $-a\tilde{C}(\tilde{x}) + b\hat{E}\left(\tilde{C}(\tilde{x})\right)$ was calculated from the solution. The results show that $b\tilde{C}(\tilde{x})\hat{E}\left(\tilde{C}(\tilde{x})\right)$ is at most about 0.2% of the size of $-a\tilde{C}(\tilde{x}) + b\hat{E}\left(\tilde{C}(\tilde{x})\right)$ and that close to the equilibrium in the middle of the membrane, the only place this term was left off, percent was orders of magnitude smaller. Therefore, calculations of the eigenvalues and eigenvectors without the $b\tilde{C}(\tilde{x})\hat{E}\left(\tilde{C}(\tilde{x})\right)$ term is reasonable. The eigenvalues and eigenvectors of the matrix that results from $\frac{\partial\tilde{C}(\tilde{x})}{\partial\tilde{x}}$ and $\frac{\partial\hat{E}\left(\tilde{C}(\tilde{x})\right)}{\partial\tilde{x}}$ allow for calculation of the vectors by which the system deviates from $\tilde{C}(\tilde{x}) = 0$. This matrix is

$$\frac{d}{dx}\begin{bmatrix} \tilde{C}(\tilde{x}) \\ \hat{E}\left(\tilde{C}(\tilde{x})\right) \end{bmatrix} = \begin{bmatrix} -a & b \\ c & 0 \end{bmatrix}\begin{bmatrix} \tilde{C}(\tilde{x}) \\ \hat{E}\left(\tilde{C}(\tilde{x})\right) \end{bmatrix}. \tag{42}$$

The eigenvalues are $\lambda = \frac{-a\pm\sqrt{a^2+4cb}}{2}$ that yield eigenvectors of $\begin{bmatrix} \frac{b}{a+\lambda_1} \\ 1 \end{bmatrix}$ and $\begin{bmatrix} \frac{b}{a+\lambda_2} \\ 1 \end{bmatrix}$. For actual values of the system, $b(a+\lambda_1)^{-1}$ and $b(a+\lambda_2)^{-1}$ are about seven orders of magnitude smaller than 1. Because of the difference in magnitude of the eigenvector components, these eigenvectors display the rapid deviation from $\tilde{C}(\tilde{x}) = 0$ expected.

2.7.1 Simulation Conditions

The following conditions are used to solve equations (41).

2.7.1.1 The Potential Drop

A potential drop of V_o over the membrane gives

$$\begin{aligned} V_o &= \Phi(C(l)) - \Phi(C(0)) = \int_0^l \frac{\partial\Phi(C(x))}{\partial x}dx \\ &= \int_0^l -E(C(x))\,dx = -10^3\int_0^l \tilde{E}\left(\tilde{C}(x)\right)dx = -10^3 l\int_0^1 \tilde{E}\left(\tilde{C}(\tilde{x})\right)d\tilde{x}. \end{aligned} \tag{43}$$

Thus,

$$\begin{aligned} -\frac{V_o}{10^3 l} &= \int_0^1 \tilde{E}\left(\tilde{C}\left(\tilde{x}\right)\right) d\tilde{x} = \int_0^1 \hat{E}\left(\tilde{C}\left(\tilde{x}\right)\right) - \frac{\alpha}{\beta} d\tilde{x} \\ &= \int_0^1 \hat{E}\left(\tilde{C}\left(\tilde{x}\right)\right) d\tilde{x} - \frac{\alpha}{\beta} = \int_0^1 \hat{E}\left(\tilde{C}\left(\tilde{x}\right)\right) d\tilde{x} - \frac{a}{b}. \end{aligned} \tag{44}$$

2.7.1.2 Global Charge Neutrality

The charge accumulations over the membrane must sum to zero. This gives

$$\frac{F}{\epsilon}\int_0^l C(x)dx = -\int_0^l \frac{d^2\Phi(C\left(x\right))}{dx^2}dx = \int_0^l \frac{dE(C\left(x\right))}{dx}dx = E(C\left(l\right)) - E(C\left(0\right)) = 0 \tag{45}$$

2.7.1.3 Determination of the Flux

Apply equation (17) to the fuel cell system gives

$$i = -nFAJ \tag{46}$$

where n is the stoichiometric number of electrons in the reaction at the anode, i is the constant current, F is Faraday's constant and J is the flux of proton $\left(mols^{-1}cm^{-2}\right)$. Therefore, the flux at the anode is $J = -i\left(nFA\right)^{-1}$. From equation (1), $n = 2$. Reasonable input parameters were taken from reference [5] as follows: a fuel cell with a membrane of length $l = 175\mu m$ has a potential difference of $V_o \approx 0.59V$ at a current density of $iA^{-1} = 1$ amp cm^{-2} for an electrode with area $A = 5cm^2$.

2.7.1.4 Additional Assumptions

Because of the fixed point argument in section 2.6.3.2, there is a point or an interval in the

middle of the membrane with a fixed proton concentration of N. Thus, the assumption of $C(l/2) = N$ or $\tilde{C}(l/2) = 0$ was made. This is reasonable because of the eigenvectors of equation (42) show deviation from $\tilde{C}(x) = 0$ could not occur in the middle of the membrane and stay within the constraints of equation 2.7.1 for a membrane of sufficient length. The concentration of Nafion, N, was calculated as the available sulfonates in the membrane. Nafion has a known density of 1.74 g/cm^3 ([24], [7])and an approximate equivalent weight of 1100 g/mol .

2.8 Calculations

Matlab was used to create a program to approximate solutions to equations (41) at steady state. Use of standard time evolution simulation methods like finite difference were not practical for the simulation of this system because of the Courant-Friedrichs-Levy (CFL) condition. The CFL condition places a restriction on the length of the time step of the simulation, based upon the terms associated with $\frac{\partial C(x,t)}{\partial x}$. The condition requires that if c is the absolute value of the term associated with $\frac{\partial C(x,t)}{\partial x}$, then $c \leq \Delta x/\Delta t$. From equation 24

$$\begin{aligned} \frac{\partial C(x,t)}{\partial t} &= D\frac{\partial^2 C(x,t)}{\partial x^2} - \frac{zF^2D}{RT\varepsilon}\left((C(x,t)+N)\left[\int_0^x C(s,t)ds + A\right]\right)_x \\ &= D\frac{\partial^2 C(x,t)}{\partial x^2} - \frac{zF^2D}{RT\varepsilon}C^2(x,t) - \frac{zF^2DN}{RT\varepsilon}C(x,t) \\ &\quad -\frac{zF^2D}{RT\varepsilon}\left(\int_0^x C(s,t)ds + A\right)\frac{\partial C(x,t)}{\partial x} \end{aligned} \tag{47}$$

which gives

$$c = \frac{zF^2D}{RT\varepsilon}\left(\int_0^x C(s,t)ds + A\right) \leq \frac{\Delta x}{\Delta t} \text{ or } \Delta t \leq \frac{\Delta x}{\frac{zF^2D}{RT\varepsilon}\left(\int_0^x C(s,t)ds + A\right)} \tag{48}$$

where $C(x,t)$ is the excess proton concentration. A simulation was created with a varying time step meeting this requirement showed that the magnitude of the term in front of the $\frac{\partial C(x,t)}{\partial x}$ term requires that the time step be so short that the computer run time is too long to complete any simulation time length of interest. Because of the magnitude difference between the coefficient in

front of $\frac{\partial^2 C(x,t)}{\partial x^2}$ and $\frac{\partial C(x,t)}{\partial x}$ in equation (47), a substitution would not be effective to lengthen Δt. Thus, another method was used.

The simulation method chosen was a shooting method within Matlab to approximate the integrals of $\tilde{C}_{\tilde{x}}$, $\hat{E}_{\tilde{x}}$ and $\tilde{E}$ from equations (41), which requires initial conditions for each equation. The behavior in the middle of the membrane is believed to be known, as discussed at the end of section 2.7.1, so the initial conditions were specified at $x = l/2$. The initial condition for $\tilde{C}_{\tilde{x}}(l/2, t)$ was determined using the eigenvectors calculated in section 2.7. The initial condition for $\hat{E}_{\tilde{x}}(l/2, t) = 0$ because $\tilde{C}(l/2, t) = 0$. The initial condition for $\tilde{E}(l/2, t) = 0$ from the one known steady state of the system. The method shoots towards a solution over a length of $l/2$. If the shooting method within the simulation returned an unrealistic solution (a solution with values of infinity), a "catch" was called within the Matlab program to stop the program, recalculate a new shorter interval and rerun the program. The new interval was calculated from the original interval by reduction of the old interval by a small percentage. After the two branches of the solution were calculated and taken out of dimensionless space, portions of the solution were used to meet the boundary conditions as specified in section 2.7.1. Starting from the end of the solution branches, places where the electric field were equal were found, satisfying equation 45. Next, the potential drop at these locations was calculated. When the potential drop calculated at two pairs of endpoint values sandwiched the value V_o, a linearization was preformed. Over ten points could be used in the linearization while keeping a r^2 value (correlation coefficient) greater than 0.99 when $l = 175\ \mu m$. The number of points used in the linearization was arbitrarily chosen to be five. Linearizations of the branch ends of the electric field and potential were calculated. Call the linearizations of the electric field $E_a(x_a)$ and $E_c(x_c)$ and the potential $P_a(x_a)$ and $P_c(x_c)$, where $E_i(x_j)$ and $P_i(x_j)$ are of the form $mx_j + b$ and the subscript a denotes the linearization at the

anode and subscript c the linearization at the cathode. Using equations 45 and 43 then give

$$\begin{aligned} E_a(x_a) - E_c(x_c) &= 0 \\ P_c(x_c) - P_a(x_a) &= V_o \end{aligned}$$

Two equations and two unknowns allows the exact solution of x_a and x_c which then specifies the portion of each branch that is usable in the solution. Next, the two branches of the solution were connected by the neutral solution for the middle of the membrane, making the solution of overall length l. The program took less than 1 minute to run on a laptop with an Intel(R) Core(TM)2 CPU with a processor speed of 1.83 GHz. A copy of the program is found in Appendix B.

2.9 Results

Figure 8 is a graph of the concentration profile that satisfies equations (41) for a membrane of length $l = 175\ \mu m$. The left side of the graph, where $x = 0$, is the anodic side of the membrane and the right side of the graph, where $x = l$, is the cathodic side of the membrane.

Figure 9 is the simulation output for the electric field. The electric field becomes positive very close to the anodic interface. This means that close to the anode, the migration force is towards the anode, while the diffusion force is toward the cathode. This is consistent with the concentration profile as diffusion is an important contributor with a large concentration gradient. Over the remainder of the membrane, diffusion appears to have little to no effect until close to the cathode. There, the strong negative electric field indicates that migration moves proton toward the anode. Here again, diffusion overcomes the migratory force and moves proton to the cathode. The magnitude of the values for the electric field is very large, but according to reference [3], they are in fact, in the normal range for an electric field in this type of system.

Figure 10 is the simulated output of the potential profile for the fuel cell system.

The asymmetry of the concentration profile, electric field and the potential profile are noted but minor. The asymmetry is hypothesized to be due to the one-sided boundedness of the

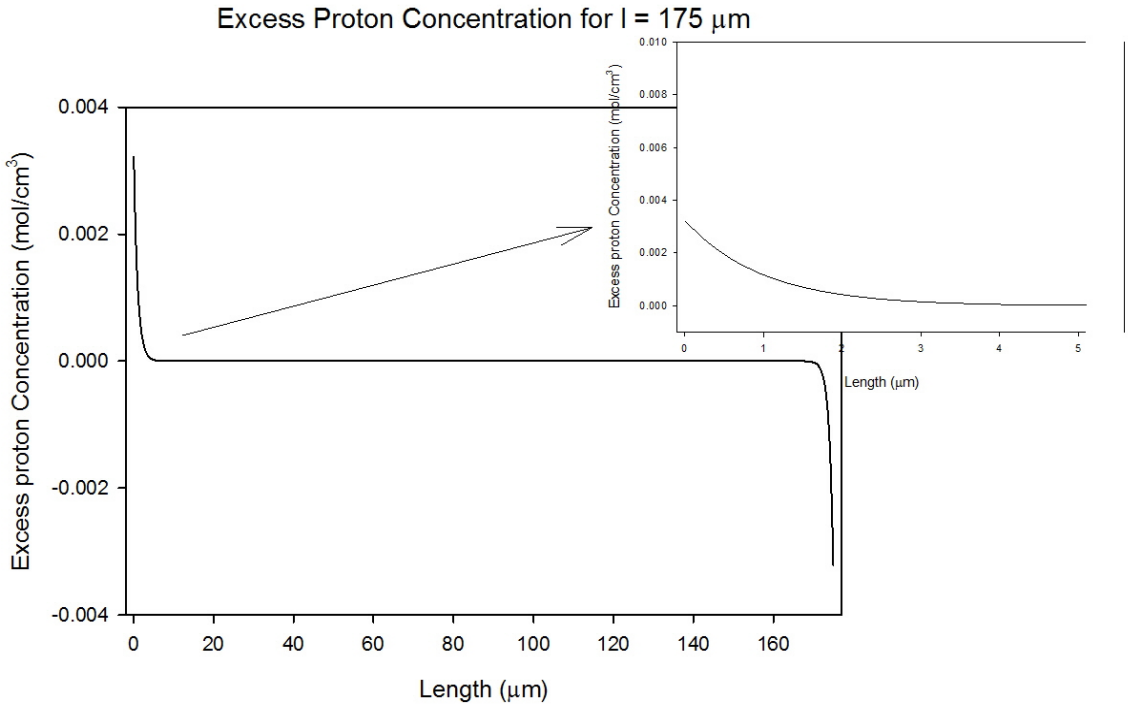

Figure 8. The simulation output of the concentration profile of a 175 μm length membrane.

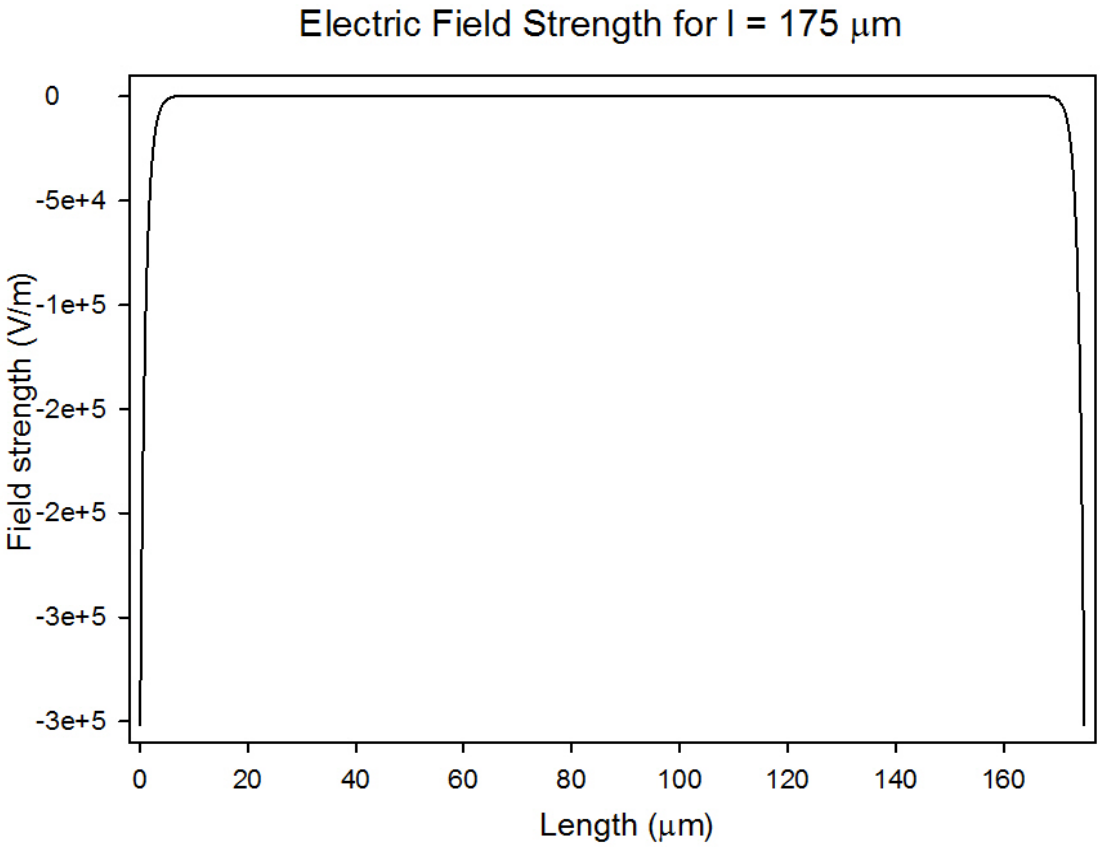

Figure 9. The simulation output of the electric field of a 175 μm length membrane.

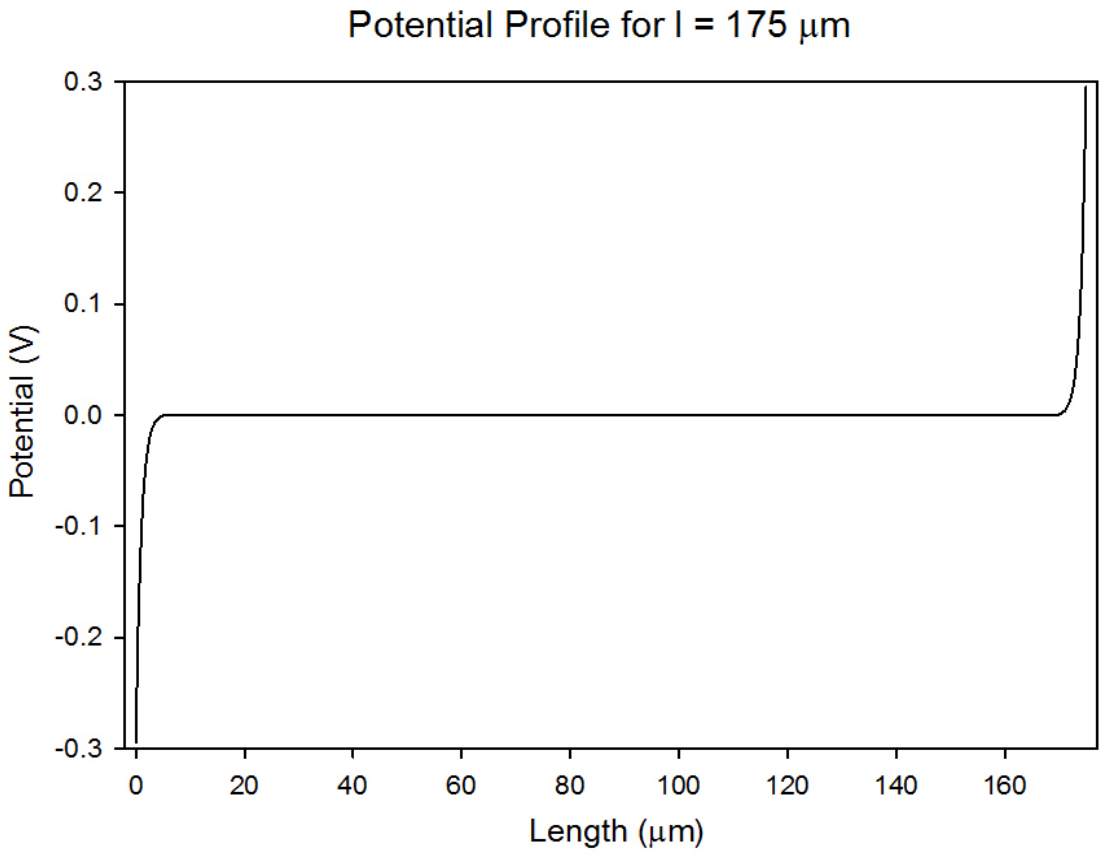

Figure 10. The simulation output of the potential profile of a 175 μm length membrane.

concentration of protons. The simulation does not allow for a negative absolute concentration of proton, but does not place a maximum concentration of proton allowed within the system. It is thought that additional membrane parameters not considered here could also yield asymmetric profiles. One such parameter is illustrated in figure 2, which speculates that Nafion aligns itself according to hydrophilic and hydrophobic portions of the molecule. Protons can only travel through the hydrophilic regions of the film. This simulation assumes a uniform film, but if figure 2 is correct, this may not be a correct assumption and could result in an upper limit on concentration of protons. Another possible reason for asymmetry is the rapid reaction as the anode releases two electrons whereas the sluggish reaction at the cathode consumes four electrons. These are both areas of future work and are not considered here explicitly.

2.9.1 Verification of the Simulation

One challenge of any simulation is verifying that the simulation program is running correctly. To verify the program used was running correctly, two checks were done. First, the number of boxes in the discretization is large enough that the simulation results don't change when a larger number of boxes is used. The second is to check that the results are correct. This is done but running the simulation for a set of equations with a known solution and getting the known solution out as a result.

The simulation results shown in section 2.10 and section 2.10.3 where created with $n = 2000$, where n is the number of boxes in the discretization. The simulation was run again with $n = 20000$, the results did not change.

To verify that the simulation results were accurate, an equation with a fixed point in the center of the interval over which the simulation was ran was needed. The equation used was

$$\bar{C}(x) = \bar{E}(x) + \bar{V}(x) = \left(x - \frac{l}{2}\right)^2 + \frac{V_o}{l}x - \frac{V_o}{2} \tag{49}$$

where

$$\bar{E}(x) = \left(x - \frac{l}{2}\right)^2 \tag{50}$$

and

$$\bar{V}(x) = \frac{V_o}{l}x - \frac{V_o}{2}. \tag{51}$$

Equation 50 has the same characteristic as $E(C(x))$ where $\bar{E}(l) - \bar{E}(0) = 0$. Equation 51 has the same characteristic as $\Phi(C(x))$ where $\bar{V}(l) - \bar{V}(0) = V_o$. In addition, $\bar{C}(x)$ has the characteristic that $\bar{C}(l/2) = 0$. The eigenvalue used in the simlation was the value that resulted from $\frac{d\bar{C}(x)}{dx}\Big|_{x=l/2}$.These equations were entered into the simulation in the form

$$\begin{aligned} dy_1 &= y_2 + y_3 \\ dy_2 &= 2 \\ dy_3 &= 0 \end{aligned}$$

where $y_1 = \bar{C}(x)$, $y_2 = \frac{d\bar{E}(x)}{dx}$ and $y_3 = \frac{d\Phi(x)}{dx}$. The resulting curves from the shooting method were as expected, generating the correct parabola for y_1 and the correct lines for y_2 and y_3.

2.10 Variation Over Length

The trends in the concentration and potential profiles are of interest in relation to the length of the membrane within the fuel cell. The following is an investigation into simulation results over various lengths.

2.10.1 Ohm's Law

The simulation looks at the steady state concentration of proton. Input parameters were taken from experimental data presented in reference [5] for specified length and current and resulting

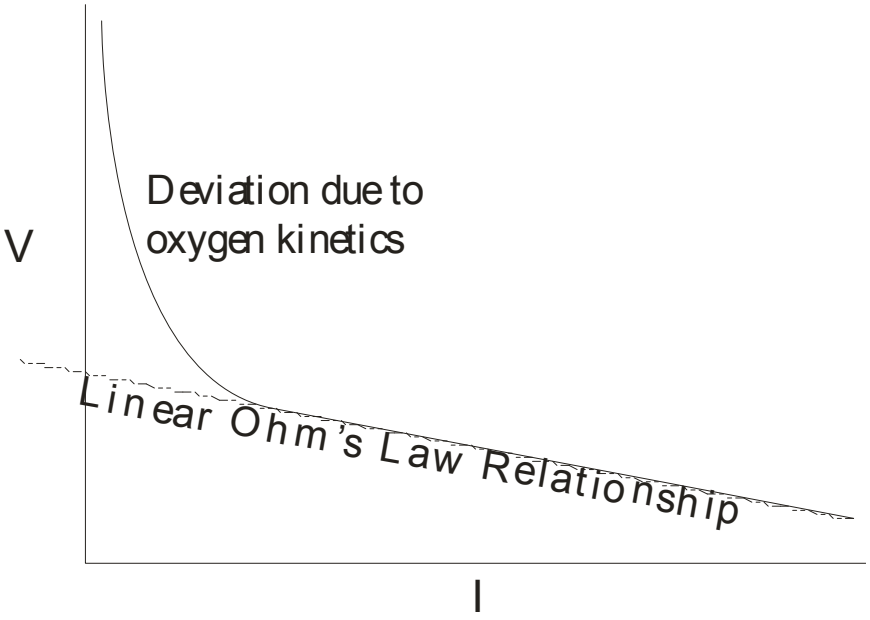

Figure 11. Ohm's Law illustration.

potential. For fixed current and potential, resistance is fixed. When membrane thickness changes, resistance over the membrane must also change. This means that either the steady state current or potential must be adjusted accordingly to allow comparison of equivalent systems. Current, potential and resistance are related by Ohm's law that states

$$V_L = IR_L, \tag{52}$$

where V_L is the potential drop over the cell (V), I is the current (amp) and R_L is the resistance (Ω). The drop, V_L, in the system is calculated as deviation from the Nernst potential ($E^o_{cell} = 1.23V$), as calculated in equation 1 minus any potential loss at the electrodes (both assumed to be zero for this simulation) and the membrane. This linear relationship between potential and current holds for high enough current and low enough potential. When current is too low or potential too high, the kinetics of one of the reactions (in this case, the oxygen kinetics at the cathode) causes the relationship to deviate from linear. Thus, if the thickness decreases by 50%, the resistance will also decrease by 50%. To keep a fixed potential, the current will have to double causing the

steady state flux at the anodic boundary to increase. The simulation assumes the system is at the mass transport limit at the anodic boundary, so to double the current will cause the anodic flux to double.

2.10.2 An Investigation into Length

A topic of interest is how the concentration profile changes when the thickness of the membrane varies. In section 2.9, concentration, electric field and potential profiles are shown for a 175 μm thick Nafion membrane. Other lengths of interest are 51 μm (approximately 2 mil) and 102 μm (approximately 4 mil), as these are commercially available thicknesses of Nafion along with 175 μm (approximately 7 mil). The simulation currently does not allow a thickness of 51 μm or less. This is likely because of the fixed point assumption and for thicknesses 51 μm and under, one cannot assume the excess proton concentration is zero in the middle of the film or the position of the zero concentration is too uncertain. It is interesting that the simulation breaks down at around the same length as membrane thickness in fuel cell. It is not clear if this is a result of the simulation method or a characteristic of the modeling equations or the constraints of the physical system. Without the fixed point assumption, there is no interval within the film where the concentration of protons and Nafion is neutral; this is why the simulation breaks down and could be the reason such thin films are not stable in fuel cells. Figures 12 through 17 show the concentration and potential profiles with varied thicknesses from 52 μm to 500 μm for fixed voltage drop and current vary as per Ohm's Law in section 2.10.1.

The shapes across the membrane for the excess proton, electric field and potential are similar. All are essentially spatially invariant across the middle of the membrane. For the excess protons, the membranes show a neutral region across the cell with steep gradients at boundaries that yield concentration polarization. That is, protons build up at the anode edge and deplete at the cathode edge, which is consistent with the membrane unable to support protons flux under the specified flux conditions. Thus, the current to sustain the potential specified for the thicker membranes

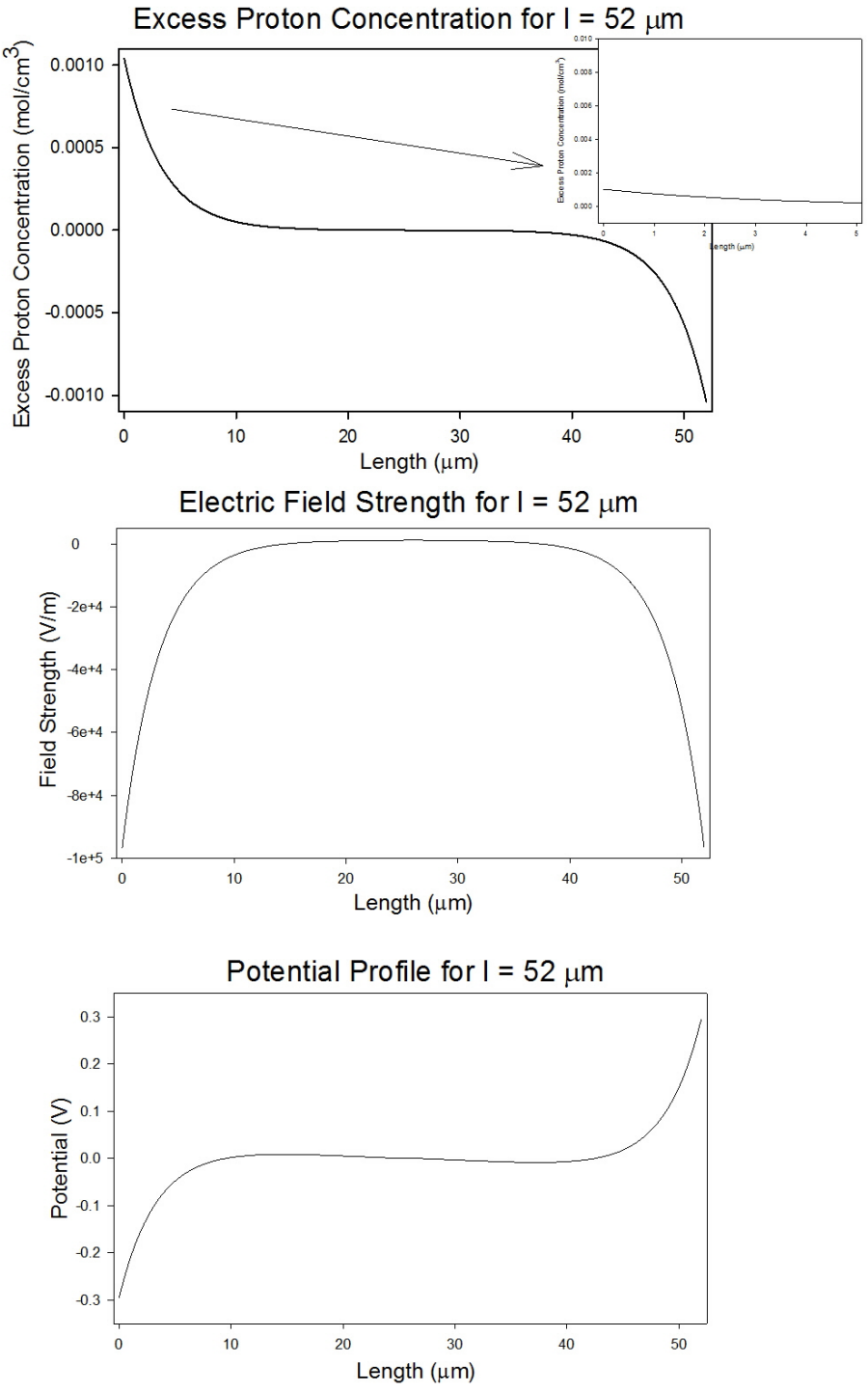

Figure 12. The simulation output of the concentration profile, electric field and potential profile for a 52 μm length membrane.

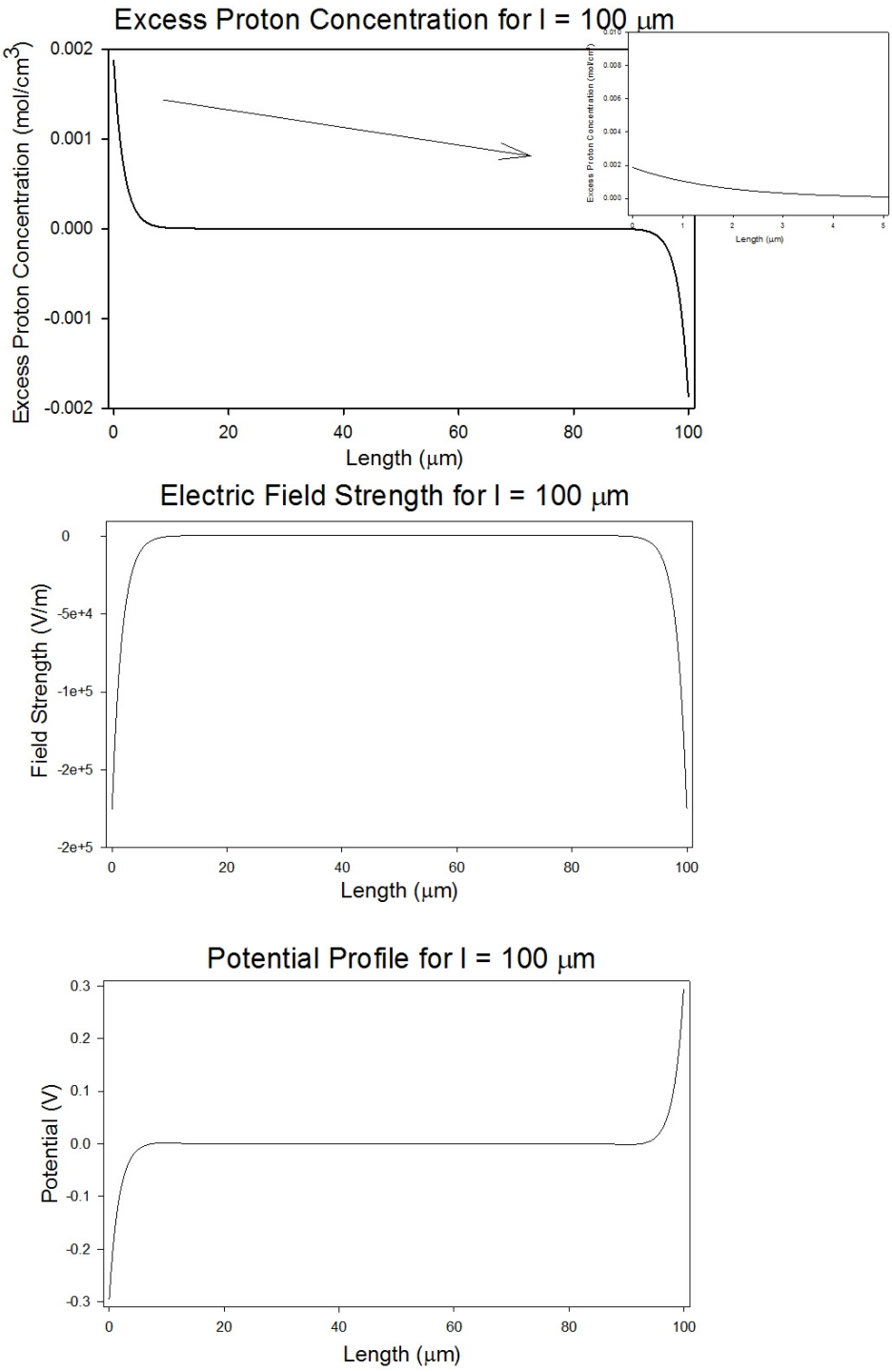

Figure 13. The simulation output of the concentration profile, electric field and potential profile for a 100 μm length membrane.

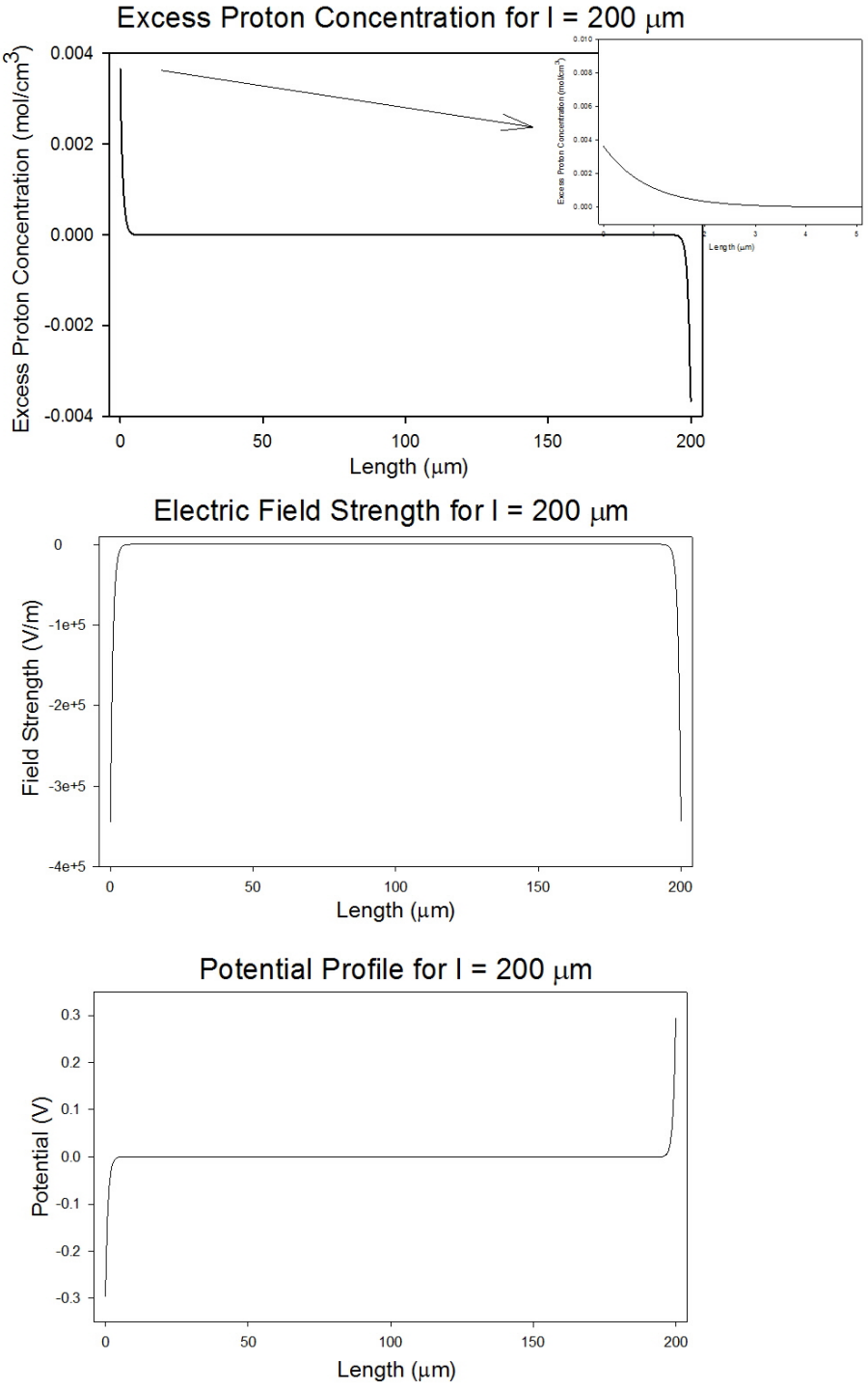

Figure 14. The simulation output of the concentration profile, electric field and potential profile for a 200 μm length membrane.

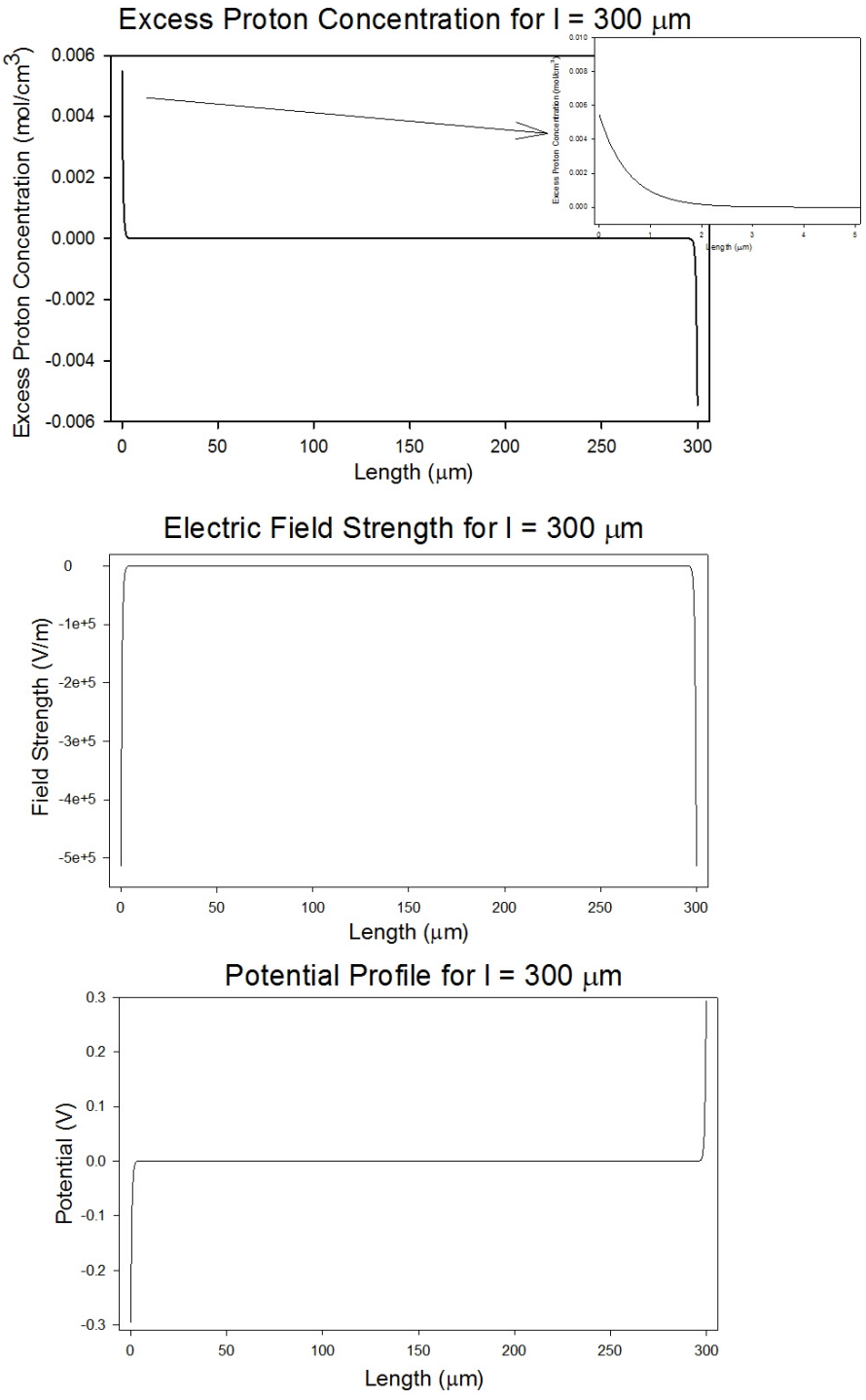

Figure 15. The simulation output of the concentration profile, electric field and potential profile for a 300 μm length membrane.

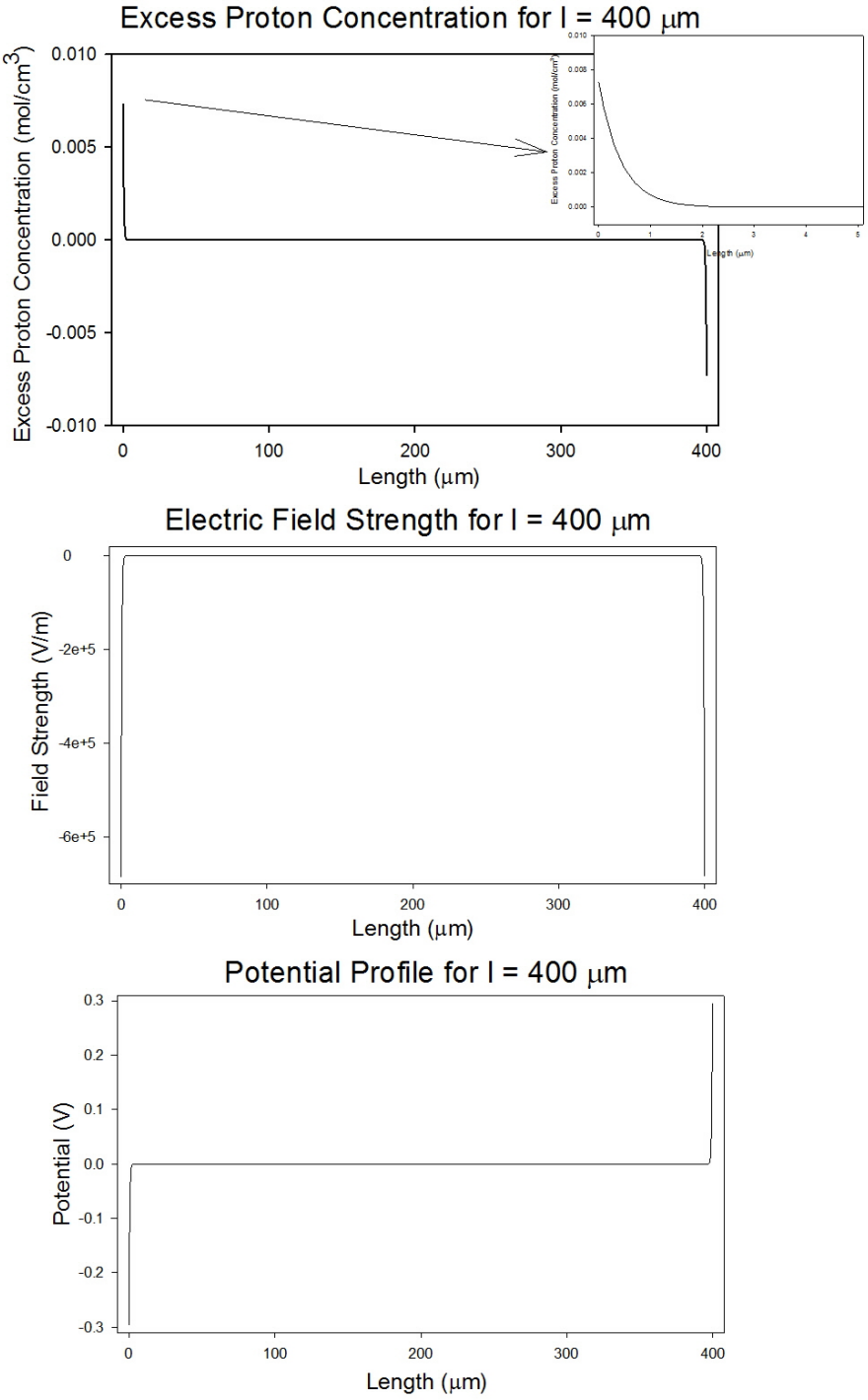

Figure 16. The simulation output of the concentration profile, electric field and potential profile for a 400 μm length membrane.

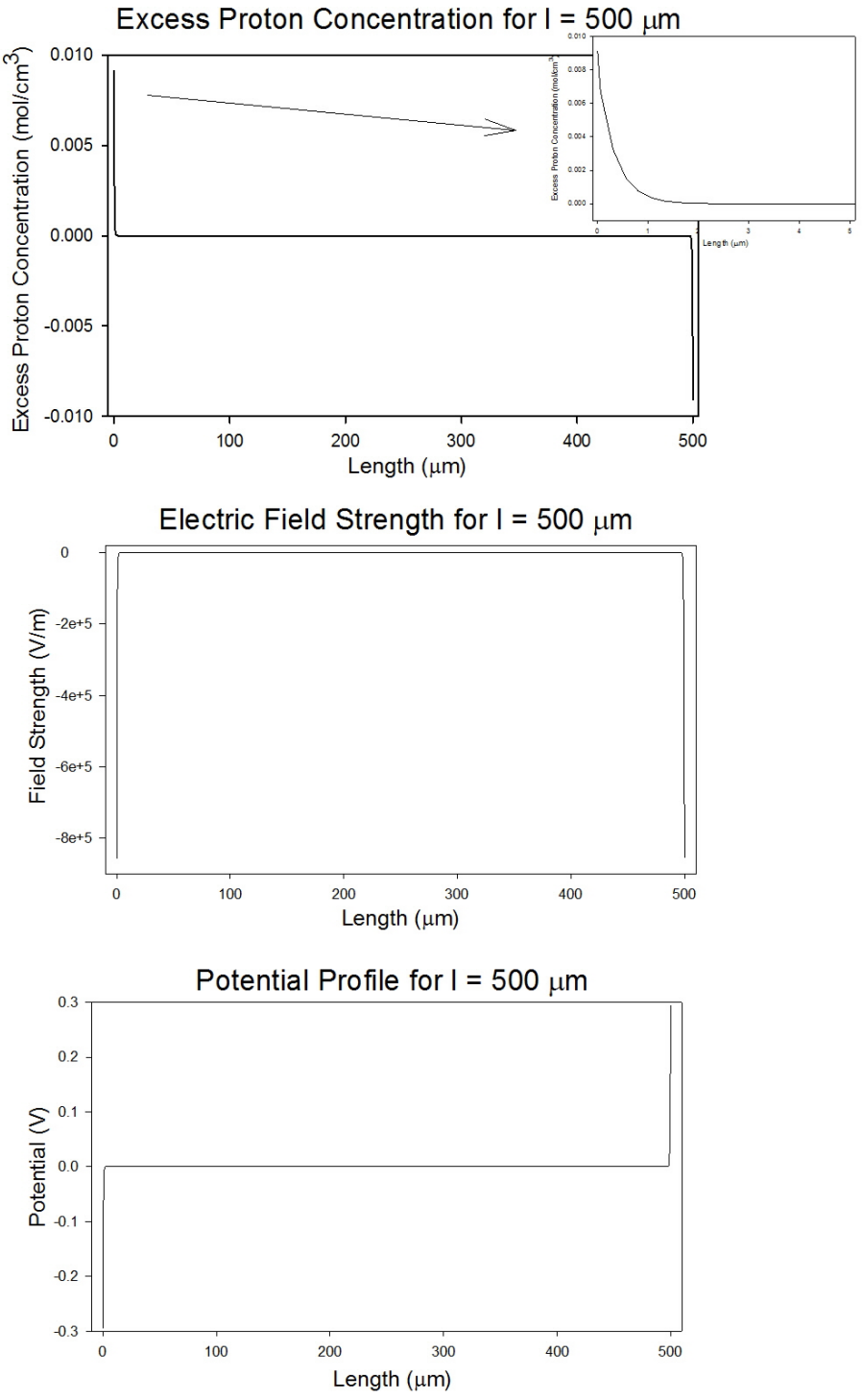

Figure 17. The simulation output of the concentration profile, electric field and potential profile for a 500 μm length membrane.

is more demanding. As the membranes become thinner, the gradients dissipate and the neutral region across the middle of the membrane reduces in length.

In summary the simulation yields stable results for physically relevant parameters. The excess proton concentration, electric field and potential plots exhibit similar characteristics as higher demands are placed on a fuel cell for a given membrane thickness. This is consistent with experimentally observed potential drops in operational fuel cells.

2.10.3 Discharge Curves for Fixed Thickness

The simulation looks at the steady state concentration of proton. Input parameters were taken from experimental data presented in reference [5] for a fixed length (175 μm) and the potentials generated at a given current demand. Reference [5] gave full current-voltage curves for laboratory fuel cells with a Nafion membrane of length 175 μm. The example curve is shown in figure 18. These curves give a current-voltage relationship outside of the linear region discussed by Ohm's Law, where nonlinearity is generated by kinetic and mass transport limitations. The next plots give concentration, electric field and potential profiles for flux-potential demands specified by the current-voltage curve in figure 18.

Several trends are shown in the profiles as current and potential vary. One trend is for small current (i) and large potential difference (V_o), the concentration profile shows a large charge separation at the boundaries and high electric field values. As the current rises and the potential lowers, the charge accumulation at the boundaries lessen and electric field values lower.

It is noted that with a large current and low potential difference, curves are not monotonic a couple microns in from the electrode boundaries. These bumps are largest and most noticeable with $i = 2.30\ A/cm^2$ and $V_o = 0.12V$ where the non-monotonic regions are about 4 microns long, starting 3 microns in from the electrodes and are about 0.0015 V high. As current goes down and potential difference rises, the bumps become smaller and shift toward the middle of the membrane, as in the $i = 1\ A/cm^2$ and $V_o = 0.59V$ where the non-monotonic region is 3 microns long, starting

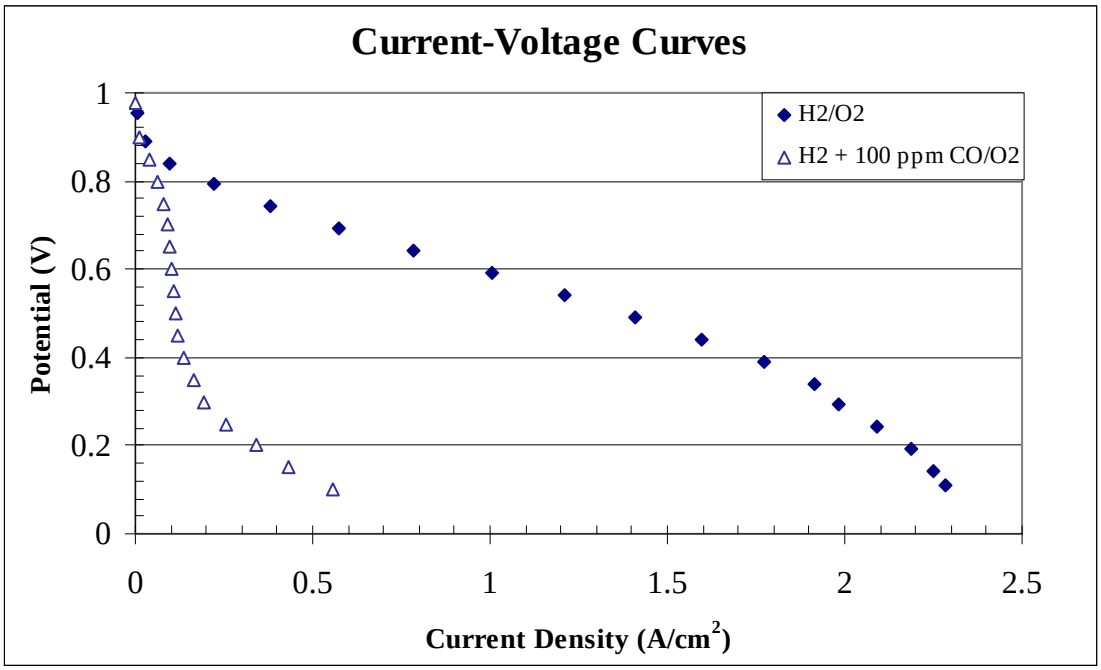

Figure 18. Discharge curve for a hydrogen oxygen fuel cell is taken from figure 62 in Wayne Gellett's thesis. The model is applied to specific current demands and voltage responses shown in this discharge curve. Model results for these points are summarized here in subsequent figures.

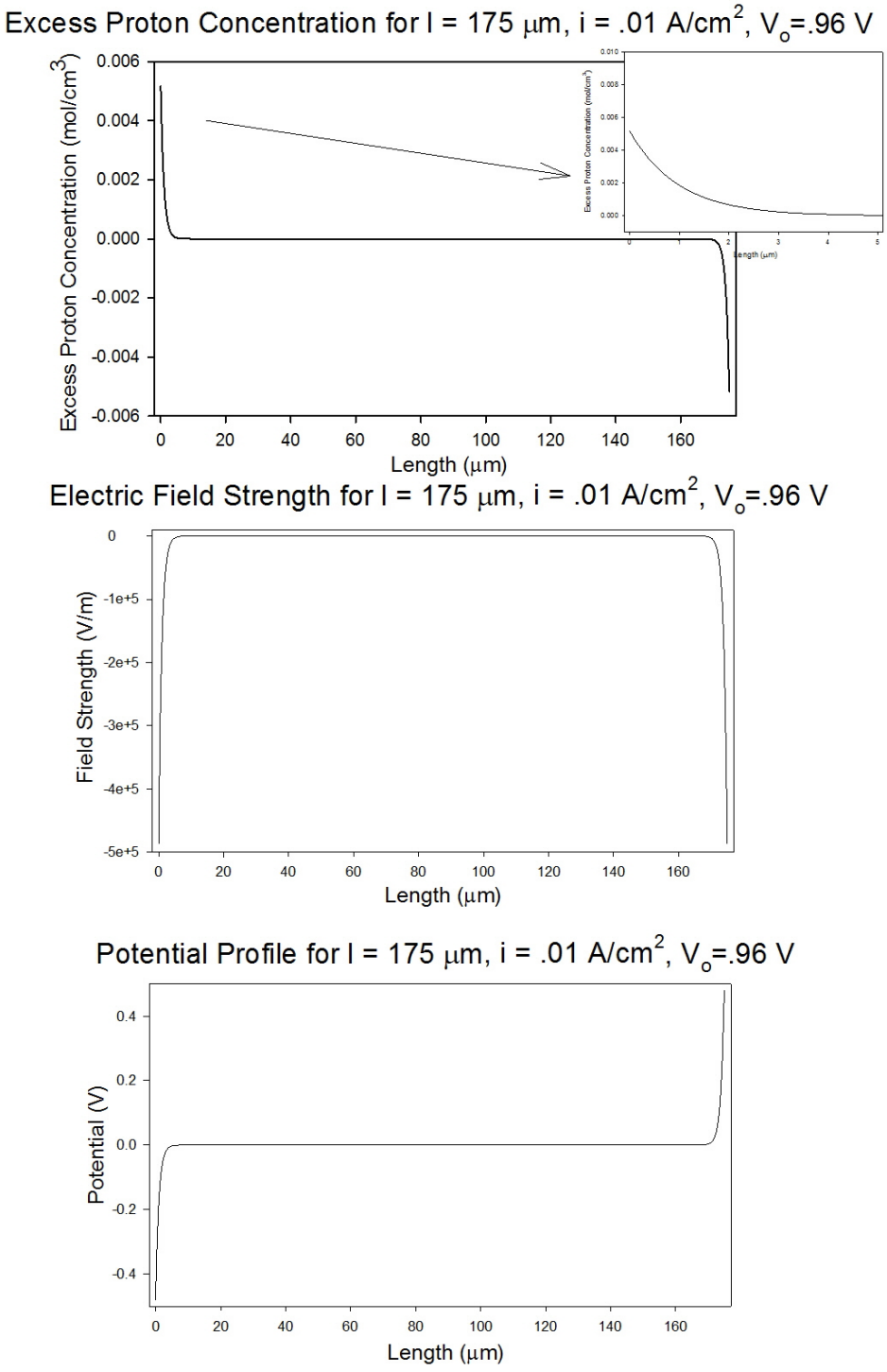

Figure 19. Excess proton concentration, electric field strength and potential profile of the Nafion membrane of a fuel cell with current 0.01 A/cm^2 and potential drop 0.96 V.

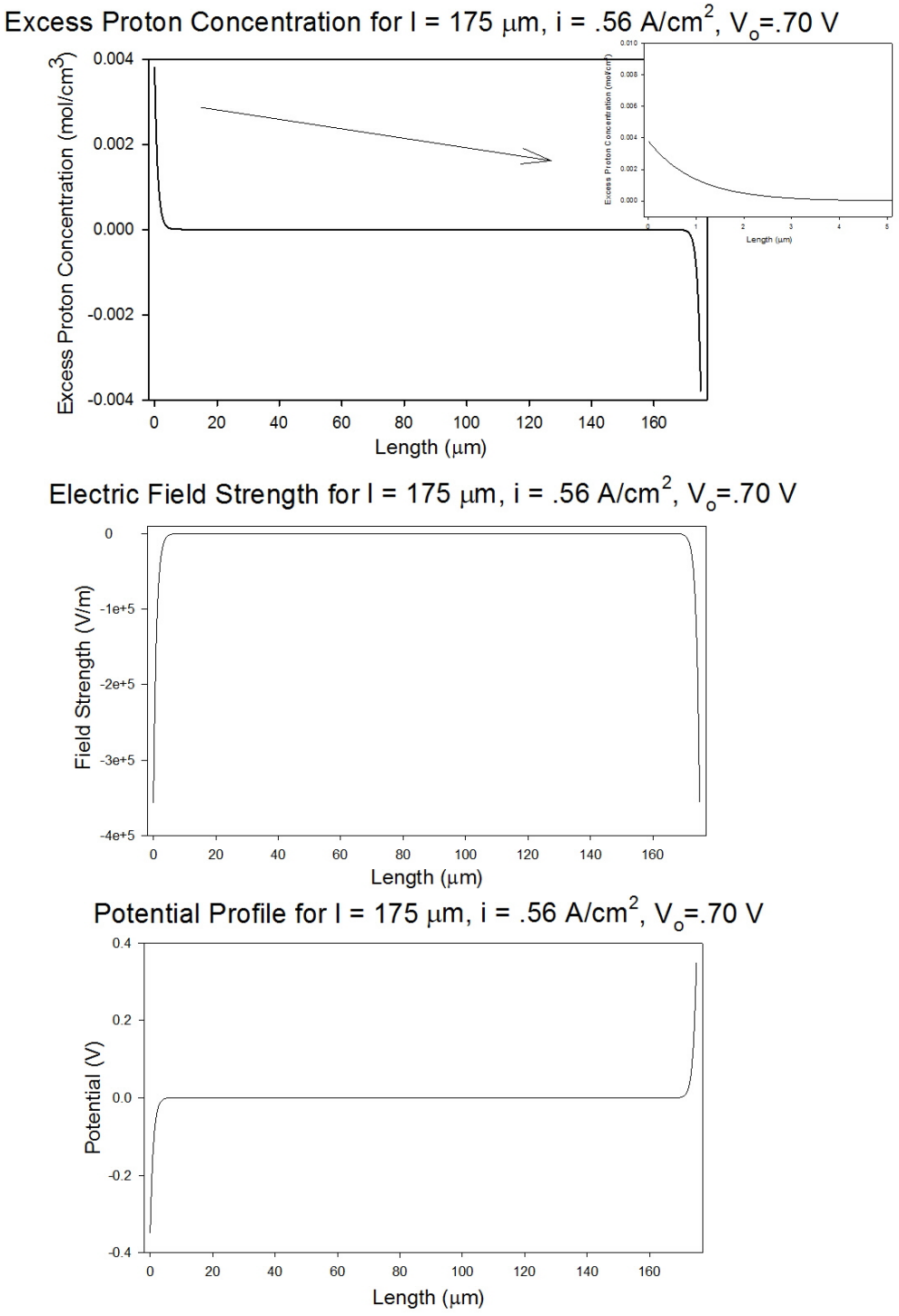

Figure 20. Excess proton concentration, electric field strength and potential profile of the Nafion membrane of a fuel cell with current 0.56 A/cm^2 and potential drop 0.70 V.

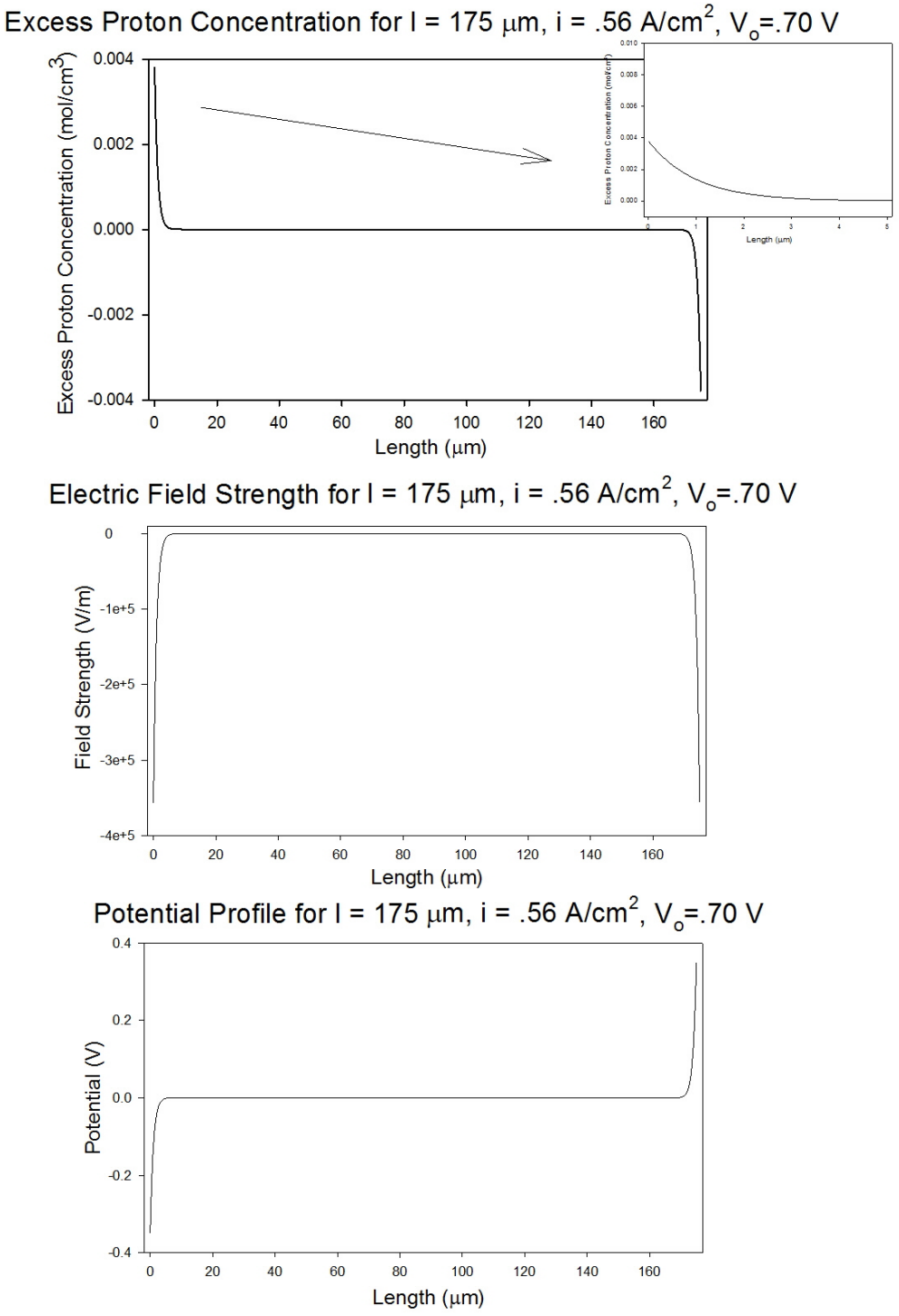

Figure 21. Excess proton concentration, electric field strength and potential profile of the Nafion membrane of a fuel cell with current 1.37 A/cm^2 and potential drop 0.44 V.

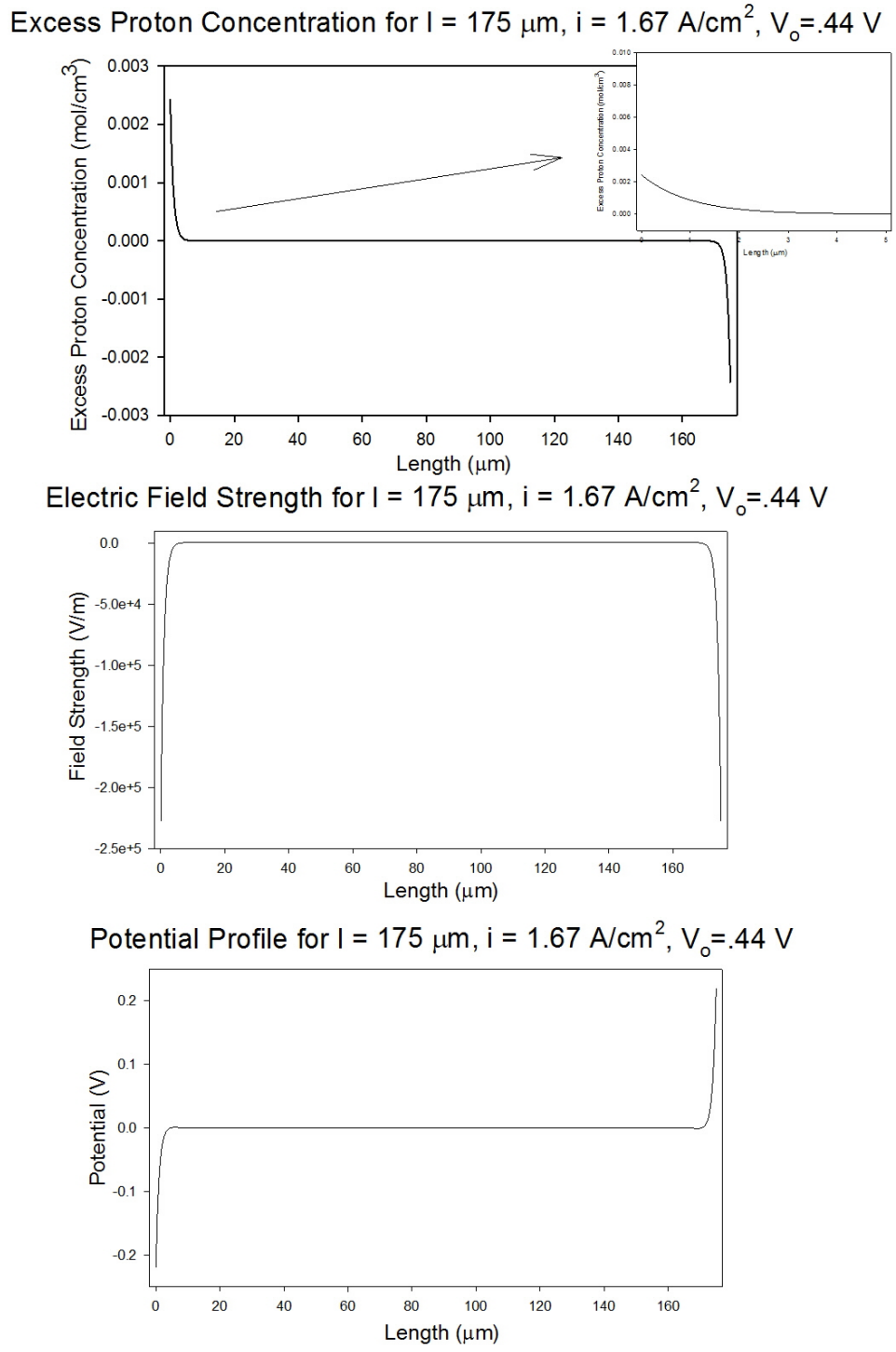

Figure 22. Excess proton concentration, electric field strength and potential profile of the Nafion membrane of a fuel cell with current 1.37 A/cm^2 and potential drop 0.44 V.

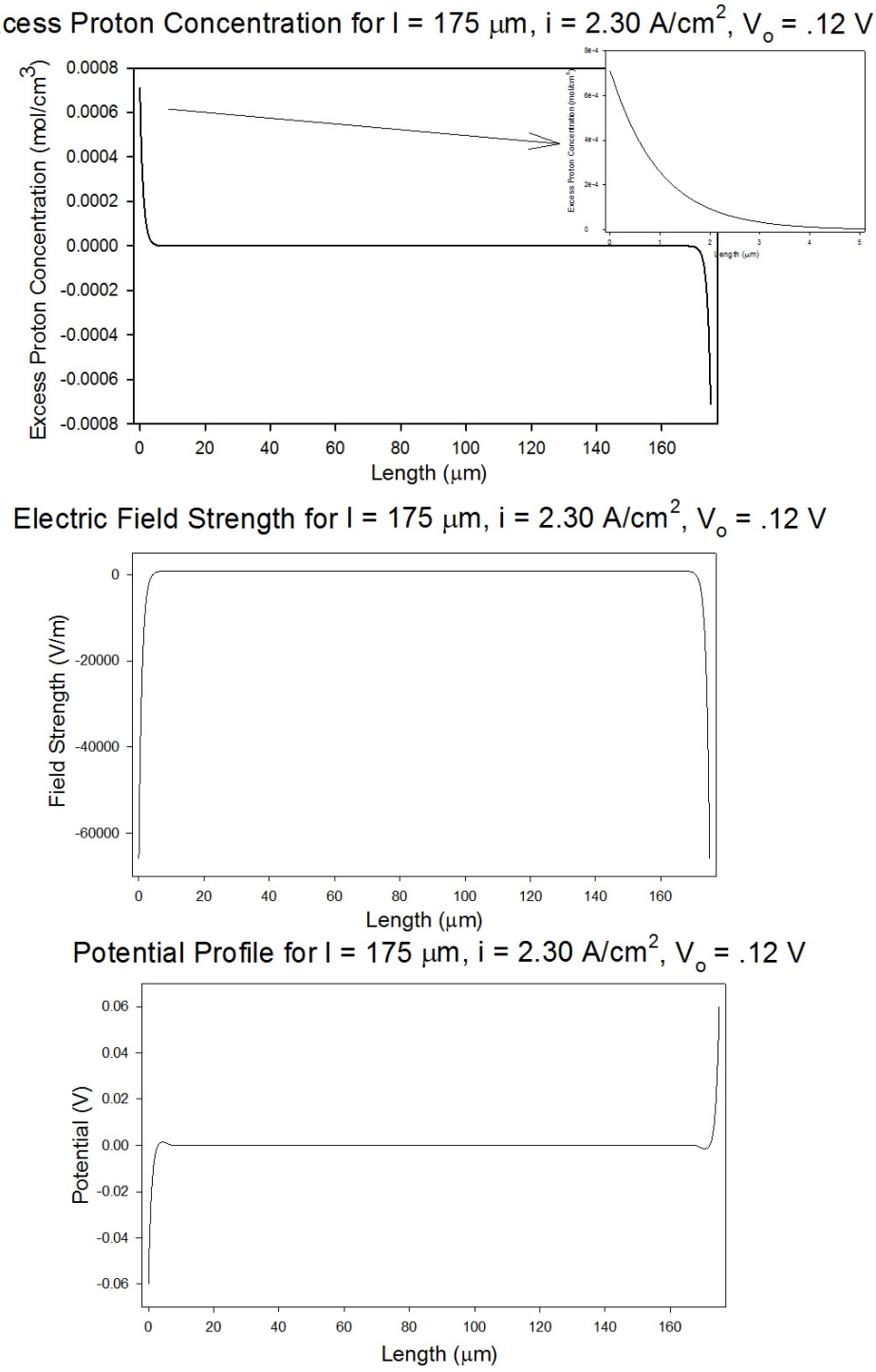

Figure 23. Excess proton concentration, electric field strength and potential profile of the Nafion membrane of a fuel cell with current 2.30 A/cm^2 and potential drop 0.12 V.

5 microns in from the electrodes and about 0.0005 V high. At the lowers current, $i = 0.01\ A/cm^2$, and largest potential difference, $V_o = 0.96V$, the bumps are undetectable. Magnified portions of the non-monotonic regions are shown in Figure 24.

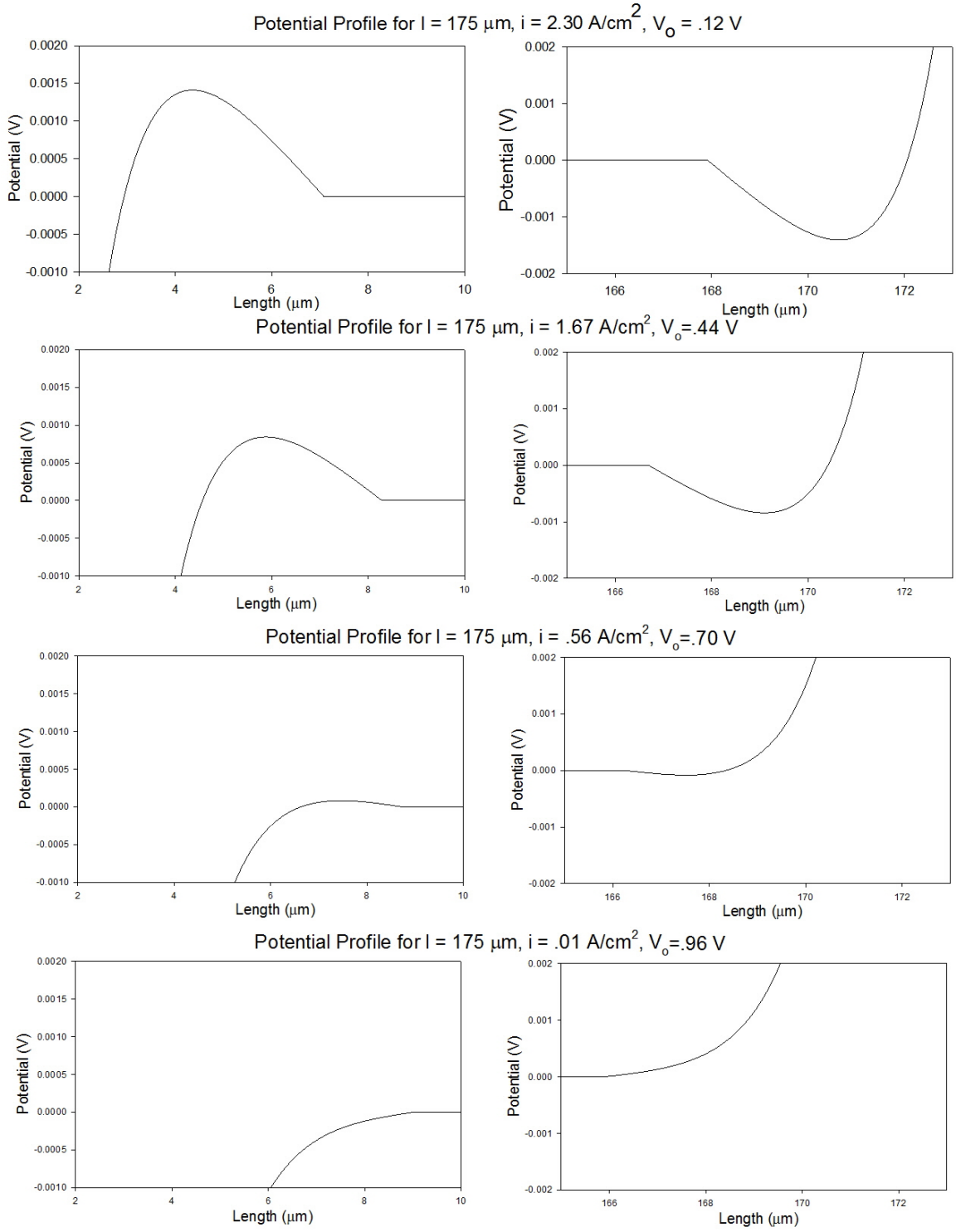

Figure 24. Magnified images of the potential profile bumps at the anode for various current and potential values.

CHAPTER 3

THE MODEL AND SIMULATION OF ELECTRON HOPPING WITHIN A PRELOADED NAFION FILM ON A MODIFIED ELECTRODE

Diffusion is usually thought of in terms of Fick's Second Law,

$$\frac{\partial C}{\partial t} = D\frac{\partial^2 C}{\partial x^2}, \tag{53}$$

where the change in the concentration of a species with respect to time equals the second derivative of concentration with respect to space multiplied by a diffusion coefficient. The diffusion coefficient takes into account how well the species moves through a system. The diffusion coefficient is usually thought of at a constant. In this chapter, a modified electrode system is investigated over which the diffusion coefficient is dependant on the concentration of the species within the system.

3.1 The Physical System

The system described in section 1.3 will be considered here. To summarize, system consists of an electrode coated with a Nafion membrane of length l, saturated with $Ru(bpy)_3^{2+}$ and placed in a bulk solution of electrolyte and $Ru(bpy)_3^{2+}$. See figure 25. The system will be at an appropriate potential such that $Ru(bpy)_3^{2+}$ oxidizes to $Ru(bpy)_3^{3+}$ when in contact with the anode, thus generating a current. The $Ru(bpy)_3^{3+}$ will diffuse out of the membrane and be replaced by $Ru(bpy)_3^{2+}$ allowing the cycle to repeat itself. The cathode for the system will be assumed far enough away that for sufficiently short periods of time, any reduction which occurs there will not affect the chemical concentrations of the system under consideration.

3.2 The Model

Experimentally, this system generates normal cyclic voltammograms. The lack of abnormal

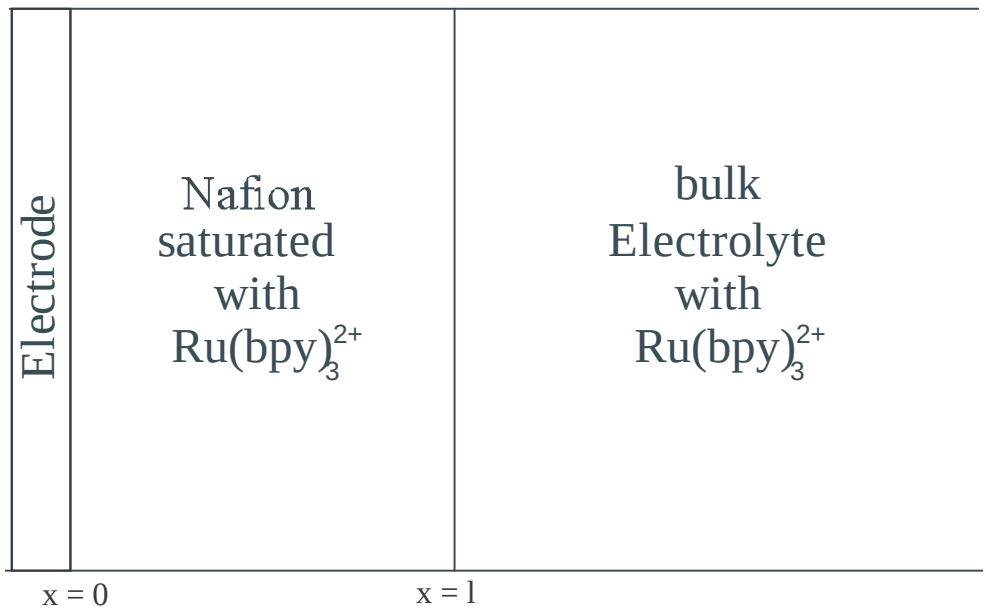

Figure 25. A schematic of the modified electrode system.

features indicates there is little to no migration present. Thus, the only portion of equation (15) needed for this model is the diffusion term,

$$\frac{\partial C}{\partial t} = \left(D \frac{\partial C}{\partial x} \right)_x . \tag{54}$$

For a constant diffusion coefficient, the resulting concentration profiles of $Ru(bpy)_3^{2+}$and $Ru(bpy)_3^{3+}$ tend toward diagonal increasing and decreasing lines, respectively, over the membrane. Voltammograms for concentration profiles like this, with a constant concentration of anion, would not look normal. Thus, the diffusion term can not be constant, but rather a function. It is believed that an electron hopping term is needed in the diffusion function. Therefore the transport equation becomes

$$\frac{\partial C}{\partial t} = \left(D\left(C\right) \frac{\partial C}{\partial x} \right)_x \tag{55}$$

where $D(C)$ is the diffusion function that accounts for both physical diffusion and electron hopping and is concentration dependant. Physical diffusion occurs when a molecule physically moves from one location to another, with the direction of movement against the concentration gradient of the molecule. Electron hopping occurs when two identical molecules, M and $\dot{M}$, both with charge

n, are in close proximity. Molecule M does not differ from molecule $\dot{M}$, the dot serves only for distinguishing between the two identical M molecules. Let e^- represent an electron capable of moving between the two molecules. For M to appear to have switched places with $\dot{M}$ only requires an electron to hop from one molecule to the other, while the rest of the molecule does not move.

$$M^{n-1} + \dot{M}^n = Me^{n-1} + \dot{M}^n \leftrightarrows M^n + \dot{M}e^{n-1} = M^n + \dot{M}^{n-1} \tag{56}$$

This idea is discussed multiple papers ([9], [21], [22]) where a mathematical model, taking into account electron hopping is presented. The theory is that the diffusion term is made up of the physical diffusion constant along with an electron hopping equation which is:

$$\begin{aligned} D_{\dot{M}e^-}(C) &= D_{phy,\ \dot{M}e^-} + \frac{k_{11}\delta^2\pi}{4}\left(C_M - C_{\dot{M}e^-}\frac{\frac{\partial C_M}{\partial x}}{\frac{\partial C_{\dot{M}e^-}}{\partial x}}\right) \\ D_M(C) &= D_{phy,\ M} + \frac{k_{11}\delta^2\pi}{4}\left(C_{\dot{M}e^-} - C_M\frac{\frac{\partial C_{\dot{M}e^-}}{\partial x}}{\frac{\partial C_M}{\partial x}}\right) \end{aligned} \tag{57}$$

where D_{phy} is the diffusion constant $\left(cm^2/s\right)$, k_{11} is the reaction rate $\left(\approx 10^8 mol\,(cm\ s)^{-1}\right)$ and δ is the distance between the center of the two molecules $\left(13.6\ \mathring{A}\right)$. Subscript $\dot{M}e^-$ denotes the concentration and diffusion terms for the molecule to be oxidized ($Ru(bpy)_3^{2+}$), and subscript M denotes the concentration and diffusion terms of the molecule to be reduced ($Ru(bpy)_3^{3+}$). Rewrite equations (55) with equations (57) gives

$$\frac{\partial C_{Ru(bpy)_3^{2+}}}{\partial t} = \left(\begin{array}{c} D_{phy,Ru(bpy)_3^{2+}} + \\ \frac{k_{11}\delta^2\pi}{4}\left(C_{Ru(bpy)_3^{3+}}\frac{\partial C_{Ru(bpy)_3^{2+}}}{\partial x} - C_{Ru(bpy)_3^{2+}}\frac{\partial C_{Ru(bpy)_3^{3+}}}{\partial x}\right) \end{array} \right)_x \tag{58}$$

$$\frac{\partial C_{Ru(bpy)_3^{3+}}}{\partial t} = \left(\begin{array}{c} D_{phy,Ru(bpy)_3^{3+}} + \\ \frac{k_{11}\delta^2\pi}{4}\left(C_{Ru(bpy)_3^{2+}}\frac{\partial C_{Ru(bpy)_3^{3+}}}{\partial x} - C_{Ru(bpy)_3^{3+}}\frac{\partial C_{Ru(bpy)_3^{2+}}}{\partial x}\right) \end{array} \right)_x . \tag{59}$$

In this dissertation, several different electron hopping equations will be considered, in addition to the one shown above.

3.2.1 The Initial Conditions

For a membrane of length l, there is a fixed concentration of Nafion throughout the membrane and no Nafion in the bulk electrolyte solution, so

$$C^{Nafion}(x,t) = \begin{array}{ll} N^* & \text{for } 0 \le x \le l \text{ and } t \ge 0 \\ 0 & \text{for } x > l \text{ and } t \ge 0 \end{array} \tag{60}$$

where N^* is determined by the molecular weight and density of Nafion. Initially, the membrane will be saturated with $Ru(bpy)_3^{2+}$. Each $Ru(bpy)_3^{2+}$.will be bonded to two Nafion molecules,

$$C^{Ru(bpy)_3^{2+}}(x,0) = \frac{N^*}{2} \text{ for } 0 \le x \le l. \tag{61}$$

Outside the membrane, there is electrolyte with a bulk concentration, C^*, of $Ru(bpy)_3^{2+}$

$$C^{Ru(bpy)_3^{2+}}(x,0) = C^* \text{ for } x > l. \tag{62}$$

One may expect that $C^* > N/2$ to ensure the Nafion film is fully loaded. Interestingly, the film will still fully load if $C^* < N/2$ because Nafion has a very high affinity for $Ru(bpy)_3^{2+}$. In a laboratory setting, C^* is typically smaller than $N/2$. This will cause a discontinuity in the initial concentration of $Ru(bpy)_3^{2+}$ at $x = l$ (the membrane/bulk interface) and require an equilibrium condition within the simulation, this is discussed later.

Within the Nafion membrane and in the bulk solution, there is no $Ru(bpy)_3^{3+}$ present initially. $Ru(bpy)_3^{3+}$ will appear as it is generated at the anode surface. Thus,

$$C^{Ru(bpy)_3^{3+}}(x,0) = 0 \text{ for } x > 0. \tag{63}$$

At the film solution interface, the concentration of $Ru(bpy)_3^{2+}$ between the film and solution is always governed by equilibrium

$$C^{Ru(bpy)_3^{2+}}\left(l^-,t\right) = \kappa C^{Ru(bpy)_3^{2+}}\left(l^+,t\right), \tag{64}$$

where $C^{Ru(bpy)_3^{2+}}(l^-,t)$, referred to as c_{l^-} hereafter, is the concentration of $Ru(bpy)_3^{2+}$ at the film/solution interface on the film side, $C^{Ru(bpy)_3^{2+}}(l^+,t)$, referred to as c_{l^+} hereafter, is the concentration of $Ru(bpy)_3^{2+}$ at the interface on the solution side and κ is the extraction parameter.. Because of this equilibrium, the flux of $Ru(bpy)_3^{2+}$ out of the solution must equal the flux of $Ru(bpy)_3^{2+}$ into the membrane giving

$$D_f^{Ru(bpy)_3^{2+}}(C)\frac{\partial C^{Ru(bpy)_3^{2+}}(l,t)}{\partial x} = D_s^{Ru(bpy)_3^{2+}}(C)\frac{\partial C^{Ru(bpy)_3^{2+}}(l,t)}{\partial x}. \tag{65}$$

This will later dictate how the membrane/solution interface is treated within the simulation. Only $Ru(bpy)_3^{2+}$ will require special treatment at this interface as equation (64) does not make sense for any other chemical in the system because there is no $Ru(bpy)_3^{3+}$ present initially and Nafion is immobile.

This will later dictate how the membrane/solution interface is treated within the simulation. Only $Ru(bpy)_3^{2+}$ will require special treatment at this interface. As $Ru(bpy)_3^{3+}$ is not initially present and the physical diffusion rate in film is smaller than in solution, $Ru(bpy)_3^{3+}$ will not require a film/solution equilibrium equation like equation 64. An equation like (64) does not make sense for Nafion either, as it is immobile.

Semi-infinite boundary conditions are assumed. This means that when $Ru(bpy)_3^{2+}$ is depleted from the bulk electrolyte solution outside of the membrane, the system can extend in the x direction to a location where the concentration of $Ru(bpy)_3^{2+}$ reaches the initial bulk $Ru(bpy)_3^{2+}$ concentration, or

$$C^{Ru(bpy)_3^{2+}}(x,t) = C^* \text{ as } x \to \infty. \tag{66}$$

Similarly, as $Ru(bpy)_3^{3+}$ is generated and released into the bulk electrolyte solution, the solution can be extended to a length where there is no $Ru(bpy)_3^{3+}$ present, or

$$C^{Ru(bpy)_3^{3+}}(x,t) = 0 \text{ as } x \to \infty. \tag{67}$$

Within the bulk electrolyte solution, there is no appreciable electron hopping between $Ru(bpy)_3^{2+}$

and $Ru(bpy)_3^{3+}$as there are fast moving counterions present from the electrolyte in concentrations much larger than that of either analyte molecule. Therefore, only physical diffusion is present in the bulk electrolyte solution which gives

$$D^{Ru(bpy)_3^{2+}}(C) = D^{Ru(bpy)_3^{3+}}(C) = D_s \text{ for } x > l. \tag{68}$$

The physical diffusion coefficient, D_s, for $Ru(bpy)_3^{2+}$ and $Ru(bpy)_3^{3+}$ within the bulk electrolyte solution is assumed equal and to have the same value as that in pure water. This is reasonable as the $Ru(bpy)_3^{2+}$ and $Ru(bpy)_3^{3+}$ are essentially the same size and the bulk electrolyte solution is mostly water with high electrolyte.

As the potential profile, $\Phi(x,t)$, will be the primary means of determining if a solution is realistic or not, conditions for the potential must be determined. It will be assumed the membrane/solution interface potential is fixed at 0 V with no potential gradient. These assumptions are reasonable because at the interface, any $Ru(bpy)_3^{3+}$ will be replaced with $Ru(bpy)_3^{2+}$ due to the negative concentration gradient of $Ru(bpy)_3^{3+}$ and Nafion has an equal affinity for both molecules. In the bulk solution, there is a high concentration of an electrolyte, like HNO_3, thus there is a potential of 0 V in the bulk solution (for reasons stated in section 2.2). This means there will be no charge build up and no charge gradient for $x \geq l$, or

$$\Phi(l,t) = 0 \text{ for } x \geq l \text{ and } t \geq 0 \tag{69}$$

$$\left.\frac{\partial \Phi(x,t)}{\partial x}\right|_{x=l} = 0 \text{ for } x \geq l \text{ and } t \geq 0. \tag{70}$$

3.2.2 The Potential Profile

Equation (18) expresses the potential over a membrane as dependent on the charges and

concentrations of the chemicals within the membrane. For the system of interest, this becomes

$$\Phi_{xx}(x,t) = \frac{-F}{\varepsilon}\left(3C_{Ru(bpy)_3^{3+}}(x,t) + 2C_{Ru(bpy)_3^{2+}} - N^*\right), \tag{71}$$

giving

$$\Phi_x(x,t) = \int_0^x \Phi_{ss}(s,t)\,ds + A \tag{72}$$

and

$$\Phi(x,t) = \int_0^x \Phi(s,t)\,ds + B. \tag{73}$$

The condition of $\frac{\partial\Phi(x,t)}{\partial x}\Big|_{x=l} = 0$ gives $A = -\int_0^l \Phi_{ss}(s,t)\,ds$, while the condition of $\Phi(l,t) = 0$ gives $B = -\int_0^l \Phi_s(s,t)\,ds$.

3.2.3 The Calculations

Steady state was not assumed for this model and is not reasonable with semi-infinite boundary conditions. Consequently, the system will start with initial conditions and be allowed to evolve over time under a one-dimensional finite difference simulation programmed in Matlab. A copy of the program can be found in Appendix C. The run time of the simulation varies, depending on the length of time the simulation was considered over. The largest simulation time considered was $t = 500$ seconds that had a run time of under 15 minutes.

3.2.3.1 Mathematical Treatment of the Membrane/Solution Interface

As stated previously, the concentration of $Ru(bpy)_3^{2+}$ is the only species present which requires special treatment at the membrane/solution interface as equilibrium was established initially by preloading the Nafion membrane with $Ru(bpy)_3^{2+}$. The treatment of the equilibrium is similar to that done in reference [10].

Upon discretization of the system, there are $x_{\max}$ boxes in the film, each of length $\Delta x = \frac{l}{x_{\max}}$. For ease of notation, let $B = x_{\max}$. The diffusion coefficient for $Ru(bpy)_3^{2+}$ is denoted by D^{2+}. See

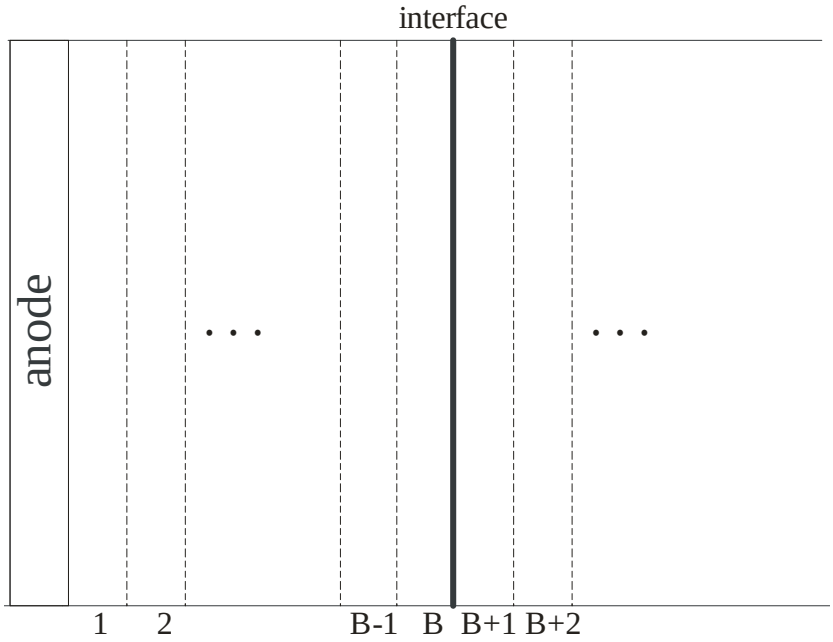

Figure 26. A schematic of the discretized modified electrode system.

figure 26. The box closest to the electrode is box 1, the box at the electrode side of the membrane solution interface is box B and the box at the solution side of the membrane solution interface is $B+1$. Concentrations are measured at the middle of each box and the distance from the middle of the box of B or $B+1$ to the membrane solution interface is $\frac{\Delta x}{2}$. Discretizing equation (65) gives

$$D^{2+}(B,t)\frac{\left(c_{l^-}-C^{2+}(B,t)\right)}{\frac{\Delta x}{2}}=D^{2+}(B+1,t)\frac{\left(C^{2+}(B+1,t)-c_{l^+}\right)}{\frac{\Delta x}{2}} \tag{74}$$

Simplify equation (74) with equations equation (64) and equation (68) gives

$$D^{2+}(B,t)\left(\kappa c_{l^+}-C^{2+}(B,t)\right)=D_s\left(C^{2+}(B+1,t)-c_{l^+}\right). \tag{75}$$

Solve equation (75) for c_{l^+} gives

$$c_{l^+}=\frac{D_sC^{2+}\left(B+1,t\right)+D^{2+}\left(B,t\right)C^{2+}\left(B,t\right)}{\kappa D^{2+}(B,t)+D_s} \tag{76}$$

with

$$c_{l^-} = \kappa c_{l^+} = \kappa \frac{D_s C^{2+}(B+1,t) + D^{2+}(B,t)\, C^{2+}(B,t)}{\kappa D^{2+}(B,t) + D_s}. \tag{77}$$

Normalize by $D^{2+}(B,t)$ and use $\gamma^2 = \frac{D_s}{D^{2+}(B,t)}$ gives

$$c_{l^+} = \frac{\gamma^2 C^{2+}(B+1,t) + C^{2+}(B,t)}{\kappa + \gamma^2} \tag{78}$$

and

$$c_{l^-} = \kappa \frac{\gamma^2 C^{2+}(B+1,t) + (B,t)\, C^{2+}(B,t)}{\kappa + \gamma^2}. \tag{79}$$

Discretizing equation (55) in time and space about spacial step B and time step n gives

$$\frac{C^{2+}(B,n+1) - C^{2+}(B,n)}{\Delta t} = \frac{\frac{D^{2+}(B,n)\left(c_{l^-} - C^{2+}(B,n)\right)}{\frac{\Delta x}{2}} - \frac{D^{2+}(B-1,n)\left(C^{2+}(B,n) - C^{2+}(B-1,n)\right)}{\Delta x}}{\Delta x} \tag{80}$$

or

$$C^{2+}(B,n+1) = C^{2+}(B,n) + \frac{\Delta t}{\Delta x^2} \begin{bmatrix} 2D^{2+}(B,n)\left(c_{l^-} - C^{2+}(B,n)\right) \\ -D^{2+}(B-1,n) C^{2+}(B,n) \\ +D^{2+}(B-1,n) C^{2+}(B-1,n) \end{bmatrix} \tag{81}$$

$$= C^{2+}(B,n) + \begin{bmatrix} 2\kappa \mathbb{D}^{2+}(B,n) \frac{\gamma^2 C^{2+}(B+1,n) + (B,n) C^{2+}(B,n)}{\kappa + \gamma^2} \\ \begin{pmatrix} \mathbb{D}^{2+}(B,n) \\ +\mathbb{D}^{2+}(B-1,n) \end{pmatrix} C^{2+}(B,n) \\ +\mathbb{D}^{2+}(B-1,n)\, C^{2+}(B-1,n) \end{bmatrix} \tag{82}$$

$$= C^{2+}(B,n) + \begin{bmatrix} \frac{2\kappa \mathbb{D}^{2+}(B,n)}{\kappa + \gamma^2} \begin{pmatrix} \gamma^2 C^{2+}(B+1,n) \\ +C^{2+}(B,n) \end{pmatrix} \\ - \begin{pmatrix} \mathbb{D}^{2+}(B,n) \\ +\mathbb{D}^{2+}(B-1,n) \end{pmatrix} C^{2+}(B,n) \\ +\mathbb{D}^{2+}(B-1,n)\, C^{2+}(B-1,n) \end{bmatrix} \tag{83}$$

where $\mathbb{D}^{2+}(j,n) = \frac{D^{2+}(j,n)\Delta t}{\Delta x^2}$. Similarly, about spacial step $B+1$

$$\frac{C^{2+}(B+1,n+1) - C^{2+}(B+1,n)}{\Delta t} = \frac{\frac{D_s\left(C^{2+}(B+2,t) - C^{2+}(B+1,n)\right)}{\Delta x} - \frac{D_s\left(C^{2+}(B+1,n) - c_{l^+}\right)}{\frac{\Delta x}{2}}}{\Delta x} \tag{84}$$

or

$$\begin{aligned} C^{2+}(B+1,n+1) &= C^{2+}(B+1,n) + \frac{\Delta t D_s}{\Delta x^2}\begin{bmatrix} C^{2+}(B+2,n) \\ -3C^{2+}(B+1,n) + 2c_{l^+} \end{bmatrix} & (85) \\ &= C^{2+}(B+1,n) + \mathbb{D}_s \begin{bmatrix} C^{2+}(B+2,n) \\ -3C^{2+}(B+1,n) \\ +2\frac{\gamma^2 C^{2+}(B+1,n) + C^{2+}(B,n)}{\kappa+\gamma^2} \end{bmatrix} & (86) \end{aligned}$$

where $\mathbb{D}_s = \frac{D_s \Delta t}{\Delta x^2}$. Equations (83) and (86) are the equations used in the modeling simulation (see Appendix C) to treat the movement of $Ru(bpy)_3^{2+}$ at the membrane solution interface equilibrium.

3.3 Possible Equations for $D(x,t)$

Equations other than equation (57) where taken into account as possible electron hopping functions and generally take the form $D_i(x,t) = D_{phy,i} + \frac{k_{11}\delta^2\pi}{4} H^i(x,t)$ where $H^i(x,t)$ is a function used to define the electron hopping phenomenon. Many of the formulas for $H^i(x,t)$ are dependant on concentrations of surrounding chemicals from a specific location $x_o \epsilon (0,l)$. Upon discretizing the system, $C^i(j,n)$ denotes the concentration of i at location x_o, $C^i(j+1,n)$ denotes the concentration of chemical i one spacial step toward the solution and $C^i(j-1,n)$ denotes the concentration of chemical i one spacial step toward the electrode. The following are the discretized versions of $H^i(x,t)$ considered:

$$\begin{aligned} H^{Ru(bpy)_3^{2+}}(j,n) &= k\begin{pmatrix} \sqrt{C^{Ru(bpy)_3^{2+}}(j+1,n) C^{Ru(bpy)_3^{3+}}(j,n)} \\ -\sqrt{C^{Ru(bpy)_3^{3+}}(j+1,n) C^{Ru(bpy)_3^{2+}}(j,n)} \end{pmatrix} & (87) \\ H^{Ru(bpy)_3^{3+}}(j,n) &= -H^{Ru(bpy)_3^{2+}}(j,n), \end{aligned}$$

where k is the mass action constant,

$$\begin{aligned} H^{Ru(bpy)_3^{2+}}(j,n) &= \sqrt{C^{Ru(bpy)_3^{2+}}(j+1,n)C^{Ru(bpy)_3^{3+}}(j,n)} \\ &\quad \pm\sqrt{C^{Ru(bpy)_3^{3+}}(j+1,n)C^{Ru(bpy)_3^{2+}}(j,n)} \\ &\quad \pm\sqrt{C^{Ru(bpy)_3^{2+}}(j,n)C^{Ru(bpy)_3^{3+}}(j-1,n)} \\ &\quad +\sqrt{C^{Ru(bpy)_3^{3+}}(j,n)C^{Ru(bpy)_3^{2+}}(j-1,n)} \\ H^{Ru(bpy)_3^{3+}}(j,n) &= \pm H^{Ru(bpy)_3^{2+}}(j,n) \end{aligned} \tag{88}$$

and

$$\begin{aligned} H^{Ru(bpy)_3^{2+}}(j,n) &= \sqrt{C^{Ru(bpy)_3^{2+}}(j+1,n)C^{Ru(bpy)_3^{3+}}(j,n)} \\ H^{Ru(bpy)_3^{3+}}(j,n) &= \sqrt{C^{Ru(bpy)_3^{2+}}(j,t)C^{Ru(bpy)_3^{3+}}(j+1,n)}. \end{aligned} \tag{89}$$

The idea for these formulas came from the ideal conditions for electron hopping. When $Ru(bpy)_3^{2+}$ and $Ru(bpy)_3^{3+}$ are in close proximity to each other, an electron may hop from $Ru(bpy)_3^{2+}$ to $Ru(bpy)_3^{3+}$, making it look as though the molecules switched places, when in fact, only an electron has moved. The likelihood of an electron to hop should then be dependant on the concentration of $Ru(bpy)_3^{2+}$ in box j and the concentration of $Ru(bpy)_3^{3+}$ in an adjacent box $j+1$ or $j-1$ and the concentration of $Ru(bpy)_3^{3+}$ in box j and the concentration of $Ru(bpy)_3^{2+}$ in box $j+1$ or $j-1$. This is illustrated in figure 27. In this figure, electrons hop both out of and into box j. In this schematic, more electrons should hop into than out of box j because the concentration of $Ru(bpy)_3^{2+}$ giving up electron is higher in box $j+1$. In addition, there is ample $Ru(bpy)_3^{3+}$ available to receive the electron on box j. As both a molecule to go from and a molecule to go to, are needed for electron hopping, the electron hopping should contain a term like $C^{Ru(bpy)_3^{2+}}(j+1,n)C^{Ru(bpy)_3^{3+}}(j,n)$. Likewise, the electrons leaving box j should be dependant on a variation of $C^{Ru(bpy)_3^{2+}}(j,n)C^{Ru(bpy)_3^{3+}}(j+1,n)$. These terms have units of mol^2/cm^6, therefore, square roots considered to get correct units of concentration.

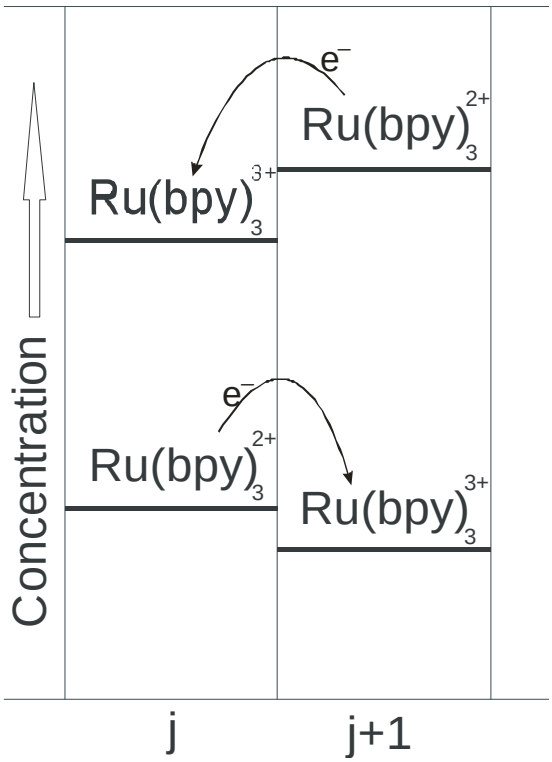

Figure 27. A schematic of a favorable proton hopping situation.

3.4 Results

All the equations considered for $D_i(C)$ yield results with unrealistic potential profiles. The following are results from using equations (57) for the electron hopping simulation run over 500 seconds. The membrane was divided into 200 boxes with the electrode at $x = 0$ and the membrane ending at $x = 200$. From figure 32, the potential profile is nonzero over a large portion of the membrane. A potential varying by more than a few millivolts will yield an abnormal looking voltammogram, thus the modeling equations considered for this system are not good representations of what is truly happens within the Nafion membrane of the modified electrode system. Concentration profiles seen in figures 28 - 31 look remarkably similar to the case where $D(C) = D_{phy}$ except ran over a longer period of time or with a larger D_{phy} value. The results for the electron hopping simulation are shown with the output from $D(C) = D_{phy}$.

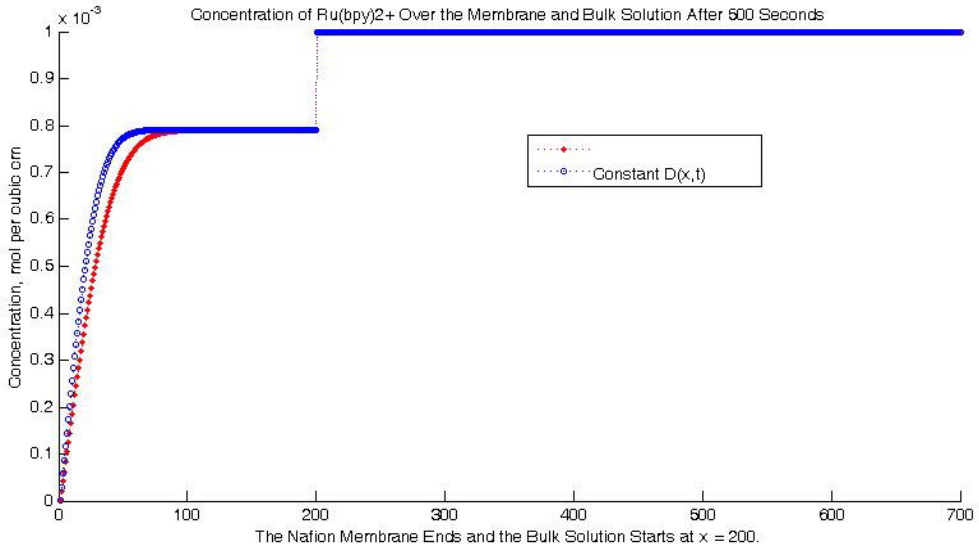

Figure 28. The concentration profile of $Ru(bpy)_3^{2+}$ over the membrane and high concentration bulk electrolyte solution for the electron hopping and constant diffusion simulations. The membrane solution interface is at x = 200.

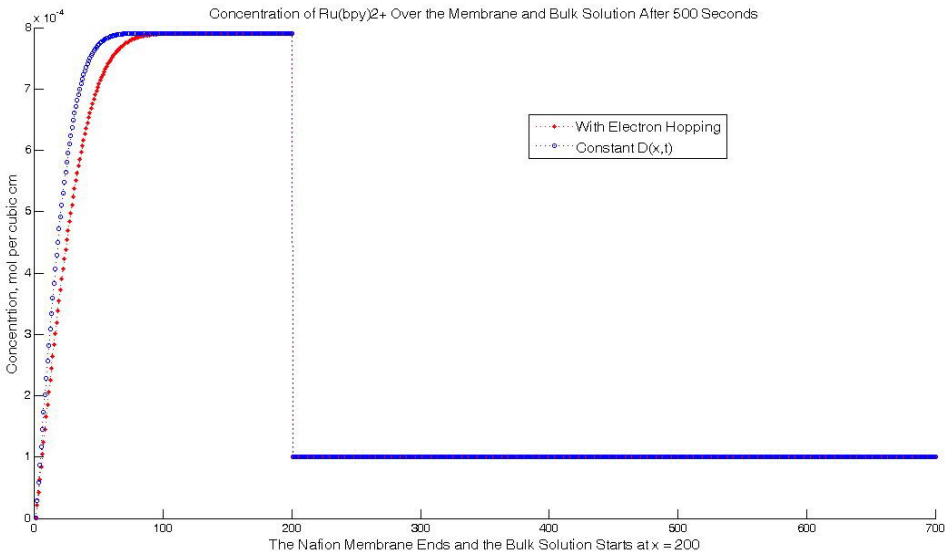

Figure 29. The concentration profile of $Ru(bpy)_3^{2+}$ over the membrane and low concentration bulk electrolyte solution for the electron hopping and constant diffusion simulations. The membrane solution interface is at x = 200.

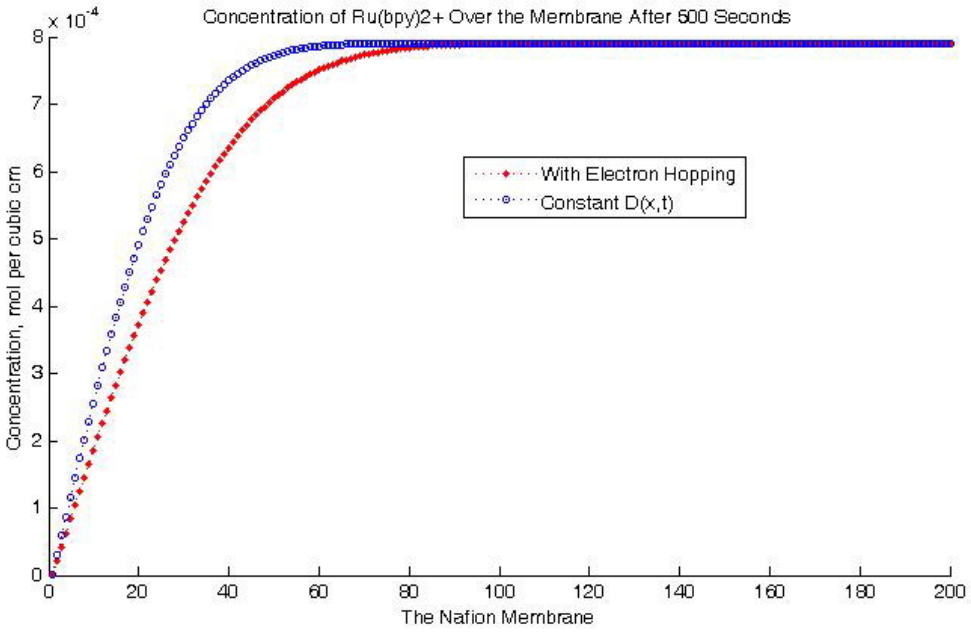

Figure 30. The concentration profile of $Ru(bpy)_3^{2+}$ over the Nafion membrane for the electron hopping and constant diffusion simulations.

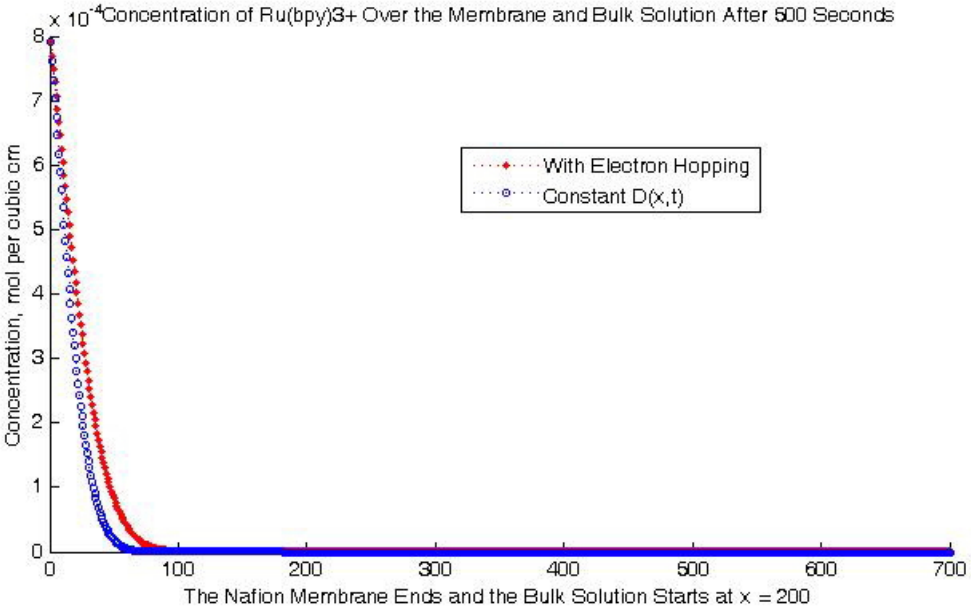

Figure 31. The concentration profile for $Ru(bpy)_3^{3+}$ over the Nafion membrane for the electron hopping and constant diffusion simulations.

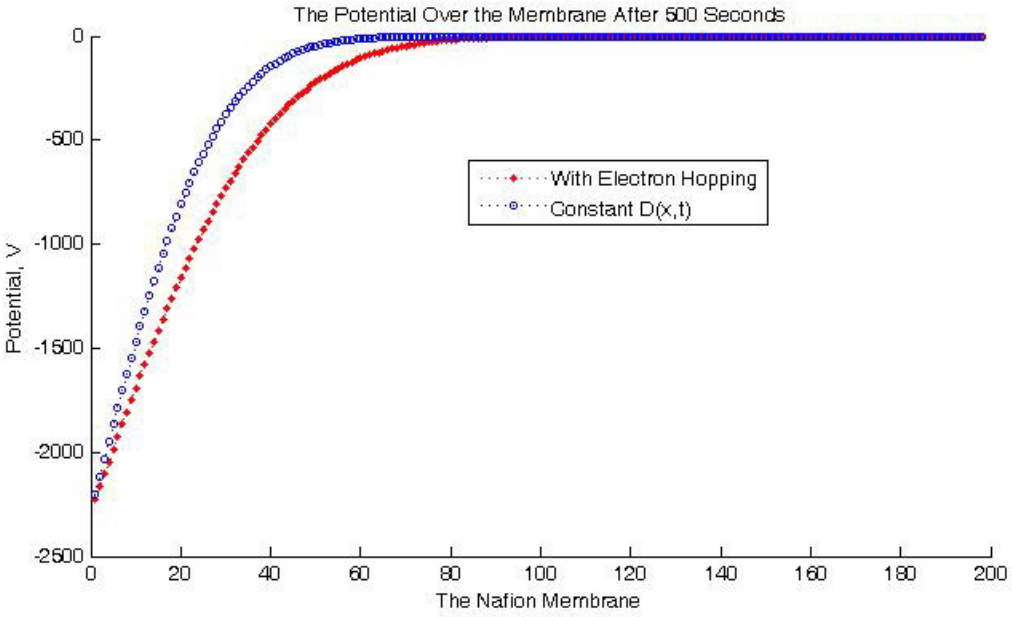

Figure 32. The potential profile over the Nafion membrane for the electron hopping and constant diffusion simulations.

CHAPTER 4

DETERMINATION THE PHYSICAL DIFFUSION RATE OF A PROBE THROUGH A MEMBRANE WITHOUT ELECTRON HOPPING

In this chapter, the simulation is presented to load a uniform film with a probe, P, under continuous cyclic voltammetry. While cyclic voltammetry sweeps run, potential versus current values are recorded on a plot, called a voltammogram. Each sweep will have a maximum current attained, shown by a peak on the voltammogram. Peak height is directly related to the concentration of the probe at the electrode surface by equation 16 for reversible electron transfer. As electron hopping requires molecules to be in close proximity to each other, low concentrations of the probe require that movement of species be dominated by physical diffusion. As the film will not be loaded initially, the time required for the peak height to grow in will correspond to the physical diffusion rate. Determining how loaded the film is will be done by comparing the peak heights from the continuous sweeps to the peak height of a fully loaded film. Thus, the physical diffusion rate can be found by monitoring the peak current as a function of the fully loaded peak height.

The model and program for this chapter are based off of the one in reference [10].

4.1 The Physical System

The system considered in this chapter will be similar to that in section 1.3. The system consists of an electrode coated with a uniform film of thickness l. Unlike section 1.3, the Nafion membrane will not be preloaded with a probe P. The modified electrode will be placed in a bulk solution of electrolyte containing a bulk concentration, C^*, of P. Over time, P will diffuse though the membrane to the electrode. At the electrode film interface, P is oxidized to P^+ at sufficient

potentials as

$$\underbrace{P^+}_{\text{oxidized form}} + e^- \rightleftharpoons \underbrace{P}_{\text{reduced form}} \quad E^{0'} = E_o \tag{90}$$

Notice that P and P^+ are the same species but differ only by one electron. While P diffuses into the membrane, cyclic voltammetry will continually monitor the concentration of P. As P reaches the electrode, current will flow if the potential is sufficiently large (close to E_o or higher). The cathode for the system will be assumed far enough away that any reduction which occurs there will not affect the chemical concentrations at the anode. As the potential goes down, any P^+ at the electrode surface will reduced back to P for potentials sufficiently small (close to E_o or lower). The physical diffusion rates for P and P^+ are taken as the same in each phase within the film and bulk solution. This assumption is reasonable as, for example, Ru(bpy)_3^{2+} does not change substantially upon oxidation to Ru(bpy)_3^{3+}. The electrode area $A\ \left(cm^2\right)$ is sufficiently large that transport is linear and the system is characterized by diffusion in one dimension, x, normal to the electrode.

4.2 The Model

In the film, $0 \leq x \leq l$, the one dimensional diffusion equation (Fick's second law) is

$$\frac{\partial C_i\left(x,t\right)}{\partial t} = D_f \frac{\partial^2 C_i\left(x,t\right)}{\partial x^2} \text{ for } 0 \leq x \leq l \tag{91}$$

where $C_i\left(x,t\right)$ is the concentration of chemical i and is dependant on the distance from the electrode, x, and time, t and diffusion coefficient D_f. For this simulation, D_f is constant.

Fick's second law applies in the solution as well, as

$$\frac{\partial C_i\left(x,t\right)}{\partial t} = D_s \frac{\partial^2 C_i\left(x,t\right)}{\partial x^2} \text{ for } x > l. \tag{92}$$

where D_s is the diffusion coefficient of chemical i in solution. As bulk solution allows for the free movement of chemical i, it contains no hopping term. As each partial differential equation is first order in time and second order in space, each phase requires one initial and two boundary

conditions for each P and P^+.

4.2.1 Initial Conditions

The initial conditions are

$$\begin{aligned} C_P(x,0) &= 0 \text{ for } 0 \leq x \leq l, \\ C_P(x,0) &= \frac{C^*}{\kappa} \text{ for } x > l, \\ \text{and } C_{P^+}(x,0) &= 0 \text{ for } 0 \leq x, \end{aligned} \tag{93}$$

where κ is the extraction parameter for the concentration of the probe in the film relative to the solution and C^* is a value which makes C^*/κ equal to the initial concentration of P in the bulk electrolyte.

4.2.2 Boundary Conditions

The solution is of sufficient extent that on the time scale of the experiment, the concentration is not depleted from the bulk at distances far from the electrode giving

$$\lim_{x\to\infty} C_P(x,t) = \frac{C^*}{\kappa}, \tag{94}$$

$$\lim_{x\to\infty} C_{P^+}(x,t) = 0. \tag{95}$$

At the film solution interface, the concentration established between the film and solution is always governed by the equilibrium

$$C_P\left(l^-,t\right) = \kappa C_P\left(l^+,t\right), \tag{96}$$

where $C_P(l^-,t)$ is the concentration of P adjacent to the film solution interface on the film side and $C_P(l^+,t)$ is the concentration of P adjacent to the interface on the solution side. The parameter κ is determined by the relationship between C^* and the concentration of P in a fully saturated membrane. For this model, there is no equilibrium condition for P^+ as diffusion across

the membrane can only occur in one direction because there is no P^+ present initially in solution and $D_f < D_s$ for both P and P^+.

4.2.3 The Equations

The current $i(t)$ is related to the flux of P to the electrode surface as

$$\frac{i(t)}{nFA} = D_f \frac{\partial C_P(0,t)}{\partial x}. \tag{97}$$

The forward (k_f) and backwards (k_b) electron transfer rates are dependant on the potential (E) and are given by

$$\begin{aligned} k_f(E) &= k^0 \exp\left[-\frac{\alpha nF}{RT}\left(E(t) - E^{o'}\right)\right] \text{ and} \\ k_b(E) &= k^0 \exp\left[\frac{(1-\alpha)nF}{RT}\left(E(t) - E^{o'}\right)\right], \end{aligned} \tag{98}$$

where k^0 is the standard heterogeneous rate constant for electron transfer at the electrode surface and α is the transfer coefficient. The parameter α characterizes the symmetry of the energy barrier for the electron transfer. For this simulation, the energy barrier is assumed symmetric, so $\alpha = .5$. Equations (98) are related to the current by

$$\frac{i(t)}{nFA} = k_f(E) C_{P^+}(0,t) - k_b C_P(0,t). \tag{99}$$

Dimensionless current is defined by

$$Z(k) = \frac{i(k)\sqrt{t_k}}{nFAC^*\sqrt{D_f}}. \tag{100}$$

Discretization of equation (99) makes all variables dimensionless (as shown in reference [10]).

Solving for the dimensionless current $Z(k)$ gives

$$Z(k) = \frac{2\sqrt{\mathbb{D}_f k_{\max}}\left(X_f(k) f_{P^+}(1,k-1) - X_b(k) f_P(1,k-1)\right)}{2\sqrt{\mathbb{D}_f k_{\max}} + X_f(k) + X_b(k)}, \tag{101}$$

where $k_{\max}$ is the number of time steps needed to complete one cyclic voltammetry sweep, f_i is the dimensionless concentration $(C_i(x,t)/C^*)$ and

$$X_f(k) = k_f(E)\sqrt{\frac{t_k}{D_f}}, \tag{102}$$

$$X_b(k) = k_b(E)\sqrt{\frac{t_k}{D_f}}. \tag{103}$$

The simulation code was taken from reference [10] and modified to account for the initial conditions of interest and to mimic several cyclic voltammetry experiments performed one after another. As seen in reference [10], equation (91) is dimensionless and discretized to the following:

$$f_i(j,n+1) = f_i(j,n) + \mathbb{D}_f\left(f_i(j-1,n) - 2f_i(j,n) + f_i(j+1,n)\right), \tag{104}$$

where $\mathbb{D}_f = D_f \Delta t/\Delta x^2$ is the dimensionless diffusion coefficient in film. The function f_i is the dimensionless concentration of species i.

At film boundary, there is no flux of the probe into the electrode. Thus, the above becomes

$$f_i(1,n+1) = f_i(1,n) + \mathbb{D}_f\left(f_i(2,n) - f_i(1,n)\right). \tag{105}$$

The equilibrium at the film solution interface is treated identical to that in Chapter 3 and is given by equations (83) and (86). The code for the simulation can be found in Appendix D. All parameters of the simulation rely on two variables, b and ω.

4.2.3.1 Parameter b

A parameter b is used in the simulation code and is the diffusion length relative to the film

thickness. The parameter b is defined by

$$b = \sqrt{\frac{l^2}{D_f t_k}} \tag{106}$$

where l is the length of the film, D_f is the diffusion rate in the film and t_k is the time to complete one cyclic voltametric sweep. For values of b greater than 1, the diffusion length is largely confined to the film. For values of b less than 1, the diffusion length extends into solution. As b is affected by t_k, and t_k depends on the scan rate, ν, of the experiment, the choice of the value of b will affect the number of space and time steps of the experiment. More can be read about the affects of the choice of b in reference [10]. The values of b used for this simulation were 0.25, 0.5, 1.2, 2.5 and 4.

4.2.3.2 Parameter ω

A parameter ω is used in the simulation code. Let $\gamma = \sqrt{D_s/D_f}$ and κ be the extraction parameter as used in equation (93). The term κ/γ is related to the ratio of the flux in the film to that in the solution. The values of κ/γ can range from 0 to infinity. To make this term more easily handled, a flux parameter ω is defined as

$$\omega = \frac{1 - \frac{\kappa}{\gamma}}{1 + \frac{\kappa}{\gamma}}. \tag{107}$$

ω is bounded between -1 and 1. The values of ω used for this simulation range from -0.5 to 0.5 with step size 0.1.

4.3 Results

The simulation output is voltammograms run continuously as a film loads with a probe. For every combination of ω and b, at least 20 consecutive voltammograms were simulated. Figure 33 is an example of the type of plots created. The arrows indicate the directions in which the peaks grew in over time. All other combinations of b and ω are similar to this one, the main difference is

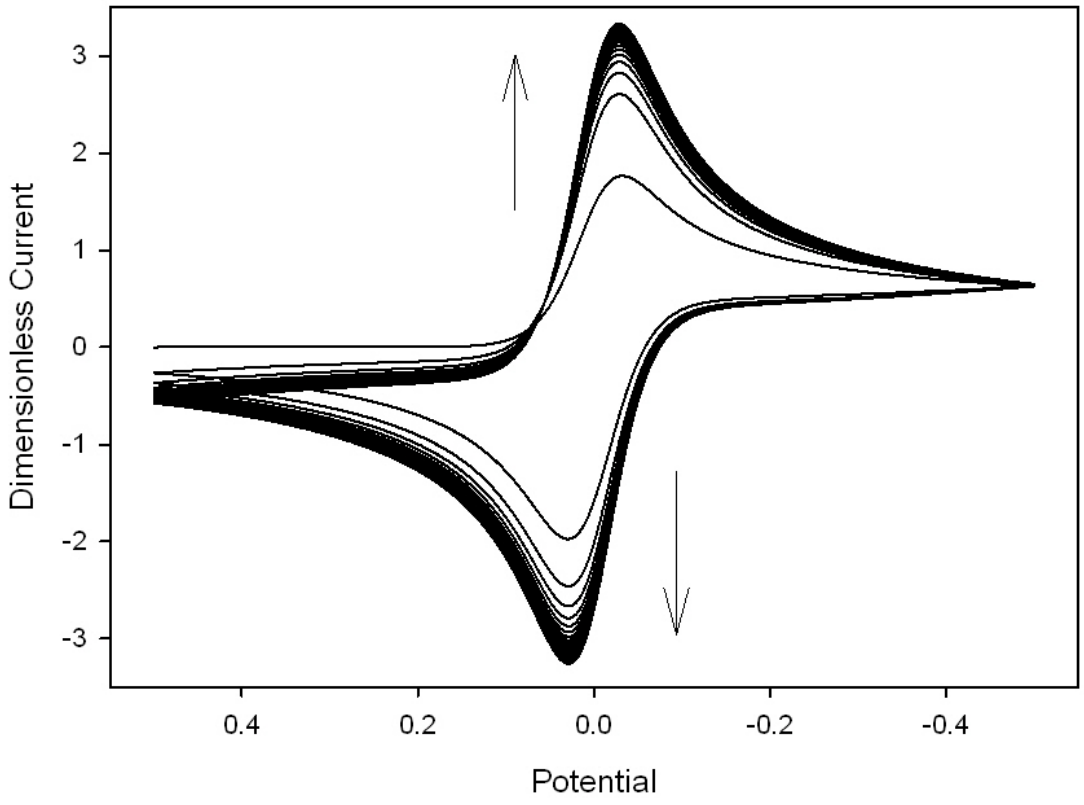

Figure 33. The output of 20 consecutive cyclic voltammetric sweeps for $b = 4$ and $\omega = -0.1$.

the rate at which the peak current values converged. For small b values and large ω values, peak currents tend to decrease as they converge, for large b values and small ω values, peaks tend to increase as they converge. It was expected that peak values grew in as they converge on a peak current, the decreasing peak values seen for small b values and large ω values was not of concern because the overall decrease was very small (less than a 10% difference between the first and last peaks in the simulation) and is due to the parameters specifying rapid loading of the film.

Figure 34 and figure 35 are of ω and b versus the dimensionless peak height at the twentieth scan. As the peak height will be known, one can get possible b and ω values for the system. Matching the b and ω for the peak height will allow an experimentalist to determine the physical diffusion of the system if the scan rate, the extraction parameter and diffusion rate in solution are known. Below are the plots of ω and b versus their dimensionless peak height.

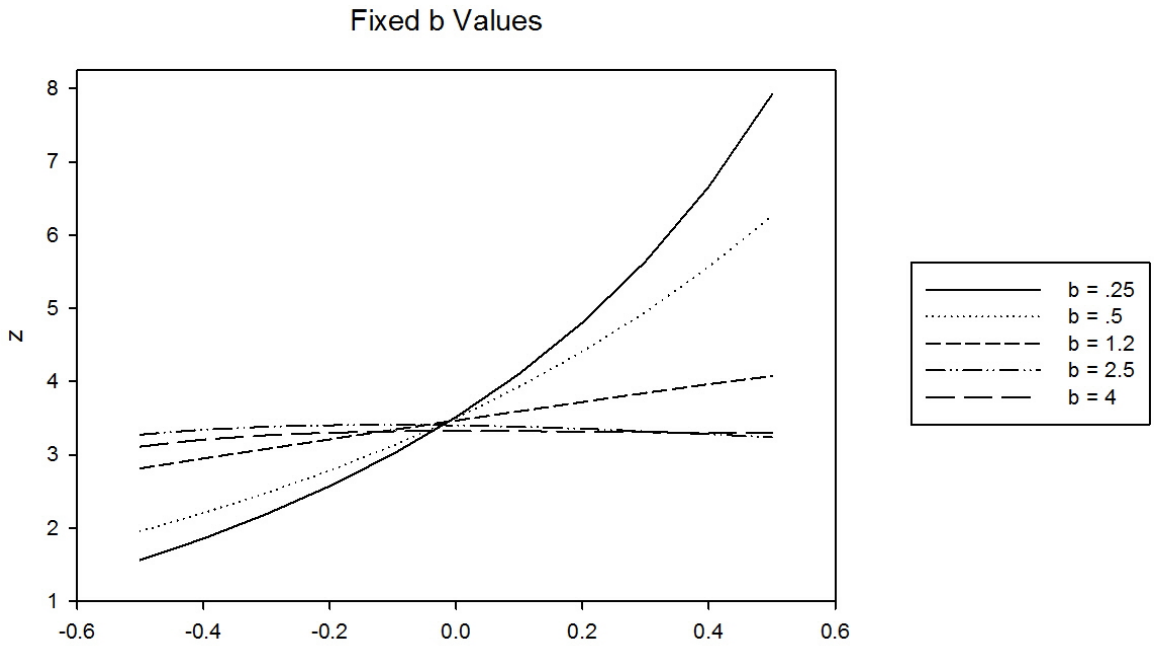

Figure 34. How ω varies with fixed b values.

One feature that stands out in the above plot is the dimensionless current values do not vary

by much when ω equals zero, in fact, they vary by less than 0.2. This is because when $\omega = 0$, the simulation parameters are such that there are is no film on the electrode. This is because $\omega = 0$ gives

$$\kappa\sqrt{D_f} = \sqrt{D_s}.$$

As the flux of molecules out of the solution must equal the flux of molecules into the film, we have that

$$D_f \left.\frac{\partial f(x,t)}{dx}\right|_{x=l} = D_s \left.\frac{\partial f(x,t)}{dx}\right|_{x=l}.$$

Substitution then gives $\kappa = 1$ and $D_f = D_s$. Thus, the simulation is that of an unmodified electrode in solution which as the system continues to steady state, the dimensionless current values when $\omega = 0$ will converge to a single value.

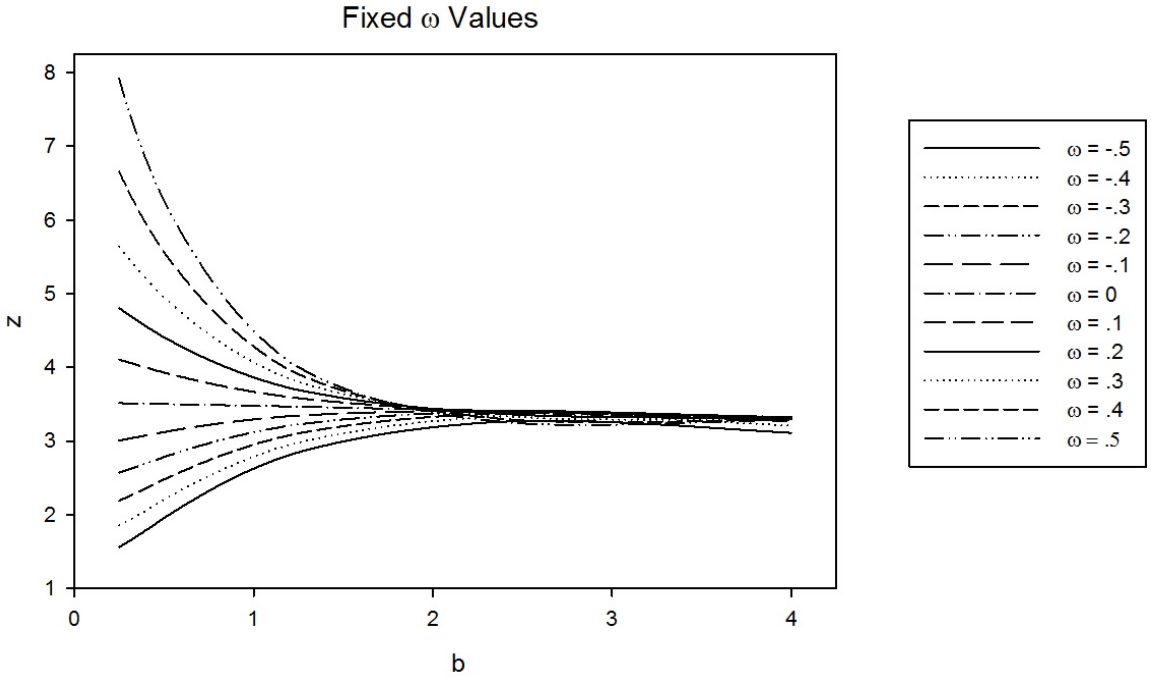

Figure 35. How b varies over fixed ω values.

One will notice that for large b values, the dimensionless current tends toward the same value. This is because b affects the diffusion layer thickness. The larger the b value, the shorter the

diffusion layer, thus for large b values, diffusion is confined to the boxes closest to the electrode, causing the concentration of probe to not change substantially except close to the electrode. Thus, the dimensionless current for any ω with a large b value, will eventually all approach the same value.

CHAPTER 5

APPLICATION OF SIMULATION MODELS AND FUTURE WORK

The work described in this thesis is on three aspects of Nafion film, namely the proton concentration through a Nafion film in a fuel cell, a test of a theory of electron hopping through a Nafion film on a modified electrode and calculation of the physical diffusion rate of a molecule without electron hopping through any type of film. This was done to better understand the delivery of probes through films that will lead to improved implementations of transport through films.

Most models of polymer modifications on electrodes assume electroneutrality. This assumption may not be appropiate in cases where the anion is fixed, as the interactions of protons with the polymer lead to unrealistic concentration profiles through the polymer when the system is polarized. It is unlikely that cations disburse uniformly through the film under such conditions. The model can guide the engineering of novel films with tailored transport properties better suited to the demands of the application.

In Chapter 3 on electron hopping, a reasonable solution was not found. It is known that a mechanism other than physical diffusion must be responsible for the transport of $Ru(bpy)_2^{2+}$ in this system. Future work in this area includes modification of the program used in Chapter 2 to take into account migration in the system. Originally migration was assumed to have no effect on the transport within the system,. It is seems possible that migration might be part of the system in a way that is concealed by the diffusion within the film.

Physical diffusion in the absence of electron hopping is important. Understanding where molecules are in a film and how they move leads to the improvement of many devices that rely on transport of probes.

APPENDIX A

C++ COMPUTER CODE FOR THE MEASUREMENT OF D_{phy}

```
#include <io.h>
#include <iostream> //originally iostream.h
#include <fcntl.h>
#include <fstream>
#include <math.h>
#include <stdio.h>
#include <time.h>
#include <vector>
using namespace std; //originally not included
int main () {
ofstream outFile1;
outFile1.open("AACurrent.txt");
if (outFile1.fail())
{
cerr << "unable to open .le Current-CA.out for output" << endl;
exit(1);
}
ofstream outFile2;
outFile2.open("ACurrent.txt");
if (outFile2.fail())
{
cerr << "unable to open .le Concentration.out for output" << endl;
exit(1);
}
ofstream outFile3;
outFile3.open("Amaxmin.txt");
if (outFile3.fail())
{
cerr << "unable to open .le maxmin.out for output" << endl;
exit(1);
}
int kmax= 1000000;
int tmax=50;
double half = kmax/2;
double kkmax;
double kk;
kkmax= kmax;
int B =20;
double dubB=B;
double F = 96485.3;
double R = 8.31447;
double T = 298;
double l = F/(R*T);
double omega=.4;//-0.7;
double b=.5;
double Df = 1.2E-9;
double Ds = 5.2E-6;
double dbx =dubB*dubB/(b*b)*2*l/(0.49*kkmax);// Df/Ds; //
double gam=1/sqrt(dbx);
double rho = 1.74; //g/cm^3
double MW = 1100; //g/mol
double N = rho/MW;
double clmin = N/2;
```

```
double clplus = .001;
double kappa=gam*(1-omega)/(1+omega); // clmin/clplus; //
double DDa = 4.9E-1; // Diffusion Coeffcients.
double DDb = 4.9E-1;
int k;
int j;
double x0= 500000.0;
double E1 = 0.5;
double E2 = -0.5;
double E0 = 0.0; // Potentials.
double E=0.0;
double enorm=0.0;
double potrang=l*(E2-E1);
double potinit=l*(E1-E0);
double z=0; // Dimensionless Current.
double d;
double alp = 0.5; // Alpha.
double fan[20001];
double fbn[20001];
double fao[20001];
double fbo[20001];
double da[20001];
double db[20001];
double zmax=0;
double zmin= 0;
double Emax= 0;
double Emin= 0;
double jmax;
int intjmax;
int t;
for( j=0;j<20001;j++) // Initializes arrays.
{
if(j<B)
{
fan[j]=0.0;
fao[j]=0.0;
fbn[j]=0.0;
fbo[j]=0.0;
}
else
{
fan[j]=1.0/kappa;
fao[j]=1.0/kappa;
fbn[j]=0.0;
fbo[j]=0.0;
}}
int r;
for ( r=0;r<B;r++) //(<= changed to < )
{
da[r]=DDa*dbx;
db[r]=DDb*dbx;
}
for ( r>=B;r<20001;r++)
{
da[r]=DDa;
db[r]=DDb;
}
//line 101
for (t=1;t<=tmax;t++) //Multiple Scans Start
```

```
{
      cout <<t<<"\n";
      double zmax=0;
      double zmin= 0;
      double Emax= 0;
      double Emin= 0;
for ( k=1;k<=kmax;k++) //TIME COUNTER STARTS.
{
kk=(t-1)*kmax+k;
jmax=B+6.0*sqrt((0.49)*kk)+10.0;
intjmax=ceil(jmax);
d=(k-0.5)/kkmax;
if (k<(kmax/2))
{
E=E1+2.0*(E2-E1)*d;
enorm= potinit+2.0*potrang*d;
}
else
{
E=E1+2.0*(E2-E1)*(1.0-d);
enorm= potinit+2.0*potrang*(1.0-d);
}
for(j=1;j<B-1;j++)
{
fan[j]=fao[j]+DDa*dbx*(fao[j+1]-2.0*fao[j]+fao[j-1]);
fbn[j]=fbo[j]+DDb*dbx*(fbo[j+1]-2.0*fbo[j]+fbo[j-1]);
}
fan[B-1]=fao[B-1]+da[B-1]*(2.0*kappa*gam*gam*fao[B]-(kappa+
3.0*gam*gam)*fao[B-1]+(kappa+gam*gam)*fao[B-2])/(kappa+gam*gam);
fbn[B-1]=fbo[B-1]+db[B-1]*(2.0*kappa*gam*gam*fbo[B]-(kappa+
3.0*gam*gam)*fbo[B-1]+(kappa+gam*gam)*fbo[B-2])/(kappa+gam*gam);
fan[B]=fao[B]+da[B]*(2.0*fao[B-1]-(3.0*kappa+gam*gam)*fao[B]
+(kappa+gam*gam)*fao[B+1])/(kappa+gam*gam);
fbn[B]=fbo[B]+db[B]*(2.0*fbo[B-1]-(3.0*kappa+gam*gam)*fbo[B]
+(kappa+gam*gam)*fbo[B+1])/(kappa+gam*gam);
for(j=B+1;j<intjmax;j++)
{
fan[j]=fao[j]+DDa*(fao[j+1]-2.0*fao[j]+fao[j-1]);
fbn[j]=fbo[j]+DDb*(fbo[j+1]-2.0*fbo[j]+fbo[j-1]);
}
fan[0]=fao[0]+da[1]*(fao[1]-fao[0]);
fbn[0]=fbo[0]+db[1]*(fbo[1]-fbo[0]);
double kf=x0*exp(-alp*enorm); // Rate constants .
double kb=x0*exp((1.0-alp)*enorm);
// CURRENT.
z=2.0*sqrt(kkmax*da[0])*(kf*fao[0]-kb*fbo[0])/(2.0*sqrt(kkmax*da[0])+kf+kb);
//{
//if (k>=3)
//{
//outFile1<<k<<", "<<kf<<", "<<kb<<", "<<E<<", "<<z<<"\n";
//outFile1<<E<<"\n";
//}
//else
//{
//outFile2<<k<<", "<<kf<<", "<<kb<<", "<<E<<", "<<z<<"\n";
//outFile2<<z<<"\n";
//}
```

```
    //}
    // Accounting for electrolyzed material
    fan[0]= fan[0]-z*sqrt(da[0]/kkmax);
    fbn[0]= fbn[0]+z*sqrt(da[0]/kkmax);
    for (j=0;j<=intjmax;j++) // Ageing.
    {
    // line 150
    fao[j]=fan[j];
    fbo[j]=fbn[j];
    }
    if (z>zmax)
    {
    zmax=z;
    Emax=E ;
    }
    if (z<zmin)
    {
    zmin=z;
    Emin=E;
    }
    } // end of k loop
    outFile3<<"t = "<<t<<", zmax = "<<zmax<<", zmin = "<<zmin<<", Emax =
"<<Emax<<
    ", Emin = "<<Emin<<", DE = "<<(Emin-Emax)*1000<<"\n" ;
    }//end of t loop
    //} in file originally, I took out
    outFile1.close();
    outFile2.close();
    outFile3.close();
    return 0;
    }
```

APPENDIX B

MATLAB COMPUTER CODE FOR THE FUEL CELL SYSTEM WITHOUT ELECTRONEUTRALITY

```
function FCfinal
clear all
global a
global b
global c
global E0
format long
%it is okay to change these first three constants to find the
%system you are finding the profile over
length = 175; %number of microns interested in
i = 1*10^4; %current, A/m^2, (from 1 amp/cm^2)
Vo = .59; %V lost over membrane
lo = 175; % length in microns data taken from
Eo = 1.23;
area = 5*10^(-4); %m^2, 5 cm^2, from Wayne's thesis
ir = i*area; %A, current used for resistance
Vr = Eo-Vo; %V lost to resistance
Ro = Vr/ir; %resistance, J s/C^2
Res = Ro*length/lo;
I = Vr/Res; %A, adjusts current for the length of interest
ne = 4; %electrons in the reactions
F = 9.64853*10^7; %C/kmol
R = 8314.47; %J/K*kmol
l = lo*10^(-6)*length/lo; %m, data taken from 50 micron length
J = I/(area*ne*F); %kmol/m^2 s
D = 1.2*10^(-9); %m^2/sec
rho = 1.74*10^6; %g/m^3, 1.74 g/cm^3 average taken from Oberbroeckling/Leddy paper
MW = 1.100*10^6; %g/kmol, taken from 1100 g/mol
N = rho/MW; %kmol/m^3
T = 298; %K
er = 20;
eo = 8.85419*10^(-12); %C^2/(J m)
e = er*eo;
alpha = -10^(-3)*l*J/(D*N);
beta = F*l/(R*T);
gamma = 10^(-3)*F*N*l/e;
delta = 10^(-3);
a=alpha/delta;
b=beta/delta;
c=gamma;
lam1 = (-a+sqrt(a*a+4*b*c))/2;
lam2 = (-a-sqrt(a*a+4*b*c))/2;
M1 = [-a-lam1 b; c -lam1];
M1(2,2) = M1(1,2)*-M1(2,1)/M1(1,1) + M1(2,2);
M1(2,1) = 0; %changes to rref
ratio1 = abs(M1(1,2)/M1(2,2));
ratio2 = abs(M1(1,1)/M1(2,2));
%if M(2,2) is small enough, have one free variable to determine the eigenvectors
if ratio1 > 10^6
if ratio2 > 10^6
PosEigVec = [-b/(-a-lam1) 1]/10000;
```

```
end
end
M2 = [-a-lam2 b; c -lam2];
M2(2,2) = M2(1,2)*-M2(2,1)/M2(1,1) + M2(2,2);
M2(2,1) = 0; %changes matrix to rref
ratio1 = abs(M2(1,2)/M2(2,2));
ratio2 = abs(M2(1,1)/M2(2,2));
%if M(2,2) is small enough, have one free variable to determine the eigenvectors
if ratio1 > 10^6
if ratio2 > 10^6
NegEigVec = [-b/(-a-lam2) 1]/10000;
end
end
E0 = -alpha/beta;
n=1000;
Ee = -alpha/beta;
IC = Vo/(10^3*l);
del1= l/2;
del2= l/2;
X1=linspace(0,del1,n);
X2=linspace(0,del2,n);
try
XI1=[NegEigVec(1,1) -.1 0]';
[X1,Y]=ode15s(@F2,X1,XI1);
catch
del1=.999*del1;
X1=linspace(0,del1,n);
end
C1=Y*[1 0 0]';
E1=Y*[0 1 0]'+E0;
V1=-Y*[0 0 1]';
C1 = N*(1+C1);
E1 = 10^(3)*E1;
V1 = V1*10^(3);
C1min = min(C1);
C1max = max(C1);
E1min = min(E1);
E1max = max(E1);
deltax1 = del1/n;
try
XI2=[PosEigVec(1,1) -.1 0]';
[X2,Y]=ode15s(@F1,X2,XI2);
catch
del2=.999*del2;
X2=linspace(0,del2,n);
end
C2=Y*[1 0 0]';
E2=Y*[0 1 0]'+E0;
V2=-Y*[0 0 1]';
C2 = N*(1+C2);
E2 = 10^(3)*E2;
V2 = V2*10^(3);
C2min = min(C2);
C2max = max(C2);
E2min = min(E2);
E2max = max(E2);
deltax2 = del2/n;
A = [E1min, E2min];
Amin = max(A);
h1 = size(X1);
```

```
h2 = size(X2);
n1 = h1(1,1);
n2 = h2(1,1);
VaAll = V1(n1)-V2(n2);
x1 = 0;
while E1(n1-x1)<Amin
x1 = x1+1;
end
x2 = 0;
while E2(n2 - x2)<Amin
x2 = x2+1;
end
for x2 = 1:n2-1
x1 = 0;
Amin = E2(n2-x2);
while E1(n1-x1)<Amin
x1 = x1+1;
end
Va(n2-x2,1) = V1(n1-x1)-V2(n2-x2);
end
xv=1;
while Va(n2-xv,1) > Vo
xv = xv+1;
end
x1 = 0;
x2 = xv-1;
Amin = E2(n2-x2);
while E1(n1-x1)<Amin
x1 = x1+1;
end
Creal = zeros(2*n, 1);
Ereal = zeros(2*n, 1);
Vreal = zeros(2*n, 1);
xfinal = zeros(2*n, 1);
Cfinal = zeros(2*n, 1);
Efinal = zeros(2*n, 1);
Vfinal = zeros(2*n, 1);
xreal = zeros(2*n,1);
for xx = 1:n2-x2
xreal(xx) = deltax2*(xx-1);
Creal(xx) = C2(n2-x2-xx+1);
Ereal(xx) = E2(n2-x2-xx+1);
Vreal(xx) = V2(n2-x2-xx+1);
end
zro = 2*n-(n2-x2+n1-x1);
deltaxmid = (l-(n2-x2)*deltax2-(n1-x1)*deltax1)/zro;
for xx = 1:zro
xreal(n2-x2+xx) = xreal(n2-x2+xx-1)+deltaxmid;
Creal(n2-x2+xx) = N;
Ereal(n2-x2+xx) = Ee*10^3;
Vreal(n2-x2+xx) = 0;
end
for xx = 1:n1-x1
xreal(n2-x2+zro+xx) = l-deltax1*(n1-x1-xx);
Creal(n2-x2+zro+xx) = C1(xx);
Ereal(n2-x2+zro+xx) = E1(xx);
Vreal(n2-x2+zro+xx) = V1(xx);
end
line = 5; %number of points used to make the linearization
FE = zeros(2,line);
LE = zeros(2,line);
FV = zeros(2,line);
```

```
LV = zeros(2,line);
FC = zeros(2,line);
LC = zeros(2,line);
for xx = 1:line
FE(1,xx) = (xx-1)*deltax2;
FE(2,xx) = Ereal(xx);
LE(1,xx) = l-(line-xx)*deltax1;
LE(2,xx) = Ereal(2*n-line+xx);
FV(1,xx) = (xx-1)*deltax2;
FV(2,xx) = Vreal(xx);
LV(1,xx) = l-(line-xx)*deltax1;
LV(2,xx) = Vreal(2*n-line+xx);
FC(1,xx) = (xx-1)*deltax2;
FC(2,xx) = Creal(xx);
LC(1,xx) = l-(line-xx)*deltax1;
LC(2,xx) = Creal(2*n-line+xx);
end
RFE = corrcoef(FE'); %gives correlation coefficient for line
RLE = corrcoef(LE'); %made at the boundaries
RFV = corrcoef(FV');
RLV = corrcoef(LV');
RFC = corrcoef(FC');
RLC = corrcoef(LC');
pFE = polyfit(FE(1,:),FE(2,:),1);
pLE = polyfit(LE(1,:),LE(2,:),1);
pFV = polyfit(FV(1,:),FV(2,:),1);
pLV = polyfit(LV(1,:),LV(2,:),1);
pFC = polyfit(FC(1,:),FC(2,:),1);
pLC = polyfit(LC(1,:),LC(2,:),1);
clear M;
M(1,1) = pFE(1,1);
M(1,2) = -pLE(1,1);
M(1,3) = pLE(1,2) - pFE(1,2);
M(2,1) = -pFV(1,1);
M(2,2) = pLV(1,1);
M(2,3) = Vo - pLV(1,2) + pFV(1,2);
Xs = rref(M);
xi = Xs(1,3);
xf = Xs(2,3);
clear total
xfinal(1) = 0;
Cfinal(1) = pFC(1,1)*xi + pFC(1,2);
Efinal(1) = pFE(1,1)*xi + pFE(1,2);
Vfinal(1) = pFV(1,1)*xi + pFV(1,2);
xfinal(2) = deltax2 - xi;
Cfinal(2) = Creal(2);
Efinal(2) = Ereal(2);
Vfinal(2) = Vreal(2);
for x = 3:2*n-1
Cfinal(x) = Creal(x);
Efinal(x) = Ereal(x);
Vfinal(x) = Vreal(x);
end
for x = 3:n2-x2
xfinal(x) = xfinal(x-1) + deltax2;
end
deltaxmid = (l-(n2-x2)*deltax2-(n1-x1)*deltax1)/zro
for xx = 1:zro
xfinal(n2-x2+xx) = xfinal(n2-x2+xx-1)+deltaxmid;
```

```
end
for xx = 1:n1-x1-2
xfinal(n2-x2+zro+xx) = l-deltax1*(n1-x1-xx);
end
xfinal(2*n-1) = 2*l-deltax1-xf;
Cfinal(2*n-1) = Creal(2*n-1);
Efinal(2*n-1) = Ereal(2*n-1);
Vfinal(2*n-1) = Vreal(2*n-1);
xfinal(2*n) = l;
Cfinal(2*n) = pLC(1,1)*xf + pLC(1,2);
Efinal(2*n) = pLE(1,1)*xf + pLE(1,2);
Vfinal(2*n) = pLV(1,1)*xf + pLV(1,2);
Vfinal(2*n)-Vfinal(1) %check potential drop
Efinal(2*n)-Efinal(1) %checks charge over membrane
sum1 = 0;
for x = 1:n2-x2
sum1 = sum1 + Cfinal(x);
end
sum1 = sum1*deltax2;
sum2 = 0;
for x = 1:n1-x1
sum2 = sum2 + Cfinal(2*n-x+1);
end
sum2 = sum2*deltax1;
sum3 = 0;
if n2-x2 < n
for x = n2-x2+1:2*n-n1+x1;
sum3 = sum3 + Cfinal(x);
end
sum3 = sum3*deltaxmid;
end
sum = sum1 + sum2 + sum3 - N*l; %gives excess protons, not good bc trap rule
%checks that ignoring b*Ctilde*Ehat is ok
Ctilde = Cfinal/N - 1;
Ehat = 10^(-3)*Efinal + alpha/beta;
for x = 1:2*n
Other(x,1) = Ctilde(x,1)*Ehat(x,1);
end
clear A
clear B
clear C
for x = 1:2*n
A(x,1) = abs(Ehat(x,1)/Other(x,1));
B(x,1) = abs(b*Ehat(x,1)/(-a*Ctilde(x,1)));
C(x,1) = abs(b*Other(x,1)/(-a*Ctilde(x,1)));
end
maxA = max(A);
minA = min(A);
maxB = max(B);
minB = min(B);
maxC = max(C);
minC = min(C);
for x = 1:2*n
All(x,1) = -a*Ctilde(x,1)+b*Ehat(x,1)*(1+Ctilde(x));
Assume(x,1) = -a*Ctilde(x,1)+b*Ehat(x,1);
Diff(x,1) = 100*(All(x,1)-Assume(x,1))/All(x,1);
end
maxDiff = max(Diff); %tells what % off by leaving out b*Ctilde*Ehat
minDiff = min(Diff);
xfinal; %delete semicolons to get output
Cfinal-N; %excess proton concentration
Vfinal; %potential
Efinal; %electric field
```

```
end
function F1=F1(T,Y)
global a
global b
global c
global E0
F1=-[-a*Y(1)+b*Y(2)*(1+Y(1));c*Y(1);Y(2)+E0];
end
function F2=F2(T,Y)
global a
global b
global c
global E0
F2=[-a*Y(1)+b*Y(2)*(1+Y(1));c*Y(1);Y(2)+E0];
end
```

APPENDIX C

MATLAB COMPUTER CODE FOR THE MODIFIED ELECTRODE WITH PROTON HOPPING

```
function HoppingDiffusion9
tic
%both directions (possible) with hopping, deltat check
totaltime = 500;
l = .01016; %cm, 4 mils
xmax = 200;
deltax = l/(xmax);
DW = 5.2*10^(-6); %cm^2/sec
Dap2 = 1.2*10^(-9); %cm^2/sec
Dap3 = Dap2;%.6*10^(-8); %cm^2/sec
%check
k11 = 10^8; %/M s
dist =13.6*10^(-8) ; %cm, 13.6 A
Dhop = k11*dist^2*pi/4; %cm^2/M*sec, will multiply by concentration in problem
length = 2.54; %cm
width = 2.54; %cm
F = 96485.3; %C/mol
eo = 8.85419^(-12); %C
er = 20;
e = eo*er;
R = 8.31447; %J/K*mol
T = 298; %K
Vo = 5;
k = 1; %mass action constant
rho = 1.74; %density, g/cm^3, density
MW = 1100; %molecular weight, g/mol
Cstar = rho/MW; %mol/cm^3
N = Cstar; %M, mol/L concentration of SO3-
bulkRu2 = 10^(-3); %concentration of Ru2 in the bulk, 1 mM
diff = bulkRu2-N/2;
kappa = N/(2*bulkRu2);
%don't have to worry about kappa for Ru3 because C(Ru3) will never get that large
Dm=.45;
time = 0;
%sec
total = xmax+500; %guess to make large enough bc D is so slow in membrane
%there is a check in loop to make sure this is okay
%r = ceil(6*sqrt(Dm*(tmax))+2);
%if r < xmax
% total = xmax + 5;
%else
% total = r;
%end
%for right now when D in membrane is larger than in film
Cold2 = zeros(total,1);
Cold3 = zeros(total,1);
Cnew2 = zeros(total,1);
Cnew3 = zeros(total,1);
CDold2 = zeros(total,1);
CDold3 = zeros(total,1);
CDnew2 = zeros(total,1);
```

```
CDnew3 = zeros(total,1);
Nafion = zeros(total,1);
charge = zeros(xmax,1);
grad2 = zeros(total,1);
grad3 = zeros(total,1);
J2 = zeros(total,1);
J3 = zeros(total,1);
D2 = zeros(xmax,1);
D3 = zeros(xmax,1);
phix = zeros(xmax,1);
phi = zeros(xmax,1);
chargeD = zeros(xmax,1);
phixD = zeros(xmax,1);
phiD = zeros(xmax,1);
%initialize
for x = 1:xmax
Cold2(x) = N/2;
Cnew2(x) = N/2;
CDold2(x) = N/2;
CDnew2(x) = N/2;
Nafion(x) = N;%all other chemcials already set to zero
end
for x = xmax+1:total
Cold2(x) = bulkRu2;
CDold2(x) = bulkRu2;
Cnew2(x) = bulkRu2;
CDnew2(x) = bulkRu2;
end
%for this while loop, Ru3 can only diffuse away and Ru2 can only diffuse in
steps = 0;
thing = 0;
while time < totaltime
%time
steps = steps+1;
%calculate gradients up to xmax
for x = 1:xmax-1
grad2(x) = (Cold2(x+1)-Cold2(x))/deltax;
grad3(x) = (Cold3(x+1)-Cold3(x))/deltax;
end
%might want to do more here if Ru2 & Ru3 at boundary
if Cold2(xmax+1)>Cstar/2
grad2(xmax) = (Cstar/2-Cold2(xmax))/deltax;
else
grad2(xmax) = (Cold2(xmax+1)-Cold2(xmax))/deltax;
end
if Cold3(xmax+1)>Cstar/3
grad3(xmax) = (Cstar/3-Cold3(xmax))/deltax;
else
grad3(xmax) = (Cold3(xmax+1)-Cold3(xmax))/deltax;
end
for x = xmax+1:total-1
grad2(x) = (Cold2(x+1)-Cold2(x))/deltax;
grad3(x) = (Cold3(x+1)-Cold3(x))/deltax;
end
%calculate D(x)'s
for x = 1:xmax
if grad2(x)~=0 %not equal to
D2(x) = Dap2+Dhop*(Cold3(x)-Cold2(x)*grad3(x)/grad2(x));
else
D2(x) = Dap2; %doesn't matter, flux is zero later
end
if grad3(x)~=0
```

```
D3(x) = Dap3+Dhop*(Cold2(x)-Cold3(x)*grad2(x)/grad3(x));
else
D3(x) = Dap3; %doesn't matter, flux is zero later
end
end
%don't have to worry about gamma 3 because C(Ru3) never gets that large
for x = xmax+1:total
D2(x) = DW;
D3(x) = DW;
end
%calculate deltat
M2 = max(D2);
M3 = max(D3);
A = [M2, M3];
M = max(A);
for x = 1:xmax
if D2(x)>thing
thing = D2(x);
end
end
deltat = Dm*deltax^2/M;
time = time+deltat;
%run through program
%do not need -J stuff, -'s cancel out
for x = 1:total
J2(x) = D2(x)*grad2(x);
J3(x) = D3(x)*grad3(x);
end
Cnew2(1) = Cold2(1)+deltat*J2(1)/deltax;
Cnew3(1) = Cold3(1)+deltat*J3(1)/deltax;
for x = 2:xmax-1
Cnew2(x) = Cold2(x)+deltat*(J2(x)-J2(x-1))/deltax;
Cnew3(x) = Cold3(x)+deltat*(J3(x)-J3(x-1))/deltax;
end
Cnew3(xmax) = Cold3(xmax)+deltat*(J3(xmax)-J3(xmax-1))/deltax;
Cnew3(xmax+1) = Cold3(xmax+1)+deltat*(J3(xmax+1)-J3(xmax))/deltax;
gamma2 = DW/D2(xmax);
DDfx = D2(xmax)*deltat/deltax^2;
DDfx1 = D2(xmax-1)*deltat/deltax^2;
DDs = DW*deltat/deltax^2;
AA = 2*kappa*DDfx/(kappa+gamma2)*(gamma2*Cold2(xmax+1)+Cold2(xmax));
BB = (2*DDfx+DDfx1)*Cold2(xmax);
CC = DDfx1*Cold2(xmax-1);
Cnew2(xmax) = Cold2(xmax)+(AA-BB+CC);
DD = 2*(gamma2*Cold2(xmax+1)+Cold2(xmax))/(kappa+gamma2);
Cnew2(xmax+1) = Cold2(xmax+1)+DDs*(Cold2(xmax+2)-3*Cold2(xmax+1)+DD);
for x = xmax+2:total
Cnew2(x) = Cold2(x)+deltat*(J2(x)-J2(x-1))/deltax;
Cnew3(x) = Cold3(x)+deltat*(J3(x)-J3(x-1))/deltax;
end
Cold2=Cnew2;
Cold3=Cnew3;
Cold3(1) = Cold3(1)+Cold2(1);
Cold2(1)=0;
end
thing
%steps
%time
time = 0;
Dm = .49;
deltat = Dm*deltax^2/DW;
while time < totaltime
```

```
%time
DM2D = deltat*Dap2/deltax^2;
DM3D = deltat*Dap3/deltax^2;
DMWD = deltat*DW/deltax^2;
gamma2 = DMWD/DM2D;
%calculate gradients up to xmax
CDnew2(1) = CDold2(1) + DM2D*(CDold2(2)-CDold2(1));
CDnew3(1) = CDold3(1) + DM3D*(CDold3(2)-CDold3(1));
for x = 2:total-1
CDnew3(x) = CDold3(x) + DM3D*(CDold3(x+1)-2*CDold3(x)+CDold3(x-1));
end
for x = 2:xmax-1
CDnew2(x) = CDold2(x) + DM2D*(CDold2(x+1)-2*CDold2(x)+CDold2(x-1));
end
AA = 2*kappa*gamma2*CDold2(xmax+1);
BB = (kappa+3*gamma2)*CDold2(xmax);
CC = (kappa+gamma2)*CDold2(xmax-1);
CDnew2(xmax) = CDold2(xmax) + DM2D/(kappa+gamma2)*(AA-BB+CC);
AA = (kappa+gamma2)*CDold2(xmax+2);
BB = (3*kappa+gamma2)*CDold2(xmax+1);
CC = 2*CDold2(xmax);
CDnew2(xmax+1) = CDold2(xmax+1)+DMWD/(kappa+gamma2)*(AA-BB+CC);
for x = xmax+2:total-1
CDnew2(x) = CDold2(x) + DMWD*(CDold2(x+1)-2*CDold2(x)+CDold2(x-1));
end
CDold2=CDnew2;
CDold3=CDnew3;
CDold3(1) = CDold3(1)+CDold2(1);
CDold2(1)=0;
time = time+deltat;
end
for x = 1:xmax
chargeD(x) = 3*CDnew3(x)+2*CDnew2(x)-Nafion(x);
charge(x) = 3*Cnew3(x)+2*Cnew2(x)-Nafion(x);
end
phixxD = -F/e*chargeD;
phixx = -F/e*charge;
for x = 1:xmax-1
phixD(x) = (phixxD(x+1)+phixxD(x))/2*deltax;
phix(x) = (phixx(x+1)+phixx(x))/2*deltax;
end
phixD = phixD-phixD(xmax-1);
phix = phix-phix(xmax-1);
for x = 2:xmax-1
phiD(x) = (phixD(x)+phixD(x-1))/2*deltax;
phi(x) = (phix(x)+phix(x-1))/2*deltax;
end
BD = phiD(xmax-1);
B = phi(xmax-1);
for x = 2:xmax-1
phiD(x) = phiD(x)-BD;
phi(x) = phi(x)-B;
end
difference2 = Cnew2-CDnew2
difference3 = Cnew3-CDnew3
Cnew2
Cnew3
figure
hold on
plot(Cnew2, ':.r')
plot(CDnew2, ':ob', 'MarkerSize',4)
title({'Concentration of Ru2 with Hopping';'mol/cm^3'})
hold off
```

```
%figure
%plot(CDnew2, ':.r')
%title({'Concentration of Ru2 without Hopping';'mol/cm^3'})
figure
hold on
plot(Cnew3, ':.r')
plot(CDnew3, ':ob', 'MarkerSize',4)
title({'Concentration of Ru3 with Hopping';'mol/cm^3'})
hold off
%figure
%plot(CDnew3, ':.r')
%title({'Concentration of Ru3 without Hopping';'mol/cm^3'})
%figure
%plot(charge, ':.r')
%title({'Charge'})
for x = 2:xmax-1
pphi(x-1)=phi(x);
pphiD(x-1)=phiD(x);
end
figure
hold on
plot(pphi, ':.r')
plot(pphiD, ':ob', 'MarkerSize',4)
title({'Potential with Hopping'})
hold off
%figure
%hold on
%for x = 2:xmax-1
% plot(x,phiD(x), ':.r')
%end
%title({'Potential without Hopping'})
%hold off
for x = 1:xmax
CCnew2(x) = Cnew2(x);
CCDnew2(x) = CDnew2(x);
end
figure
hold on
plot(CCnew2, ':.r')
plot(CCDnew2, ':ob', 'MarkerSize',4)
title({'Rubpy2 with Hopping'})
hold off
%figure
%hold on
%for x = 1:xmax
% plot(x,CDnew2(x), ':.r')
%end
%title({'Rubpy2 without Hopping'})
%hold off
toc
thing
end
```

APPENDIX D

DERIVATION OF POISSON'S EQUATION FROM GAUSS' LAW FOR ELECTRICITY

Gauss' law for electricity states

$$\Theta = \oint_S E \cdot da = \frac{1}{\varepsilon_o} \int_V \rho dV = \frac{Q_a}{\varepsilon_o} \tag{D.1}$$

where Θ is the electric flux, E is the electric field, da is the differential area on a closed surface S with an outward facing surface normal to its direction, Q_a is the charge enclosed by surface S, ρ is the charge density at a point in V, ε_o is the electric constant and $\oint_S$ is the integral over the surface S enclosing volume V. In differential form, equation (D.1) becomes

$$\nabla \cdot D = \rho \tag{D.2}$$

where ∇ is the del operator representing divergence, D is the electric displacement field and ρ is the charge density. If it is assumed that the medium is linear, isotropic and homogeneous, then

$$D = \varepsilon E = \varepsilon_r \varepsilon_o E \tag{D.3}$$

where ε is the electric permittivity of the medium, ε_o is the vacuum permittivity and ε_r is the relative permittivity. This gives

$$\nabla \cdot D = \nabla \cdot \varepsilon E = \rho \tag{D.4}$$

or

$$\nabla \cdot E = \frac{\rho}{\varepsilon_r \varepsilon_o}. \tag{D.5}$$

Any sufficiently smooth, rapidly decaying vector field can be resolved into irrotational (curl-free) and solenoidal (divergance-free) component vector fields. This implies that any vector field F can

be considered to be generated by a pair of potentials, a scalar potential Ψ and a vector potential A. The resulting Helmholtz decomposition of a vector field splits the vector field into a sum of gradient and curl as follows:

$$F = -\nabla G\left(\nabla \cdot F\right) + \nabla \times G\left(\nabla \times F\right) \tag{D.6}$$

where G is the Newtonian potential operator. If $\nabla \cdot F = 0$, the F is solenoidal (divergence-free). So the above becomes

$$F = \nabla \times G\left(\nabla \times F\right) = \nabla \times A \tag{D.7}$$

where A is the vector potential for F. If $\nabla \times F = 0$, then F is curl-free (irrotational) and the above becomes

$$F = -\nabla G\left(\nabla \cdot F\right) = -\nabla \Phi \tag{D.8}$$

where Φ is the scalar potential function for F. In general, the negative gradient of the scalar potential is equated with the irrotational component and the curl of the vector potential is equated with the solenoidal component, giving

$$F = -\nabla \Phi + \nabla \times A. \tag{D.9}$$

Thus, for an electric field, the curl is zero (so $\nabla \times A = 0$), giving

$$F = -\nabla \Phi \tag{D.10}$$

and equation (D.5) becomes

$$\nabla \cdot E = \nabla \cdot \nabla \Phi = \nabla^2 \Phi - \frac{\rho}{\varepsilon_r \varepsilon_o}. \tag{D.11}$$

The total change Q_a of a region over a volume can be calculated by

$$Q_a = \int_V \alpha_q\left(r\right) dV = \sum \alpha_q\left(r\right) \Delta V = \sum_i n_i \zeta_i \Delta V \tag{D.12}$$

$$= \sum_i e n_i z_i \Delta V = N_A e \sum_i C_i z_i \Delta V = F \sum_i C_i z_i \tag{D.13}$$

where $\alpha_r\left(r\right)$ is the amount of electric charge over a volume, n_i is the number of species i, ζ_i is the

charge of species i, e is the elementary charge and z_i is the charge of species i.

As

$$\rho = \sum_V Q_a = F \sum_i C_i z_i \tag{D.14}$$

this gives

$$\nabla^2 \Phi = -\frac{F}{\varepsilon} \sum_i C_i z_i. \tag{D.15}$$

REFERENCES

[1] Tjarnhage, T.; 1996, Thin Polymer Phospholipid Films for Biosensors, Umea University, July 19, 2010, www.foa.se/surfbiotech/tt/Films.html

[2] Image received from Tim Paschkewitz, 2009, Johna Leddy Lab, University of Iowa

[3] Bard, A. J.; Faulkner, L. R.; Electrochemical Methods, Fundamentals and Applications, 2nd Ed., New York, John Wiley and Sons, Inc. 2001

[4] Leddy, J; Iverson, E; Vanderborgh, N.; Modeling of the Electrode/Ionomer Interface in a Proton Exchange Membrane Fuel Cell; Proceedings from the Electrochemical Conference, 1995, 310 - 322

[5] Gellet, W.L., 2004, Magnetic microparticles on Electrodes: Polymer Electrolyte membrane Fuel Cells, Carbon monoxide Oxidation and Transition Metal Complex Electrochemistry, Doctoral Thesis, The University of Iowa, pgs. 138, 146

[6] Image received from Heung Chan Lee, 2009, Johna Leddy Lab, University of Iowa

[7] Minteer, S. D., 2000, Magnetic Field Effects on Electron Transfer Reactions, Doctoral Thesis, The University of Iowa, pgs. 1 - 5, 32

[8] Image received from Dr. Johna Leddy, 2010, advisor, University of Iowa

[9] Dahms, H.; Electronic Conduction in Aqueous Solution; Journal of Physical Chemistry; 72, 1, 1968, 362 - 364

[10] Hettige, C., 2007, characterization and models for Uniform and Non-Uniform Films on Electrodes, Doctoral Thesis, The University of Iowa, pgs 1 - 62, 183 - 186

[11] Feldberg, S W; On the Dilemma of the Use of the Electroneutrality Constraint in Electrochemical Calculations; Elecom; 2, 2000, 453 - 456

[12] Feldberg, S W; Bond, Alan M; Analysis of Simulated Reversible Cyclic Voltametric Responses for a Charged Redox Species in the Absence of Added Electrolyte; J. Phys. Chem, 102, 1998, 9966 - 9974

[13] Djilali, N; Secanell, M; Carnes, B; Suleman,A; Numerical Optimization of Proton Exchange Membrane Fuel Cell Cathodes; Electrochimica Acta; 52, 2007, 2668 - 2682

[14] Seddiq, M.; Khaleghi, H.; Mirzaei, M.; Numerical analysis of Gas Cross Over Through the Membrane in a Proton Exchange Membrane Fuel Cell; Journal of Power Sources; 161; 2006; 371-379

[15] Ascher, U. M; Ruuth, S. J; Spiteri, R.J.; Implicit-Explicit Runge-Kutta Methods for Time-Dependant Partial Differential Equations; Applied Numerical Mathematics; 25; 1997; 151 - 167

[16] Kassam, A; Trefethen, L. N; Fourth-Order Time Stepping for Stiff PDEs; SIAM Journal of Scientific Computing; 26; 4; 2005; 1214 - 1233

[17] Ascher, U. M; Ruuth, S. J; Wetton, B. T. R; Implicit-Explicit Methods for Time-Dependant Partial Differential Equations; SIAM Journal on Numerical Analysis; 32; 2;1997; 797 - 823

[18] Choi, Y. S; Chan, K; Fractional Step Algorithm for a Model Problem in Electrochemistry; Mathematics and Computers in Simulation; 34, 1992; 101 - 112

[19] Kwok, Y; Wu, C. C. K; Fractional Step Algorithm for Solving a Multi-Dimensional Diffusion-Migration Equation; Numerical Methods for partial Differential Equations; 11, 1995, 389 - 397

[20] Baldy, C J; Elliott, M C; Feldberg, S W; Electron Hopping in Immobilized Polyvalent and/or Multicouple Redox Systems; J. Electroanal. Chem; 203, 1990; 53 - 65

[21] Ruff, I.; Experimental Evidence of Electronic Conduction in Aqueous Solutions; Electrochimica Acta; 15, 1970; 1059-1061

[22] Ruff, I; Friedrich, V.J.; Transfer Diffusion. I. Theoretical; Journal of Physical Chemistry; 75; 21; 1971; 3297-3302

[23] Paddison, S.J; Reagor, D. W; Zawodzinski, T. A. Jr; High Frequency Dielectric Studies of Hydrated Nafion; Journal of Electroanalytical Chemistry; 459; 1998; 91 - 97

[24] Leddy, J; Oberbroecking, K; Dunwoody, D; Minteer, S; Density of Nafion Exchanged with Transition Metal Complexes and Tetramethyl Ammonium, Ferrous and Hydrogen Ions: Commerical and Recast Films; Analytical Chemistry; 74; 2002; 4794 - 4799

[25] Becker, A. J.; Motupally, S.; Weidner, J.W.; Diffusion of Water in Nafion 115 Membranes; Journal of the Electrochemical Society; 147; 9; 200; 3171 - 3177

[26] Berning, T; Lu, D. M; Djilali, N; Three-Dimensional Computational Analysis of Transport Phenomena in a PEM Fuel Cell; Journal of Power Sources; 106; 2002;

284 - 294

[27] Berning, T; Djilali, N.; Three-Dimensional Computational Analysis of Transport Phenomena in a PEM Fuel Cell - A Parametric Study; Journal of Power Sources; 124; 2003; 440 - 452

[28] Bernardi, D. M; Verbrugge, M, W.; Mathematical model of a Gas Diffusion Electrode Bonded to a Polymer Electrolyte; AIChE Journal; 37; 8; Aug. 1991; 1151 - 1163

[29] Williams, M. V; Kunz, H. R; Fenton, J. M.; Operation of Nafion based PEM fuel cells with no external humidification: influence of operating conditions and gas diffusion layers, Journal of Poer Sources, 135, 2004, 122 - 134

[30] Ciureanu, M; Effects of Nafion Dehydration in PEM Fuel Cells, Journal of Applied Electrochemistry, 43, 2004, 705 - 714